University of Stavanger

Faculty of Science and Technology

MASTER'S THESIS

Study program/ Specialization: M.Sc, Petroleum Engineering / Drilling	Spring semester, 2015 Open access
Writer: Morten Adamsen Husvæg	…… (Writer's signature)
Faculty supervisor: Mesfin Belayneh External supervisor(s):	
Thesis title: ROP Modelling and Analysis	
Credits (ECTS): 30	
Key words: ROP Modelling Analysis Multiple regression Least square Bourgoyne & Young's model D-exponent MSE Microsoft Excel	Pages: ……127…… Stavanger, …….. Date/year

ABSTRACT

A total of six techniques are developed to model ROP for a new well. The techniques attain coefficients or specific values from a close-by already drilled well. Using these and drilling parameters, the proposed method predicts ROP for the new well. The techniques are mainly developed and influenced by Bourgoyne & Young's model, d-exponent model and MSE model.

The techniques are tested by comparison with six wells; three close-by wells from the Ormen Lange field, and three close-by wells from the Morvin field. Thereby each well may be tested with each technique with coefficients or values from two different close-by wells. The results display both the actual ROP and modelled ROP plots for comparison. In order to thoroughly assess the validity of the techniques an analysis of the results is also performed.

ACKNOWLEDGEMENTS

I would like to acknowledge and express my appreciations for the supervision and guidance of Mesfin Belayneh, whom has been continuously available for support and comments. I would also like to thank Svein Finnestad from the Norwegian Petroleum Directorate, for the valuable well data provided.

Stavanger, May 28, 2015

Morten Adamsen Husvæg

TABLE OF CONTENTS

ABSTRACT i

ACKNOWLEDGEMENTS ii

LIST OF FIGURES v

LIST OF TABLES ix

NOMENCLATURE x

LIST OF ABBREVIATIONS xi

1 INTRODUCTION 1

1.1 Background 1

1.2 Problem formulation 1

1.3 Objective 2

2 LITERATURE STUDY 3

2.1 Drill bits 3

2.1.1 Bit optimization 3

2.1.2 Roller-Cone Bits 4

2.1.3 Diamond Bits 6

2.2 ROP models 7

2.2.1 MSE 7

2.2.2 Bourgoyne & Young 9

2.2.3 Warren 11

2.2.4 Modified Warren 13

2.2.5 Diamond bit model 14

2.2.6 Real-Time Bit Wear Model 16

2.3 Factors affecting ROP 17

2.4 Principles of multiple regression 18

2.5 Least square parameter 19

2.6 Dillability d-exponent 19

2.7 Well-to-well correlation 21

3 ROP MODELLING 22

3.1 Multiple regression 23

3.2 Least square 26

3.3 Multiple Regression and Least Square with Bourgoyne & Young model 29

3.4 D-exponent 33

3.5 MSE 35

4 ROP MODELLING ANALYSIS 37

4.1 Plot comparison 38

4.2 Time comparison 43
5 RESULTS & DISCUSSION 49
5.1 Multiple Regression 50
5.2 Least Square 59
5.3 Multiple Regression with Bourgoyne & Young's Model 68
5.4 Least Square with Bourgoyne & Young's Model 77
5.5 D-Exponent 86
5.6 MSE 92
5.7 Analysis: Plot comparison 98
5.8 Analysis: Time comparison 103
6 CONCLUSION 106
REFERENCES 109

LIST OF FIGURES

Figure 1: Roller-cone bit (inserts) [10] 5
Figure 2: PDC bit profiles [18] 6
Figure 3: D-exponent plot example [59] 20
Figure 4: Multiple regression data analysis (Microsoft Excel) 24
Figure 5: Equation 3.1 applied in Microsoft Excel 25
Figure 6: Multiple regression procedure flowchart 26
Figure 7: Error squared of least square method 27
Figure 8: Sum of error squared in least square method 28
Figure 9: Solver Add-inn in Microsoft Excel 28
Figure 10: Least square procedure flowchart 29
Figure 11: Bourgoyne & Young's model drilling effects calculated in Microsoft Excel 30
Figure 12: Applying coefficients to the drilling effects to produce ROP with equation 3.7 31
Figure 13: Multiple regression and least square with Bourgoyne & Young's model procedure flowcharts 32
Figure 14: D-exponents calculated in Microsoft Excel 33
Figure 15: ROP calculated by d-exponents in Microsoft Excel 34
Figure 16: D-exponent model procedure flowchart 34
Figure 17: MSE calculated in Microsoft Excel 36
Figure 18: ROP calculated by MSE in Microsoft Excel 36
Figure 19: MSE model procedure flowchart 36
Figure 20: Analysis organization (by field) 38
Figure 21: Plot showing 5% and 10% deviation limits 39
Figure 22: Equation 4.1 applied in Microsoft Excel 40
Figure 23: Finding the average percentage of plot within 5/10 % of ROP in Microsoft Excel 40
Figure 24: Plot analysis organization (by well) 41
Figure 25: Plot analysis organization (by coefficient set) 41
Figure 26: Plot nalysis organization (by each field) 42
Figure 27: Plot analysis organization (overall) 43
Figure 28: Predicted ROP averaged in Microsoft Excel 44
Figure 29: Equation 4.2 applied in Microsoft Excel 45
Figure 30: Time analysis organization (by well) 46
Figure 31: Time analysis organization (by coefficient set) 46
Figure 32: Time analysis organization (by field) 47
Figure 33: Time analysis organization (overall) 48
Figure 34: Multiple regression method in well 6305/7-D-1 51
Figure 35: Multiple regression method in well 6305/7-D-2 51
Figure 36: Multiple regression method in well 6305/7-D-3 51
Figure 37: Multiple regression method in well 6506/11-A-1 52
Figure 38: Multiple regression method in well 6506/11-A-2 52
Figure 39: Multiple regression method in well 6506/11-A-3 52
Figure 40: Multiple regression - 6305/7-D-1 with coefficients from 6305/7-D-2 53
Figure 41: Multiple regression - 6305/7-D-1 with coefficients from 6305/7-D-3 53
Figure 42: Multiple regression - 6305/7-D-2 with coefficients from 6305/7-D-1 54
Figure 43: Multiple regression - 6305/7-D-2 with coefficients from 6305/7-D-3 54
Figure 44: Multiple regression - 6305/7-D-3 with coefficients from 6305/7-D-1 55

Figure 45: Multiple regression - 6305/7-D-3 with coefficients from 6305/7-D-2 55
Figure 46: Multiple regression - 6506/11-A-1 with coefficients from 6506/11-A-2 56
Figure 47: Multiple regression - 6506/11-A-1 with coefficients from 6506/11-A-3 56
Figure 48: Multiple regression - 6506/11-A-2 with coefficients from 6506/11-A-1 57
Figure 49: Multiple regression - 6506/11-A-2 with coefficients from 6506/11-A-3 57
Figure 50: Multiple regression - 6506/11-A-3 with coefficients from 6506/11-A-1 58
Figure 51: Multiple regression - 6506/11-A-3 with coefficients from 6506/11-A-2 58
Figure 52: Least square method in well 6305/7-D-1 60
Figure 53: Least square method in well 6305/7-D-2 60
Figure 54: Least square method in well 6305/7-D-3 60
Figure 55: Least square method in well 6506/11-A-1 61
Figure 56: Least square method in well 6506/11-A-2 61
Figure 57: Least square method in well 6506/11-A-3 61
Figure 58: Least square - 6305/7-D-1 with coefficients from 6305/7-D-2 62
Figure 59: Least square - 6305/7-D-1 with coefficients from 6305/7-D-3 62
Figure 60: Least square - 6305/7-D-2 with coefficients from 6305/7-D-1 63
Figure 61: Least square - 6305/7-D-2 with coefficients from 6305/7-D-3 63
Figure 62: Least square - 6305/7-D-3 with coefficients from 6305/7-D-1 64
Figure 63: Least square - 6305/7-D-3 with coefficients from 6305/7-D-2 64
Figure 64: Least square - 6506/11-A-1 with coefficients from 6506/11-A-2 65
Figure 65: Least square - 6506/11-A-1 with coefficients from 6506/11-A-3 65
Figure 66: Least square - 6506/11-A-2 with coefficients from 6506/11-A-1 66
Figure 67: Least square - 6506/11-A-2 with coefficients from 6506/11-A-3 66
Figure 68: Least square - 6506/11-A-3 with coefficients from 6506/11-A-1 67
Figure 69: Least square - 6506/11-A-3 with coefficients from 6506/11-A-2 67
Figure 70: Multiple regression with Bourgoyne & Young's model in well 6305/7-D-1 69
Figure 71: Multiple regression with Bourgoyne & Young's model in well 6305/7-D-2 69
Figure 72: Multiple regression with Bourgoyne & Young's model in well 6305/7-D-3 69
Figure 73: Multiple regression with Bourgoyne & Young's model in well 6506/11-A-1 70
Figure 74: Multiple regression with Bourgoyne & Young's model in well 6506/11-A-2 70
Figure 75: Multiple regression with Bourgoyne & Young's model in well 6506/11-A-3 70
Figure 76: Multiple regression with Bourgoyne & Young's model - 6305/7-D-1 with coefficients from 6305/7-D-2 71
Figure 77: Multiple regression with Bourgoyne & Young's model - 6305/7-D-1 with coefficients from 6305/7-D-3 71
Figure 78: Multiple regression with Bourgoyne & Young's model - 6305/7-D-2 with coefficients from 6305/7-D-1 72
Figure 79: Multiple regression with Bourgoyne & Young's model - 6305/7-D-2 with coefficients from 6305/7-D-3 72
Figure 80: Multiple regression with Bourgoyne & Young's model - 6305/7-D-3 with coefficients from 6305/7-D-1 73
Figure 81: Multiple regression with Bourgoyne & Young's model - 6305/7-D-3 with coefficients from 6305/7-D-2 73
Figure 82: Multiple regression with Bourgoyne & Young's model - 6506/11-A-1 with coefficients from 6506/11-A-2 74
Figure 83: Multiple regression with Bourgoyne & Young's model - 6506/11-A-1 with coefficients from 6506/11-A-3 74

Figure 84: Multiple regression with Bourgoyne & Young's model - 6506/11-A-2 with coefficients from 6506/11-A-1 _____ 75
Figure 85: Multiple regression with Bourgoyne & Young's model - 6506/11-A-2 with coefficients from 6506/11-A-3 _____ 75
Figure 86: Multiple regression with Bourgoyne & Young's model - 6506/11-A-3 with coefficients from 6506/11-A-1 _____ 76
Figure 87: Multiple regression with Bourgoyne & Young's model - 6506/11-A-3 with coefficients from 6506/11-A-2 _____ 76
Figure 88: Least square with Bourgoyne & Young's model in well 6305/7-D-1 _____ 78
Figure 89: Least square with Bourgoyne & Young's model in well 6305/7-D-2 _____ 78
Figure 90: Least square with Bourgoyne & Young's model in well 6305/7-D-3 _____ 78
Figure 91: Least square with Bourgoyne & Young's model in well 6506/11-A-1 _____ 79
Figure 92: Least square with Bourgoyne & Young's model in well 6506/11-A-2 _____ 79
Figure 93: Least square with Bourgoyne & Young's model in well 6506/11-A-3 _____ 79
Figure 94: Least square with Bourgoyne & Young's model - 6305/7-D-1 with coefficients from 6305/7-D-2 _____ 80
Figure 95: Least square with Bourgoyne & Young's model - 6305/7-D-1 with coefficients from 6305/7-D-3 _____ 80
Figure 96: Least square with Bourgoyne & Young's model - 6305/7-D-2 with coefficients from 6305/7-D-1 _____ 81
Figure 97: Least square with Bourgoyne & Young's model - 6305/7-D-2 with coefficients from 6305/7-D-3 _____ 81
Figure 98: Least square with Bourgoyne & Young's model - 6305/7-D-3 with coefficients from 6305/7-D-1 _____ 82
Figure 99: Least square with Bourgoyne & Young's model - 6305/7-D-3 with coefficients from 6305/7-D-2 _____ 82
Figure 100: Least square with Bourgoyne & Young's model - 6506/11-A-1 with coefficients from 6506/11-A-2 _____ 83
Figure 101: Least square with Bourgoyne & Young's model - 6506/11-A-1 with coefficients from 6506/11-A-3 _____ 83
Figure 102: Least square with Bourgoyne & Young's model - 6506/11-A-2 with coefficients from 6506/11-A-1 _____ 84
Figure 103: Least square with Bourgoyne & Young's model - 6506/11-A-2 with coefficients from 6506/11-A-3 _____ 84
Figure 104: Least square with Bourgoyne & Young's model - 6506/11-A-3 with coefficients from 6506/11-A-1 _____ 85
Figure 105: Least square with Bourgoyne & Young's model - 6506/11-A-3 with coefficients from 6506/11-A-2 _____ 85
Figure 106: 6305/7-D-1 and 6305/7-D-2 d-exponents compared _____ 86
Figure 107: 6305/7-D-1 with d-exponent from 6305/7-D-2 _____ 86
Figure 108: 6305/7-D-2 with d-exponent from 6305/7-D-1 _____ 86
Figure 109: 6305/7-D-1 and 6305/7-D-3 d-exponents compared _____ 87
Figure 110: 6305/7-D-1 with d-exponent from 6305/7-D-3 _____ 87
Figure 111: 6305/7-D-3 with d-exponent from 6305/7-D-1 _____ 87
Figure 112: 6305/7-D-2 and 6305/7-D-3 d-exponents compared _____ 88
Figure 113: 6305/7-D-2 with d-exponent from 6305/7-D-3 _____ 88
Figure 114: 6305/7-D-3 with d-exponent from 6305/7-D-2 _____ 88
Figure 115: 6506/11-A-1 and 6506/11-A-2 d-exponents compared _____ 89

Figure 116: 6506/11-A-1 with d-exponent from 6506/11-A-2 _____ 89
Figure 117: 6506/11-A-2 with d-exponent from 6506/11-A-1 _____ 89
Figure 118: 6506/11-A-1 and 6506/11-A-3 d-exponents compared_____ 90
Figure 119: 6506/11-A-1 with d-exponent from 6506/11-A-3 _____ 90
Figure 120: 6506/11-A-3 with d-exponent from 6506/11-A-1 _____ 90
Figure 121: 6506/11-A-2 and 6506/11-A-3 d-exponents compared_____ 91
Figure 122: 6506/11-A-2 with d-exponent from 6506/11-A-3 _____ 91
Figure 123: 6506/11-A-3 with d-exponent from 6506/11-A-2 _____ 91
Figure 124: 6305/7-D-1 and 6305/7-D-2 MSE compared _____ 92
Figure 125: 6305/7-D-1 with MSE from 6305/7-D-2_____ 92
Figure 126: 6305/7-D-2 with MSE from 6305/7-D-1_____ 92
Figure 127: 6305/7-D-1 and 6305/7-D-3 MSE compared _____ 93
Figure 128: 6305/7-D-1 with MSE from 6305/7-D-3_____ 93
Figure 129: 6305/7-D-3 with MSE from 6305/7-D-1_____ 93
Figure 130: 6305/7-D-2 and 6305/7-D-3 MSE compared _____ 94
Figure 131: 6305/7-D-2 with MSE from 6305/7-D-3_____ 94
Figure 132: 6305/7-D-3 with MSE from 6305/7-D-2_____ 94
Figure 133: 6506/11-A-1 and 6506/11-A-2 MSE compared _____ 95
Figure 134: 6506/11-A-1 with MSE from 6506/11-A-2_____ 95
Figure 135: 6506/11-A-2 with MSE from 6506/11-A-1_____ 95
Figure 136: 6506/11-A-1 and 6506/11-A-3 MSE compared _____ 96
Figure 137: 6506/11-A-1 with MSE from 6506/11-A-3_____ 96
Figure 138: 6506/11-A-3 with MSE from 6506/11-A-1_____ 96
Figure 139: 6506/11-A-2 and 6506/11-A-3 MSE compared _____ 97
Figure 140: 6506/11-A-2 with MSE from 6506/11-A-3_____ 97
Figure 141: 6506/11-A-3 with MSE from 6506/11-A-2_____ 97

LIST OF TABLES

1. Multiple regression - 6305/7-D-1 coefficients
2. Multiple regression - 6305/7-D-2 coefficients
3. Multiple regression - 6305/7-D-3 coefficients
4. Multiple regression - 6506/11-A-1 coefficients
5. Multiple regression - 6506/11-A-2 coefficients
6. Multiple regression - 6506/11-A-3 coefficients
7. Least square - 6305/7-D-1 coefficients
8. Least square - 6305/7-D-2 coefficients
9. Least square - 6305/7-D-3 coefficients
10. Least square - 6506/11-A-1 coefficients
11. Least square - 6506/11-A-2 coefficients
12. Least square - 6506/11-A-3 coefficients
13. Multiple regression with Bourgoyne & Young's model - 6305/7-D-1 coefficients
14. Multiple regression with Bourgoyne & Young's model - 6305/7-D-2 coefficients
15. Multiple regression with Bourgoyne & Young's model - 6305/7-D-3 coefficients
16. Multiple regression with Bourgoyne & Young's model - 6506/11-A-1 coefficients
17. Multiple regression with Bourgoyne & Young's model - 6506/11-A-2 coefficients
18. Multiple regression with Bourgoyne & Young's model - 6506/11-A-3 coefficients
19. Least square with Bourgoyne & Young's model - 6305/7-D-1 coefficients
20. Least square with Bourgoyne & Young's model - 6305/7-D-2 coefficients
21. Least square with Bourgoyne & Young's model - 6305/7-D-3 coefficients
22. Least square with Bourgoyne & Young's model - 6506/11-A-1 coefficients
23. Least square with Bourgoyne & Young's model - 6506/11-A-2 coefficients
24. Least square with Bourgoyne & Young's model - 6506/11-A-3 coefficients
25. Plot comparison analysis, 6305/7 wells within 5%
26. Plot comparison analysis, 6305/7 wells within 10%
27. Plot comparison analysis, 6506/11 wells within 5%
28. Plot comparison analysis, 6506/11 wells within 10%
29. Time comparison analysis, 6305/7 wells
30. Time comparison analysis, 6506/11 wells
31. Overall plot compared results
32. Overall time compared results

NOMENCLATURE

ρ – Fluid density

ρ_c – ECD at the hole-bottom

γ_f – Fluid specific gravity

μ - Bit specific coefficient of sliding friction / Apparent viscosity / Plastic viscosity

A – Area

A_B – Bit area

C_b – Cost of bit

C_f – Drilling cost per foot drilled

C_r – Cost of rig

d – Bit diameter / D-exponent

D – Depth

d_B – Bit diameter

d_c – Corrected d-exponent

d_n – Bit nozzle diameter

e – Specific energy

F – Thrust

f_c – Chip hold down function

F_j – Jet impact force

F_{jm} – Modified jet impact force

g_p – Pore pressure gradient of formation

h – Tooth wear hight

hr – Hour

ln – Natural logarithm

log – Logarithm

m – Meter

N – Rotational speed (RPM)

Norm – Normalized

P – Penetration of each cutter

P_e – Effective differential pressure

P_w – Penetration loss due to wear of cutter

q – Flow rate

Q – Least square sum

R – ROP

S – Rock strength

T – Torque

t_b – Rotating time

t_c – Non-rotating time

t_t – Trip time

V_D – Volume each cutter is worn down per rotation

v_f – Return fluid velocity

v_n – Nozzle velocity

w – Bit weight

$ – Dollars

LIST OF ABBREVIATIONS

B&Y – Bourgoyne & Young's model

COR – Correction factor

coeff. – Coefficient(s)

D-Exp – D-exponent

DG – Dull grade

ECD – Equivalent circulating density

FLOW – Flowrate

FP – Formation pressure

GPM – Mud flow rate

IADC – International Association of Drilling Contractors

KA – Apparent nozzle area of bit

LS – Least square

Mult. Reg. – Multiple regression

MW – Mud weight

MSL – Mean sea level

MSE – Mechanical specific energy

NPP – Normal pore pressure

PDC – Polycrystalline diamond compact

ROP – Rate of penetration

RPM – Revolutions per minute

TRQ – Torque

TVD – True vertical depth

WOB – Weight on bit

WOB_{mech} – Mechanical weight on b

1 INTRODUCTION

1.1 Background

Drilling after hydrocarbon resources generally occur deep down in the ground through various layers of rocks. The essentials in drilling are breakage, crushing and cutting of fragments out of the rock surface to reach deeper into the ground. Rotary drilling is the standard penetration method for oil and gas wells. Teale [1] described rotary drilling as a combination of two actions: cutting and indention. The rotating movement cuts the rock, simultaneously as it pushes into the rock to indent. The work done or required energy to excavate a unit volume of rock was introduced by Teale as specific energy or mechanical specific energy (MSE) [1]. The speed of the drilling process is given in rate of penetration (ROP), presenting the drilling in feet drilled per hour.

The petroleum industry is a high grossing industry, but also a high cost industry. Therefore, there has always been a focus on cutting costs and increasing efficiency. Given the recent unexpected drop in oil prices and the subsequent rise in uncertainty related to future price levels, the focus on cost reduction and efficiency considerations have increased dramatically. One of the most costly aspect of the industry is exploration and drilling, and therefore has a lot of potential for optimization and reducing costs. Planning and predicting future drilling operations based on controllable variables will be essential in order to realize these efficiency gains. This may be aided by ROP modelling and analysis.

1.2 Problem formulation

Drilling operations have significant potential for optimizing and reducing costs. This thesis aims to develop new techniques in modelling ROP more accurately, and to improve the prediction of ROP for new wells. These techniques can be utilized to better plan and optimize drilling expenses. This thesis is going to address issues such as:

- How field data may be used to analyze and develop ROP models for new nearby wells
- How literature documented models can be modified with the idea of coupling operational parameters

- How d-exponent and MSE data obtained from an old well can be utilized for a new nearby well

1.3 Objective

The objective of this thesis comprises the following:

- Literature study on bits and ROP models and methods
- Develop new techniques to model the ROP
- Test the new techniques on three wells from 6305/7 and three wells from 6506/11
- Analyze the results to identify the validity and performance of the techniques.
- Analyze the results to identify the best technique to model ROP

2 LITERATURE STUDY

2.1 Drill bits

The drill bit is the main tool of the drilling process, positioned at the end of the drill string. Its rotation cuts and the weight on bit indents, resulting in penetration of the formation. Drilling fluid circulates through the bit to decrease bit wear by cooling, and to help the penetration rate by removing cuttings. There is a great selection of bits available, where rotary drilling has two main groups of bits in which we find numerous varieties of bit designs. These are roller-cone bits and fixed-cutter or diamond bits.

2.1.1 Bit optimization

The most important factor affecting the drilling rate is considered by the industry to be the bit selection [6]. Importance of the drill bit in the overall drilling cost is seen in the cost equation 2.1, which expresses the significance of drill bit optimization. During the planning phase, the primary analysis is drill bit optimization [2].

$$C_f = \frac{(t_r+t_t+t_c)C_r+t_rC_m+C_b}{\Delta D} \quad (2.1)$$

Where C_f is drilling cost [$/ft], t_r: the drilling time [hr], t_t: the trip time [hr], t_c: the connection time [hr], C_r: the rig cost [$/hr], C_m: the downhole motor cost [$/hr], C_b: the cost of bit [hr], and ΔD is the formation drilled, in [ft].

Drill bits have been continuously developed and improved since the introduction of the drill bit. They are designed and optimized to produce low cost drilling, increase operational time of the bit to minimize tripping, and to provide stable and safe operations. All these aspects result in lower drilling costs, in accordance with cost equation 2.1 and minimizing drilling risks.

The selection of bit is foremost dependent on the formation type being drilled [5]. There are many operating factors affecting the performance of the drill bit, mainly the WOB, RPM, mud properties, hydraulic efficiency and formation properties [3][7]. The drill bit elements affecting

the drilling rate are bit diameter, bit weight, bit wear and bit hydraulic [4]. Bit selection for specific conditions are often based on mathematical predictions from models, rule of thumb, trial and error, or a combination of these [8]. While roller-cone bits have a more complex geometry than diamond bits, the diamond bits have a very wide selection in bit and cutter design [17]. The result is a much greater variation of bit performance for diamond bits [9].

2.1.2 Roller-Cone Bits

Roller-cone bits can be categorized by insert or milled tooth. Insert bits have a cutting structure consisting of a sequence of inserts pressed into the cone. Milled tooth bits have a cutting structure of teeth milled out of the cone. Tooth design and bearing types vary greatly for roller-cone bits, making them applicable for several formation types. Milled tooth bits are usually used in soft formations. Insert bits are appropriate for a wider variety of formations, including hard formations.

Three cones and legs of similar size, connected to a pin, normally make up roller-cone bits. The cones are mounted on each of their bearings, and able to rotate with respect to the bit body. Connection to the drill string is provided by the pin section. Drilling fluid is pumped down the drill string and through the nozzles of the bit. Openings by the legs provide fluid circulation, and give the possibility to achieve high pressure jetting through the nozzles of the bit. A representation of a typical roller-cone bit is provided below in Figure 1 [10] (with alterations).

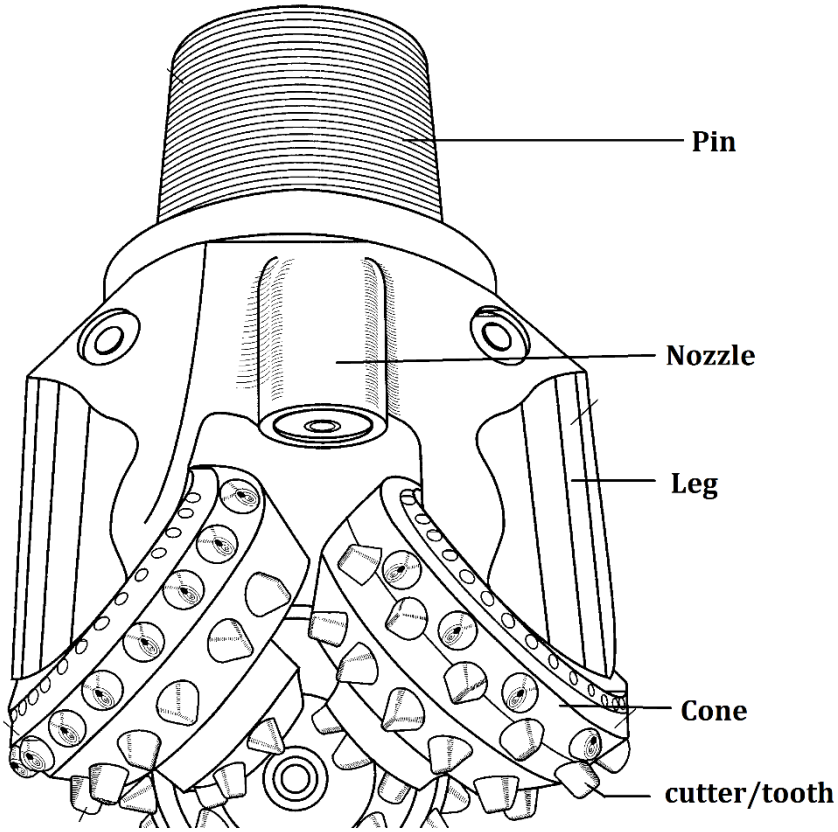

Figure 1: Roller-cone bit (inserts) [10]

Roller-cone bits are made of steel, which requires sufficient hardenability, yield strength, heat treatment, machinability, and impact resistance. Design of the bit has generally four focus areas: geometry and type of cutting structure, hydraulic requirements, material selection, and mechanical operating requirements. The bit design is chosen based on how it will operate and in what conditions it will operate in. Operating factors influencing the bit design are primarily weight on bit, rotary speed and hydraulics. Operating conditions such as formation, depth, drilling fluid, and hole deviation are also important parts considered when designing a bit. The geometry and type of cutting structure is the significant design area of the bit for providing an efficient penetration. Wear-resistance is also important during the selection of geometry and type of cutting structure. Cutter shape and grade is normally differentiated by its placement on the cone for insert teeth. There is a number of available geometries, sizes and grades for cutters to be optimized depending on the cutters location and conditions.

2.1.3 Diamond Bits

Diamond bits can be regarded as fixed-cutter bits, as the bits have no separately moving parts. Diamond is the hardest readily available material, thus using it as material provides superior hardness. Both rotating as one piece and using diamond material gives a long bit life. The diamond bits are mainly used in soft to moderate formation. In hard formations, the bit has limitations regardless of recent developments [15]. Limitations such as low ROP and high wear is also a result for deep continental gas developments [16]. Two categories of diamond bits are currently on the marked: Polycrystalline Diamond Compact Bits and Natural Diamond Bits. The Polycrystalline Diamond Compact (PDC) Bit is the most common diamond bit, relatively equal in popularity as the roller-cone bit. PDC bits uses inexpensive, fabricated diamonds. Their long bit life and capability of maintaining a high ROP has resulted in wide popularity. Fixed-cutters induce a shearing action more effective than the crushing of the inserts or teeth on the cones of the roller-cone bit [11-14]. A PDC bit is designed based on four considerations: materials, formation properties, hydraulic conditions, and mechanical parameters. There are four different types of blade profiles for a PDC bit:

1. Flat profile – for hard and non-abrasive formations
2. Short parabolic – for hard and medium abrasive formations
3. Medium parabolic – for medium/hard and abrasive formations
4. Long parabolic – for soft and abrasive formations

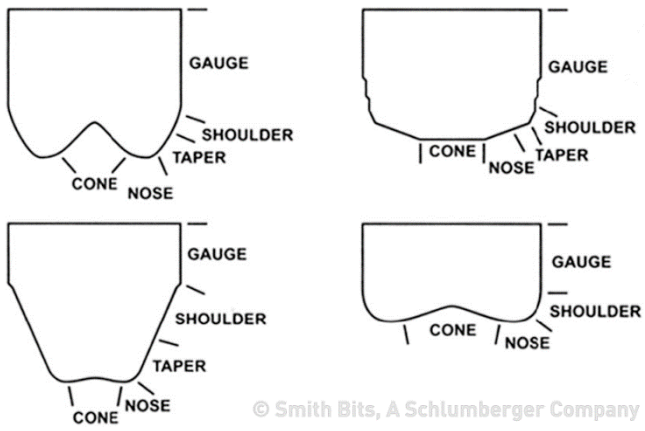

Figure 2: PDC bit profiles [18]

Figure 2 [18] shows various PDC bit profiles, broken into five zones: cone, nose, taper, shoulder, gauge (from center). The profile or shape of the bit is dependent on cutter placements, cutter geometry, cutter density, hydraulics, well geometry, and formation. All elements need to be considered to design a bit capable of high ROP and low bit wear. The shape will have a direct influence on steerability, stability, ROP, durability, fluid circulation, and cutter density.

2.2 ROP models

The two leading drilling optimization methods are rate of penetration (ROP) and mechanical specific energy (MSE) models. Both models optimize by considering the important variables during the drilling operation. These variables can affect the models in a complex way. Many ROP and MSE models have been developed and modified, with mathematically or experimentally derived relationships among the variables. [19]

ROP models may be used to calculate formation drillability including the effects of drilling variables. Optimizing the drilling operation by use of ROP models is managed by varying the drilling variables to achieve the ideal drilling situation during the entire bit run. Mechanical specific energy models may detect changes in drilling efficiency during drilling operations, providing a tool to enhance instantaneous ROP by optimizing the drilling variables similarly as the ROP model. [19]

2.2.1 MSE

In “The Concept of Specific Energy in Rock Drilling” [1] from 1965, Teale discusses the fundamental problems and implications in rock working or mining operations. We can relate this work on rock excavation to drilling. The paper focuses on the applied energy for crushing, as this was accepted as a significant factor and there had been several attempts to relate it to drilling [20]. Besides the work of Walker and Shaw [21], no identified work has been done on the relationship between energy and crushing by drilling and indention. Walker and Shaw managed to calculate the energy needed to grind different sizes of steel and rock.

Teale was certain such a relationship had to have a vital part in understanding the rock excavating processes. The factor introduced was 'specific energy', work done to excavate a unit volume of rock. In other words, the work/energy required to drill a certain amount of rock. In order to drill a certain amount of rock, it was obvious to Teale that there had to be a theoretical minimum energy required.

For a rotary non-percussive drilling process, Teale proposed that work is done by the thrust (F) and torque (T) because of the indention and rotation actions. Then the total work performed within one minute could be derived by including the rotation speed (N) and the rate of penetration (u) to give F u + 2πN T (in.lb). With the area of excavation or hole (A) the amount of rock drilled is Au (in^3). By dividing work with volume (Au), specific energy (e) is given as:

$$e = \frac{F}{A} + \frac{2\pi}{A}\frac{NT}{u} \tag{2.2}$$

or

$$MSE = \frac{WOB}{A_B} + \frac{120\pi NT}{A_B ROP} \tag{2.3}$$

These equations are the original formulas of what has become mechanical specific energy (MSE), a concept introduced and formulated by Teale originally as 'specific energy'. Since then MSE has been further researched and the model has been modified several times. MSE can be monitored to ensure drilling efficiency by detecting when it changes [22]. An increase in MSE results in a higher demand of work to drill and thereby a lower drilling efficiency.
Pessier and Fear [23] introduced a formulation of torque into the MSE equation in 1992. Measurements-while-drilling (MWD) measured torque; however, the majority of field data was given in the form of WOB, RPM and ROP measurements. Therefore a method to compute more reliable torque values, by using a bit specific coefficient of sliding friction (μ), bit diameter and WOB was added to give:

$$T = \mu \frac{d_B\, WOB}{36} \tag{2.4}$$

By use of this formulation of torque, Pessier and Fear modelled MSE as:

$$MSE = WOB\left(\frac{1}{A_B} + \frac{13{,}33\ \mu\ N}{d_B\ ROP}\right) \tag{2.5}$$

2.2.2 Bourgoyne & Young

Initial drilling models proposed for drilling optimization were largely established upon limited data and imprecise results. Bourgoyne & Young [4] introduced an ROP model that is considered the most suitable for real-time drilling optimization and an essential optimization method as it is based on statistical past drilling values [24]. The modeling is done by a multiple regression analysis of the past drilling data, including effects of variables, to produce the rate of penetration. Effects on ROP included in the model are formation strength, formation depth, formation compaction, pressure differential (bottom hole), bit weight and diameter, rotary speed, bit wear, and bit hydraulics.

This rate of penetration model predicts the effect of the included eight drilling variables (x_j) on the penetration rate (dD/dt). In a given formation, the modeling is done by determining the eight constants (a_j). The model is mathematically given by:

$$\frac{dD}{dt} = \exp(a_1 + \sum_{j=2}^{8} a_j x_j) \tag{2.6}$$

The model can also be expressed clearer, with the exponential function integrated:

$$ROP = f_1 * f_2 * f_3 * f_4 * f_5 * f_6 * f_7 * f_8 \tag{2.7}$$

where f_{1-8} represents the various normalized effects on ROP [19].

Effect of formation strength or rock drillability is represented by the a_1 constant and x_1, or $f_1 = \exp(2.303\ a_1)$. Constant a_1 is proportional to the inversed natural logarithm of the squared drillability strength parameter mentioned by Maurer [25].

Effect of formation depth (D [ft]) is denoted by the a_2 constant, where x_2 is given by:

$$x_2 = 10000{,}0 - D \tag{2.8}$$

$f_2 = \exp(2.303\ a_2(10000 - D))$. Therefore in a normal compacted formation, the ROP decreases exponentially with depth. This trend was found in Murray's [26] micro-bit and field data, as well as Combs' [27] field data.

Effect of formation compaction or pore pressure is represented by the a_3 constant and x_3. The ROP is assumed to exponentially increase with the pore pressure gradient of the formation (g_p [lb/gal]). The effect of under-compaction on ROP was suggested by compaction theory, thus x_3 is defined by equation 2.9 and $f_3 = e^{2.303\ a_3 D^{0,69}(g_p - 9)}$.

$$x_3 = D^{0,69}(g_p - 9{,}0) \tag{2.9}$$

Effect of differential pressure is represented by constant a_4 and x_4. It is assumed an exponential decrease in ROP with increasing bottom-hole-pressure, based on indications from field data [27] [28] and laboratory data [29] [30]. Therefore, the x_4 is given by:

$$x_4 = D(g_p - \rho_c) \tag{2.10}$$

Here ρ_c is the ECD at the bottom of the hole [lb/gal]. Whereas $f_4 = e^{2.303\ a_4 D(g_p - P_c)}$.

Effect of bit diameter (d [in]) and bit weight (w [lb]) (w/d) is expressed by constant a_5 and x_5. Indications from several sources [27] [31-35] assume the ROP as directly proportional to the term $(\frac{W}{d})^{a_5}$. The normalized $e^{a_5 x_5}$ term is equal to 1.0 for 4000 lb/in bit. Consequently, x_5 is determined by:

$$x_5 = \ln\left(\frac{\frac{w}{d} - \left(\frac{w}{d}\right)_t}{4.0 - \left(\frac{w}{d}\right)_t}\right) \tag{2.11}$$

Drill-off tests are used to estimate threshold bit weight $\left(\frac{W}{d}\right)_t$. Bit weight exponent values have been reported ranging from 0.6 – 2.0. $f_5 = \left(\frac{\frac{w}{d} - \left(\frac{w}{d}\right)_t}{4.0 - \left(\frac{w}{d}\right)_t}\right)^{a_5}$.

Effect of rotary speed (N) is represented by constant a_6 and x_6. Sources [27] [31-35] indicate that the ROP should be assumed directly proportional to N^{a_6}. The normalized $e^{a_6 x_6}$ term is equal to 1.0 for 100 RPM, giving x_6 as:

$$x_6 = \ln(\frac{N}{100}) \tag{2.12}$$

Rotary speed exponent values have been reported ranging from 0.4 – 0.9 (from very hard formations to very soft formations) [35]. The f_6 term is: $f_6 = (\frac{N}{60})^{a_6}$.

Effect of tooth wear (h) is represented by constant a_7 and x_7. Tooth wear has been modeled by various sources [31] [32] with complex terms. However, for multiple regression a simpler approach is more suitable. Fractional worn away tooth height (h) is used to determine x_7 in equation 2.13. While $f_7 = e^{-a_7 * h}$.

$$x_7 = -h \tag{2.13}$$

Effect of bit hydraulics is denoted by the constant a_8 and x_8, and based on Eckel's [36] microbit experiments. Eckel discovered that the ROP was proportional to Reynolds number group $(\frac{\rho q}{\mu\, d_n})^{0,5}$. Here ρ is mud density [lb/gal], q is flow rate [gal/min], μ is the apparent viscosity [cp], and d_n is the bit nozzle diameter [in]. Giving x_8 by equation 2.14.

$$x_8 = \frac{\rho q}{350\, \mu d_n} \tag{2.14}$$

Apparent viscosity is not measured regularly and therefore estimated by: $\mu = \mu_p + \frac{\tau_y}{20}$.

The f_8 term with jet impact force (F_j [klb$_f$]) is $f_8 = (\frac{F_j}{1000})^{a_8}$.

2.2.3 Warren

Warren developed models to predict the rate of penetration for soft formation bits. The models are generated from laboratory work, by combining rotary speed, bit type, bit size, rock strength and weight on bit to calculate the rate of penetration. A large-scale drilling rig was used to obtain experimental data. The main intention of the models is to describe the relationship between the variables that control the rate of penetration. The initial model assumes perfect cleaning conditions. Warren then modified his own model to account for more realistic, imperfect cleaning conditions.

Development of new models for soft formations was needed, as there was a lack of an adequate existing model. Galle and Woods [37] had at the time the most commonly used model for soft formation drilling. However, Randall and Estes [38] explains the inadequacy of that model, where applying the model in real conditions violates an assumption of the model. Maurer's [25] 'perfect cleaning' model was found not applicable in general for soft formation bits. Deviation occurred constantly in the results from experimental data in soft-formation conditions used with the Maurer model.

Warren presented the perfect-cleaning model in 1981 [39]. In the "Drilling Model for Soft-Formation Bits" paper, it is described that developing the drilling model was done with dimensional analysis and generalized response curves. A model by Wardlaw [40] was modified to better comply with experimental data acquired from a laboratory test. The model modified to best comply with the experimental data is given by equation 2.15.

$$\mathrm{ROP} = \left(\frac{\mathrm{aS^2d^3}}{\mathrm{N^bWOB^2}} + \frac{\mathrm{c}}{\mathrm{Nd}}\right)^{-1} \tag{2.15}$$

The first term describes the maximum rate that a bit can crush rock into cuttings by $\left(\frac{aS^2d_b^3}{N^bWOB^2}\right)$. The second term considers the applied WOB to more teeth, and as the WOB increases, the teeth penetrate deeper into the rock. Here a, b and c are bit constants in the penetration model. The bit constants do not need to change when the variables alter to retain adequate ROP prediction. Extensive field tests were performed, where the model's prediction ability was investigated by drilling with several variable changes. The relatively small difference between predicted and measured ROP in the tests are perhaps a result of changes in hydraulics, as there is no correction for this in the model.

In 1987, Warren presented the imperfect cleaning model [8]. To simplify the complex modeling required to give a good ROP prediction, Warren understood that a basic model had to be developed first. The perfect cleaning model is this basic model, the starting point. Refining the basic model is done by adding new terms. If the physics of the process is controlled correctly, the new terms will not dismiss the initial model.

Warren explained that under steady state conditions, the cuttings removal rate from the bit is equivalent to the rate new chips forms. This infers that the rate of penetration is affected by cuttings generation process or cuttings removal process, or a combination of them both. As the basic model does not account for cuttings removal, this term had to be added. To account for cuttings removal, Warren used dimensional analysis to isolate variables consisting of the impact force and mud properties. These were incorporated into equation 2.15 to express the imperfect cleaning model by:

$$\mathrm{ROP} = \left(\frac{aS^2 {d_b}^3}{N\,WOB^2} + \frac{b}{N d_b} + \frac{c d_b \gamma_f \mu}{F_{jm}}\right)^{-1} \tag{2.16}$$

Here F_{jm} is the modified impact force that removes variation in impact pressure and is given by $F_{jm} = \left(1 - {A_v}^{-0,122}\right)F_j$ where $A_v = \frac{v_n}{v_f} = \frac{0,15 d_b^2}{3 d_n^2}$ and $F_j = 0{,}000516 \rho q v_n$.

2.2.4 Modified Warren

Work continued in modifying Warren's model, by adding new conditions that affect the ROP. There are numerous actions and processes going on during drilling and resulting in penetration. It is not likely that it would be possible to completely model the penetration process, at least not with all inputs known. However, work continued to build on the basic model Warren started to strengthen the model's precision, as more quantifiable conditions are included. [8]

In 1993, Hareland and Hoberock [41] introduced a modified Warren model. It was known that "chip hold down effects" has an important impact on the rate of penetration [42] [43]. However, it was not included in Warren's models. Hareland and Hoberock defined the effect with $f_c(P_e)$, given by:

$$f_c(P_e) = c_c + a_c(P_e - 120)^{b_c} \tag{2.17}$$

Here a_c, b_c and c_c constants are dependent on the lithology and P_e is differential pressure [44]. This equation gave the most reasonable fit to the data tested using a varied bottom hole pressure,

and for different lithologies. The modified equation including "chip hold down effect" resulted as:

$$ROP = \left[f_c(P_e)\left(\frac{aS^2{d_{bit}}^3}{RPM*WOB^2} + \frac{b}{RPM*d_{bit}}\right) + \frac{cd_{bit}\rho\mu}{I_m}\right]^{-1} \quad (2.18)$$

Another essential effect missing in this equation is bit wear. It was known that bit wear impaired the rate of penetration; however, there were no available published rate of penetration models for dull bits. Hareland and Hoberock [41] noticed equation 2.18 experienced problems when the bit was dull, by wear or missing teeth. Therefore, a wear term was introduced and represented by W_f, given by equation 2.19.

$$W_f = 1 - \frac{\Delta BG}{8} \quad (2.19)$$

Where ΔBG represent the bit wear change and is given as $\Delta BG = W_c \sum_{i=1}^{A} WOB_i * RPM * Ar_{abrj} * S_i$. Here S is rock compressive strength which is a function of lithology and confining pressure, calculated by $S = S_o(1 + a_s P_e^{b_s})$.

Bit wear W_f included in the ROP model gives the following final equation:

$$ROP = W_f\left[f_c(P_e)\left(\frac{aS^2{d_{bit}}^3}{RPM*WOB^2} + \frac{b}{RPM*d_{bit}}\right) + \frac{cd_{bit}\rho\mu}{I_m}\right]^{-1} \quad (2.20)$$

2.2.5 Diamond bit model

Unlike the Warren and Warren modified models produced for roller-cone bits, the following model is designed to be applied when drilling with diamond bits. The model relates the ROP to the quantity removed by the scraping action of a diamond bit [45]. Bit types that can use the model includes Polycrystalline Diamond Compact Bits, Natural Diamond Bits and any Geoset Bits [9]. Useful application areas for the model are in planning drilling operations, during drilling, drilling optimization and post drilling analysis.

Several models have previously been developed for diamond bits. Appl and Rowley [46] introduced one of the initial models, assuming "a plastic coulomb rock failure with Mohr circle failure criteria" [9] back in 1968. In 1976, Peterson [47] used the equivalent blade concept and a static loading condition to produce a model. Neither of the models were applicable in normal drilling scenarios. A time consuming and often inaccurate model was developed by Warren and Sinor [48] [17] in 1986-1987. The model required detailed information and was not considered practical. No models were developed on the performance of geoset bits.

Hareland and Rampersad's [9] diamond bit model presented here uses cutter geometries, cutter wear, bit design parameters, formation properties and operating conditions. The principle of the model is based on that a weight applied on the bit will cause each cutter (diamond) to penetrate a certain depth depending on the number of cutters, cutter size and rock strength. Rotating the bit will additionally scrape the rock away. The model developed for a Natural Diamond Bit is:

$$\mathrm{ROP} = \frac{14{,}14\ \mathrm{N_s RPM}}{\mathrm{D_B}} \left[\left(\frac{\mathrm{d_s}}{2}\right)^2 \cos^{-1}\left(1 - \frac{4\mathrm{W_{mech}}}{\mathrm{N_s d_s^2 \pi \sigma_c}}\right) - \left(\frac{2\mathrm{W_{mech}}}{\mathrm{N_s \pi \sigma_c}} - \frac{4\mathrm{W_{mech}^2}}{(\mathrm{N_s d_s \pi \sigma})^2}\right)^{\frac{1}{2}} \left(\frac{\mathrm{d_s}}{2} - \frac{2\mathrm{W_{mech}}}{\mathrm{N_s \pi \sigma_c d_s}}\right) \right] \quad (2.21)$$

For a Natural Diamond Core Bit model is:

$$\mathrm{ROP} = 14{,}14\ \mathrm{N_s RPM} \left(\frac{\sqrt{\mathrm{D_o^2 + D_i^2}}}{\mathrm{D_o^2 + D_i^2}}\right) \left[\left(\frac{\mathrm{d_s}}{2}\right)^2 \cos^{-1}\left(1 - \frac{4\mathrm{W_{mech}}}{\mathrm{N_s d_s^2 \pi \sigma_c}}\right) - \left(\frac{2\mathrm{W_{mech}}}{\mathrm{N_s \pi \sigma_c}} - \frac{4\mathrm{W_{mech}^2}}{(\mathrm{N_s d_s \pi \sigma})^2}\right)^{\frac{1}{2}} \left(\frac{\mathrm{d_s}}{2} - \frac{2\mathrm{W_{mech}}}{\mathrm{N_s \pi \sigma_c d_s}}\right) \right] \quad (2.22)$$

Anomalies from the complexity in the rock bit interaction gave the need for a lithology correction factor, COR. The factor can be calculated with lab data or a drill-off test [49], and is given by $\mathrm{COR} = \mathrm{a}/(\mathrm{RPM^b\ x\ WOB^c})$. Where a, b, and c are cutter geometry correction factors. With this correction factor the ROP can be calculated by equation 2.23 [46].

$$\mathrm{ROP} = \frac{14{,}14\ \mathrm{N_s\ RPM\ (A_V - A_{Vw})\ COR}}{\mathrm{D_{bit}}} \quad (2.23)$$

Where A_V is the projected front area of each cutter and A_{Vw} is the projected worn area of a cutter, given by $A_V = \left(\frac{d_s}{2}\right)^2 cos^{-1}\left(1 - \frac{2P}{d_s}\right) - \sqrt{d_s\,P - P^2}\left(\frac{d_s}{2} - P\right)$ and $A_{Vw} = \left(\frac{d_s}{2}\right)^2 cos^{-1}\left(1 - \frac{2P_w}{d_s}\right) - \sqrt{d_s\,P_w - P_w^2}\left(\frac{d_s}{2} - P_w\right)$.

Here P is the penetration of each cutter and P_w is penetration loss due to wear of cutter, given by $P = \frac{2}{\pi\, d_s}\left(\frac{WOB_{mech}}{S\,N_s} - \frac{\pi P_w d_s}{2}\right)$ and $P_w = \sqrt{\frac{2\,V_D}{\pi\, d_s}}$. The volume each cutter has worn down per rotation, V_D, is calculated by $V_D = C_a \sum_{i=1}^{n} \frac{WOB_{mech}\,RPM\,S\,Ar_{abr}}{N_s\,R_e}$. Where R_e is introduced, the equivalent bit radius given by $R_e = \frac{D_{bit}}{2\sqrt{2}}$. WOB_{mech} is mechanical WOB and is defined by $WOB_{mech} = WOB_{applied} - \Delta p A_p$. Here $WOB_{applied}$ is the applied WOB and $\Delta p A_p$ is the pump-off force on the bit face, where Δp is calculated by $\Delta p = \frac{GPM^2\rho}{12031(KA)^2}$. KA is the apparent nozzle area of the bit.

2.2.6 Real-Time Bit Wear Model

Rashidi, Hareland and Nygaard [19] based a model on two past approaches for drilling optimization: Mechanical specific energy (MSE) and Borgouyne and Young's inverted ROP model. As mentioned earlier in this paper, MSE can be used to optimize drilling variables and ROP instantaneously during drilling. ROP models vary drilling parameters to optimize for an entire bit run. The advantage of the ROP model is that drillability, bit wear and the effect of changing mud weight is included, while the advantage of the MSE model is that it is applicable in real-time. A combination of these two approaches was modified to be used for real-time bit wear estimation.

A new model for MSE was proposed to give a relationship between drillability from the ROP model and MSE, introduced by equation 2.24.

$$MSE = K_1\left(\frac{1}{f_1}\right)^{K_2} \tag{2.24}$$

Here f_1 is the formation drillability term in the Burgouyne and Young ROP model, and is related to the model by equation 2.25.

$$f_1 = \frac{ROP}{f_2 * f_3 * f_4 * f_5 * f_6 * f_7 * f_8} \tag{2.25}$$

Where the bit wear h in function f_7 is altered, and given by $h = \frac{(Depth_{Current} - Depth_{In})}{(Depth_{Out} - Depth_{In})} * \frac{DG}{8}$.

Here DG is the dull grade value between 0-8 (IADC).

The K_1 constant from equation 2.24 is used for real-time estimation of the wear function. A normalized inversion of K_1 is introduced to compensate for trends of K_1 and bit wear against depth, given as equation 2.26.

$$Norm\left(\frac{1}{K_1}\right) = 1 - A * h^B \tag{2.26}$$

Constant B here was obtained most accurately by regressive software. Equation for the constant is $B = 5{,}6392 * h + 0{,}4212$. The proposed model showed encouraging results with data, and has become an important initial model for further real-time analysis [50].

2.3 Factors affecting ROP

The drilling factors can be divided into two groups as dependent and independent variables (Barr and Brown 1983) (Ambrose 1987) (Shah 1992). The dependent variables are determined by the drilling conditions and independent variables. Whereas the independent variables may be controlled and changed before and during drilling [51]. A similar dividing can be to classify by controllable and environmental variables, where also formation related factors are included [4].

The controllable variables are like the independent variables directly and instantly adjustable. These include:

- Weight on bit (WOB)
- Rotations per minute (RPM)
- Bit type
- Hydraulics

The environmental variables are similarly to the dependent variables not controllable; however also include the formation factors. Although the drilling fluid may be directly changed, it is included as an environmental variable as it is dependent on the drilling conditions and there is a certain fluid required for the drilling operation [4]. The environmental variables include:

- Drilling fluid
- Torque
- Formation properties

Additionally Equivalent Circulating Density (ECD) and cuttings transport affects the ROP [24]. Observations indicate that the ROP increases with decreased ECD. Ozbayoglu et al. [52] analyzed effects of cuttings transport on drilling parameters. Efficient hole cleaning is essential during drilling, this is controlled by a number of factors:

- Hole angle
- Fluid velocity
- Fluid properties (rheological properties and density)
- Cuttings size, shape, and concentration
- Annular size
- Rate of pipe rotation and pipe eccentricity
- Fluid flow regime (laminar or turbulent)

2.4 Principles of multiple regression

A multiple regression model is a regression model with two or more regression variables [53]. Multivariate analysis characterizes an observation factor by several variables [54]. This method takes into account changes of several properties simultaneously. The multiple regression

equation of Y on X_1, X_2… is commonly given by $Y = b_0 + b_1 X_1 + b_2 X_2 + \ldots$ [55]. Where b_0 is the intercept and b_1, b_2… are analogues to the slope in linear regression equation, also called regression coefficients [55]. This flexible method of data analysis can be applicable when a quantitative variable is to be examined in relation to other factors [56].

2.5 Least square parameter

The least squares method minimizes the square sum of residual between observed output and predicted output [57]. The least square sum is minimized to attain parameter estimates, mathematically expressed by equation 2.27.

$$Q = \sum_{i=1}^{n} [y_i - f(x_i; b)]^2 \tag{2.27}$$

Where unknown parameters of b is in the regression function f(x; β) estimated by minimizing the squared sum deviation [57]. The x values are coefficients. Observed output is represented by y_i here, while predicted output is $f(x_i; b)$. Q is then the sum of the error squared.

2.6 Dillability d-exponent

The drillability d-exponent normalizes the ROP by removing effects of external drilling parameters such as pressure and rock strength. This exponent increases with depth in normally pressured formations, proportionally to the rock strength. When drilling into abnormally pressured shale however, the exponent will decreases with depth. Here the drilling experiences an under-compacted section, where the decreased density and increased porosity results in a more drillable formation. If all other drilling parameters stay unchanged, the rate of penetration will increase in this section. ROP also increases by having less pressure differential between drilling fluid and pore pressure. These abnormal pressure zones are detected far earlier by a bit with no wear, than a worn down bit. A dull bit may be far into the abnormally pressured zone before the transition is detected. A projected plot of the d-exponent is in figure 3. [58] [59]

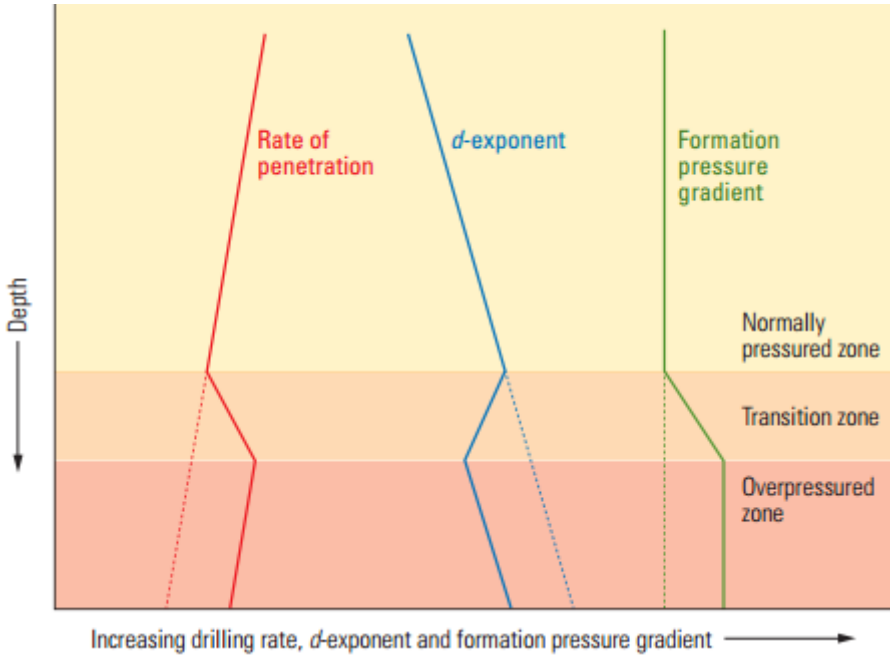

Figure 3: D-exponent plot example [59]

Using changes of ROP values by themselves as indicator of abnormal pressure is not ideal. Therefore, the drillability exponent is used to normalize or correct the drilling rate. This gives a more effective indicator of pore pressure and abnormally pressured zones. The basic drillability exponent (d) originates from work by Bingham (1965) and Jordan and Shirley (1967) [60], and the mathematical formulation of the d-exponent is given as equation 2.28.

$$d = \frac{\log\left(\frac{ROP}{60\,RPM}\right)}{log\left(\frac{12\,WOB}{10^6\,d_B}\right)} \tag{2.28}$$

This equation tries to correct the rate of penetration for changes in WOB, RPM and hole size. In 1971, Rehm et al. [61] produced a corrected d-exponent for changes in mud weight. The corrected d-exponent (d_c) is given by equation 2.29.

$$d_c = d\left(\frac{NPP}{ECD}\right) \tag{2.29}$$

Here NPP is normal pore pressure gradient, and ECD is equivalent circulating density. This correction is universally used as it makes the exponent more sensitive to mud weight changes and increasing pore pressure, yet it is without a thorough theoretical basis [58].

Three limitation of the drillability exponent have been expressed [58]:

- The drillability exponent requires clean shale or clean argillaceous limestone
- Large increase in mud weight results in lower values of the corrected drillability exponent (d_c)
- The corrected drillability exponent (d_c) is affected by lithology, type of bit, bit wear, poor hydraulics, unconformities, and motor or turbine runs.

2.7 Well-to-well correlation

It is already a policy to use survey data from nearby drilled wells or exploration wells in the planning of other adjacent wells [62], although well-to-well correlation is not exact. The reason we may do so is because the formation properties within an area generally changes only with depth, not horizontally [63]. Most sediments deposit in layers [64]. Thereby when drilling two vertical holes close-by, they will most likely go through the same formation properties and pressure regimes at approximately the same depths. Correlating formations can help engineers in designing close-by wells and help identifying drilling risks [65]. The pressure regime is especially of importance, with respect to selecting drilling fluid design and equipment [66].

3 ROP MODELLING

Rate of penetration modelling in this thesis is done by using multiple formulas and techniques on relevant drilling data in order to give a good estimate of the ROP. Drilling data from the Norwegian Sea is used to ensure realistic testing of the models. The data is processed to be compatible with the use of Microsoft Excel. In this thesis, the modelling of ROP is based on using coefficients or certain values from neighboring wells to predict the ROP and comparing these with actual data. Thereby attempting to improve the ability to predict the ROP for wells to be drilled close-by an already drilled well. These coefficients and values are attained by use of the models and/or techniques described in this paper.

Drilling data from two fields in the Norwegian Sea is used to verify the accuracy of the models presented in this thesis. Each field is represented by three close-by wells. The drilling data was provided by the Norwegian Petroleum Directorate in the form of "Final Well Report" mud log reports for each well in portable document format (PDF). With the exception of ECD, all the pertinent data are listed for every 5-meter depth. ECD data are derived from its plotted values. The data is processed with Nitro Pro 9 software to Microsoft Excel format. Further structural editing of the data was required to make it compatible for processing with in Microsoft Excel.

Three of the wells are from block 6305/7, better known as part of the Ormen Lange field. Located 120 kilometers north-west of Kristiansund, Ormen Lange is Europe's third largest gas field [67]. The three wells used in this thesis are from the D-template of the Shell operated development, wells 6305/7-D-1 H, 6305/7-D-2 H and 6305/7-D-3 H. These wells were drilled in 2010/2011 at a water depth of 853.8 m MSL, the total depth varied from 2889.8 m to 2896.1 m TVD.

The Statoil operated Morvin field is the location of the other three wells, in block 6506/11. Morvin is a subsea satellite located 200 kilometers offshore from the approximately middle of Norway [68]. The wells used in this thesis are 6506/11-A-1 H, 6506/11-A-2 H and 6506/11-A-3 H, from Template A. These wells were drilled in 2009-2011 with a total depth varying 4466.3 m – 4696.7 m TVD.

Having two areas with three neighboring wells each provides several possibilities for testing the presented methods of predicting ROP. Six wells may each undergo an ROP prediction by each presented method with two separate sets of data by close-by wells. Including two separate locations of well data that will increase the legitimacy of the results.

The method of implementing the techniques and models to predict rates of penetration in this thesis is largely based on the well-to-well correlation procedure. Together with drilling data, coefficients are used to obtain the ROP for a well. These same coefficients are then used together with "planned" drilling data for a close-by well to predict the ROP of this well. It is assumed the neighbor well will experience similar effects from drilling parameters on the ROP. Several techniques are tested in this thesis to determine these coefficients. Multiple regression technique and least square technique are both presented in this thesis to obtain coefficients (3.1 and 3.2). Both the techniques are also tested with the Bourgoyne & Young model (3.3 and 3.4). Two models have been altered to similarly be used to correlate well-to-well. Instead of using a selection of coefficients, a specific value is calculated based on well data and ROP. This value is then used in the same model for a close-by well to calculate the ROP. This procedure is done with a drillability d-exponent model (3.5) and a MSE model (3.6).

3.1 Multiple regression

Multivariate analysis characterizes an observation factor by several variables, taking into account changes of several properties simultaneously. In this thesis, the observation factor (Y) is the rate of penetration. Relevant drilling factors make up the regression variables ($X_{1\text{-}7}$). These data are processed with a regression data analysis in Microsoft Excel. From this analysis, the required coefficients ($b_{0\text{-}7}$) are computed. With these coefficients, it is possible to compute values for the observation factor.

Relevant drilling data for each well is uploaded in each their Microsoft Excel file. The data used for the multiple regression analysis in this thesis is RPM, flow rate, mud weight, formation pressure, bit diameter, WOB and torque, together with the observation factor ROP. Performing the regression data analysis in Microsoft Excel (Figure 4), ROP is input as the Y-area. The remaining data is selected as the X-area. Depth is included only as a reference and is not selected

as part of the analysis. The analysis then provides output data it has computed, where the coefficients are of interest. The first value of coefficients is the intercept (b_0). The following coefficients ($b_{1\text{-}7}$ or "X-variable 1-7") are to be multiplied with the regression variables according to their order (Figure 5). ROP is modelled by equation 3.1.

$$Y = b_0 + b_1 X_1 + b_2 X_2 + b_3 X_3 + b_4 X_4 + b_5 X_5 + b_6 X_6 + b_7 X_7 \quad (3.1)$$

Where the equation becomes as equation 3.2 with Y and $X_{1\text{-}7}$ assigned.

$$ROP = b_0 + b_1\, RPM + b_2\, Flowrate + b_3\, Mudweight + b_4\, FormationPressure + b_5\, BitDiameter + b_6\, WOB + b_7\, Torque \quad (3.2)$$

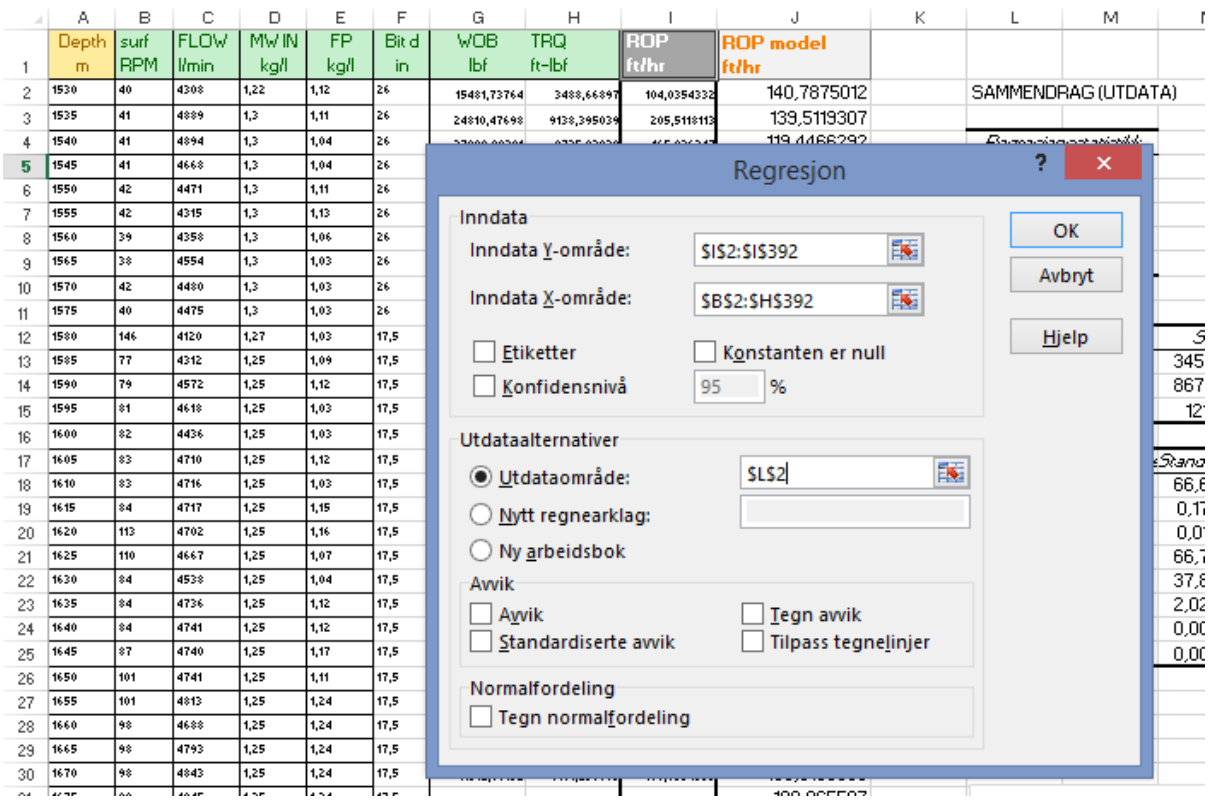

Figure 4: Multiple regression data analysis (Microsoft Excel)

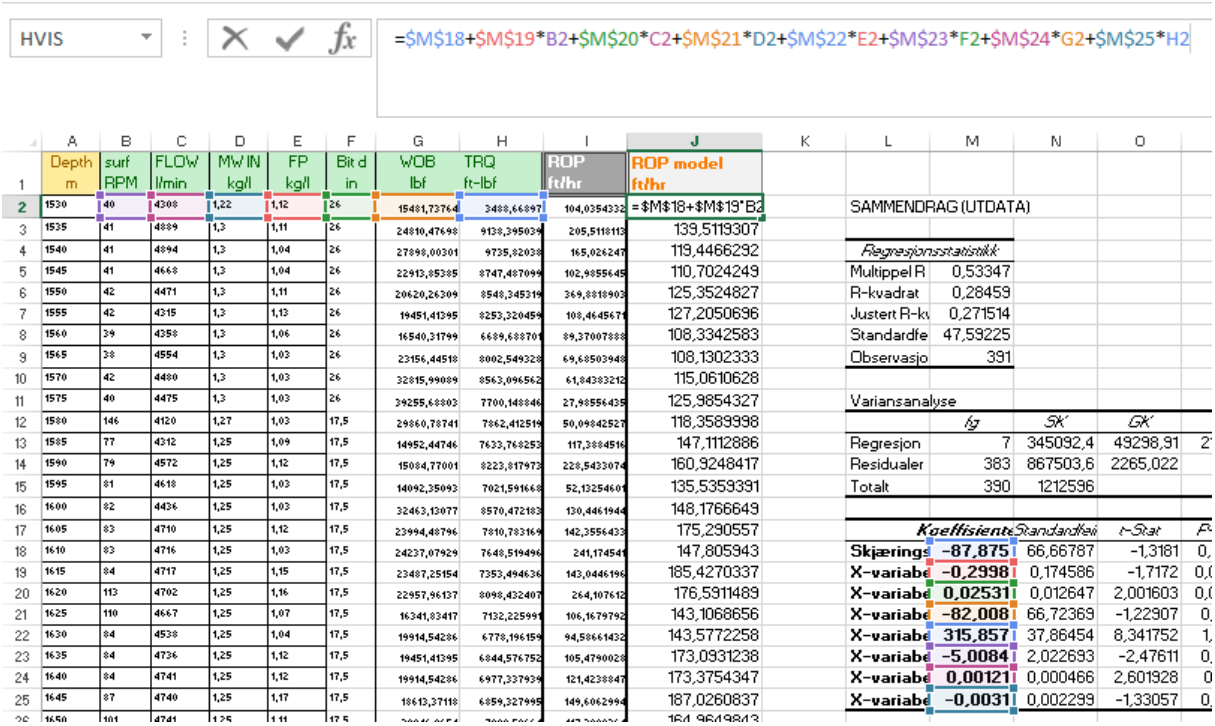

Figure 5: Equation 3.1 applied in Microsoft Excel

In Microsoft Excel, equation 3.3 is used for row two of drilling data. The coefficients are listed from cell Q18 to Q25 and are denoted by a $ sign to keep their value constant for the whole procedure. Cell columns B, C, D, E, F, G and H contain the regression variables, varying with depth intervals by rows. The equation computes the modelled ROP for each row by changing the row reference number.

$$= \$M\$18 + \$M\$19 * B2 + \$M\$20 * C2 + \$M\$21 * D2 + \$M\$22 * E2 + \$M\$23 * F2 + \$M\$24 * G2 + \$M\$25 * H2 \quad (3.3)$$

This multiple regression procedure (Figure 6) is done for each well, providing each with a set of coefficients. Each set of well coefficients is then applied in the model to produce ROP values for the two neighboring wells. With this method, it is possible to predict ROP values of the neighboring wells. All wells are tested with two sets of coefficients, from the two close-by wells. This is accomplished simply by replacing the well's own coefficients with coefficients of a neighbor well. Equation 3.2 can be used with the replaced coefficients to predict the ROP values for the well.

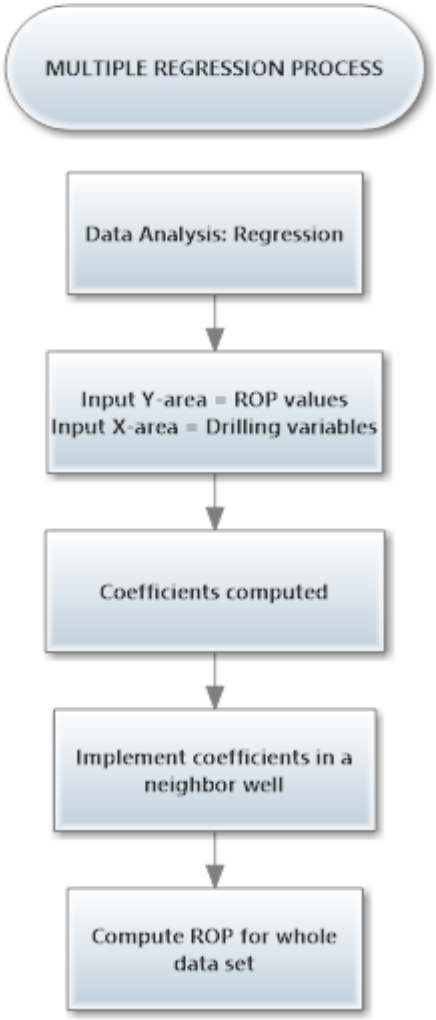

Figure 6: Multiple regression procedure flowchart

3.2 Least square

Least square analysis minimizes the sum of error between an observed factor and a predicted factor by estimating parameters. In this thesis the parameters are the relevant drilling variables available while coefficients are altered to minimize the sum of error between observed and predicted factor. The observed factor (y_i) and the factor to be predicted is the rate of penetration. With the altered coefficients, it is possible to compute the predicted ROP.

The same data used for multiple regression analysis is used in the least square analysis. Error squared between the actual ROP and predicted ROP is conducted for each row of the set of data (figure 7). These are then summed up to give the sum of error squared (figure 8), given by

equation 3.4. The predicted ROP is computed by the equation 3.6, where the coefficients ($b_{0\text{-}7}$) are designed to minimize the sum of error squared. This is done by using Solver Add-inn in Microsoft Excel, to minimize the calculated sum of error squared value, by changing the coefficients.

$$Q = \sum_{i=1}^{n} [y_i - f(x_i; b)]^2 \tag{3.4}$$

The equation can be expressed as equation 3.5 with y_i and $f(x_i;b)$ assigned.

$$Sum\ of\ error\ squared = \sum_{i=1}^{n} \left[ROP_{observed} - ROP_{predicted}\right]^2 \tag{3.5}$$

Where $ROP_{predicted}$ is modelled by equation 3.6.

$$ROP_{predicted} = b_0 + b_1\, RPM + b_2\, Flowrate + b_3\, Mudweight + b_4\, FormationPressure + b_5\, BitDiameter + b_6\, WOB + b_7\, Torque \tag{3.6}$$

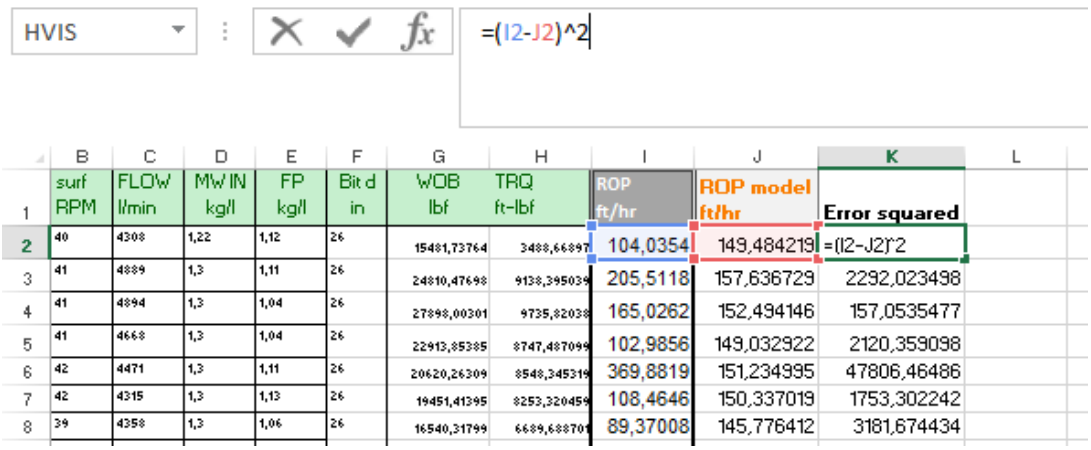

Figure 7: Error squared of least square method

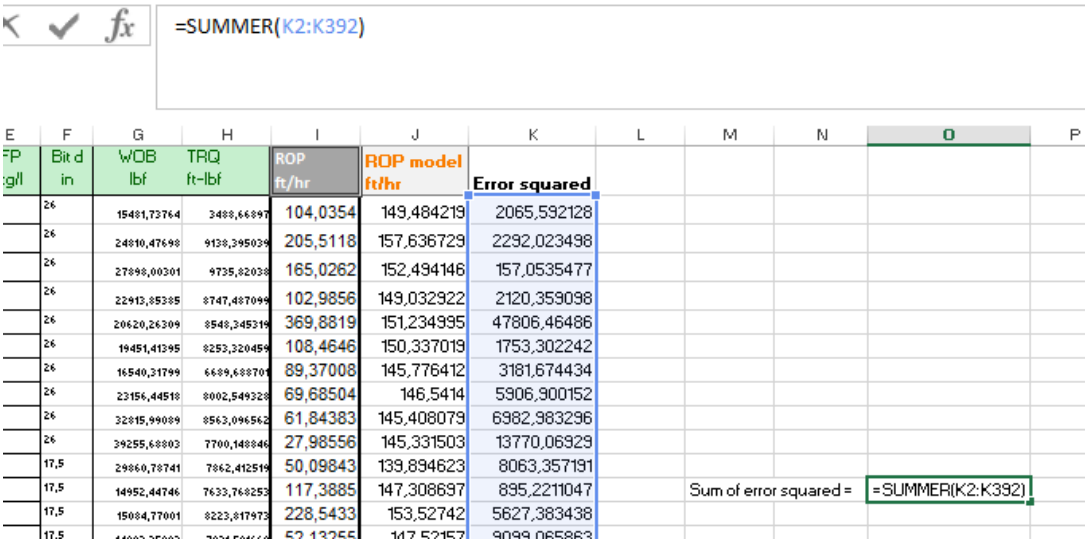

Figure 8: Sum of error squared in least square method

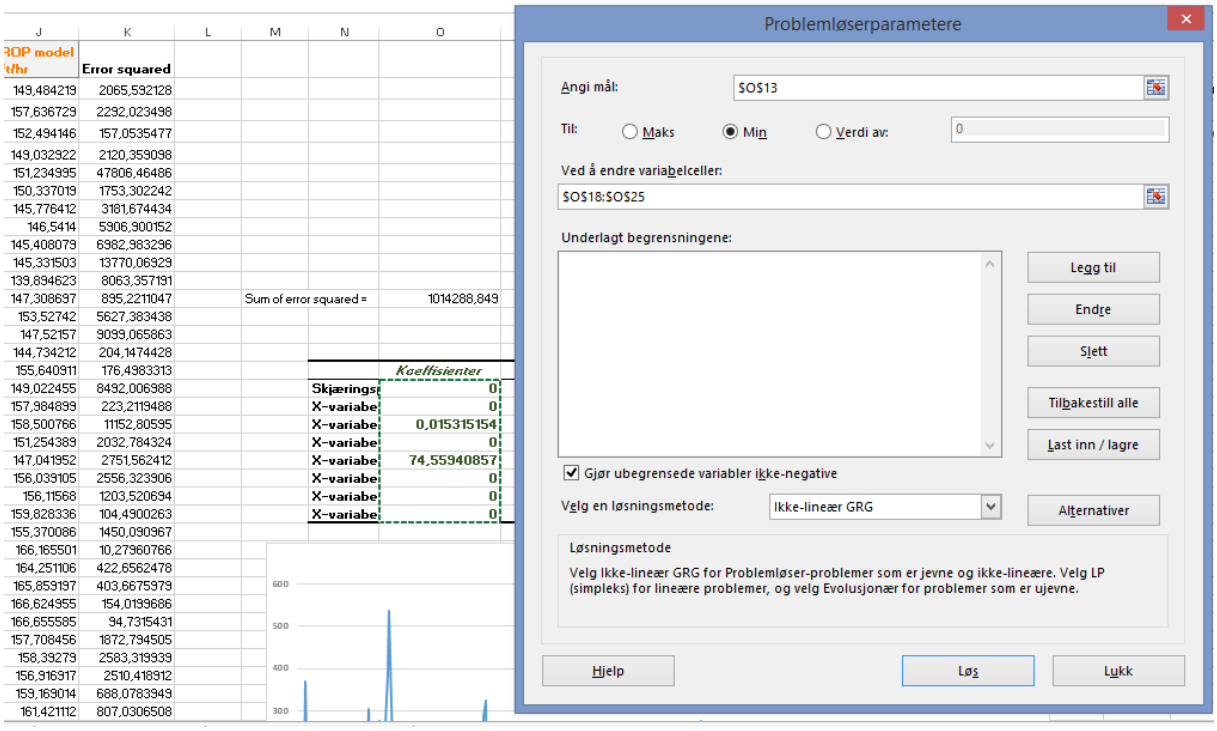

Figure 9: Solver Add-inn in Microsoft Excel

When the new coefficients are computed with the Solver Add-inn (figure 9) to minimize the sum of error squared, they are implemented in equation 3.6 to compute the ROP. This procedure (figure 10) is tested for each of the six well data sets, with the belonging two neighboring wells' least square coefficients.

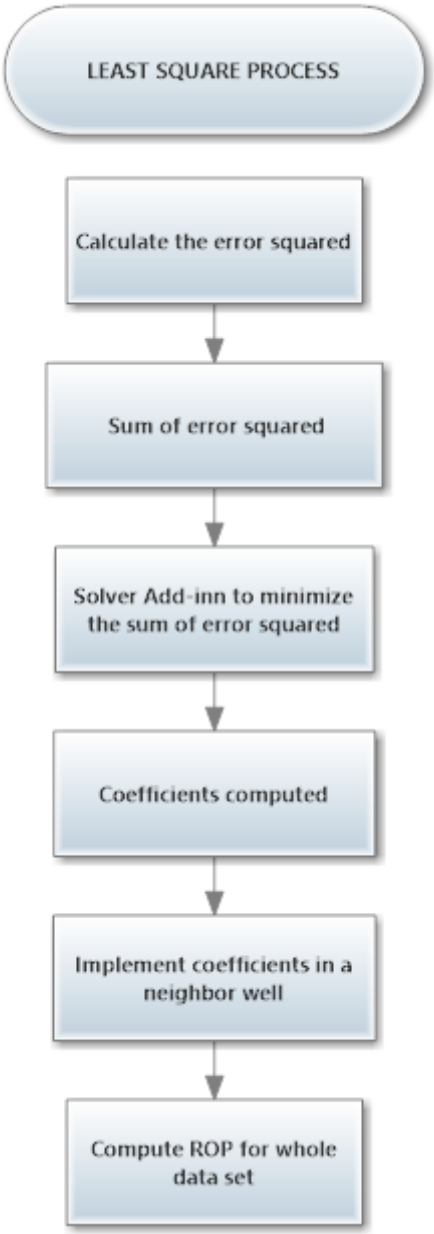

Figure 10: Least square procedure flowchart

3.3 Multiple Regression and Least Square with Bourgoyne & Young model

This rate of penetration model predicts the influence of seven drilling effects ($x_{2\text{-}8}$) on the ROP. In a given formation, this is done by determining eight coefficients ($a_{1\text{-}8}$). The seven drilling effects are given by equations 2.8 through 2.14. These drilling effects together with the coefficients make up the model as equation 2.6. By computing the seven drilling effects and then performing a multiple regression analysis, eight coefficients are achieved with one as an intercept. Bourgoyne & Young's model is given by equation 2.6, used with multiple regression

technique. In the least square technique, the coefficients used in equation 2.6 are designed to minimize the error squared between observed ROP and predicted ROP.

The drilling data available and used for the particular modelling in this thesis is depth, RPM, flow rate, mud weight, formation pressure, bit diameter, WOB, ECD, torque and observed ROP. Depth is converted to feet and flow rate into gallons per minute. Mud weight, formation pressure and ECD are converted to pounds per gallon. These converted values are then ready to be implemented in the equations to determine drilling effects $x_{1\text{-}8}$, as seen in figure 11. The natural logarithm is applied on both sides of the equation to give equation 3.7.

$$\ln ROP = a_1 + a_2 * x_2 + a_3 * x_3 + a_4 * x_4 + a_5 * x_5 + a_6 * x_6 + a_7 * x_7 + a_8 * x_8 \qquad (3.7)$$

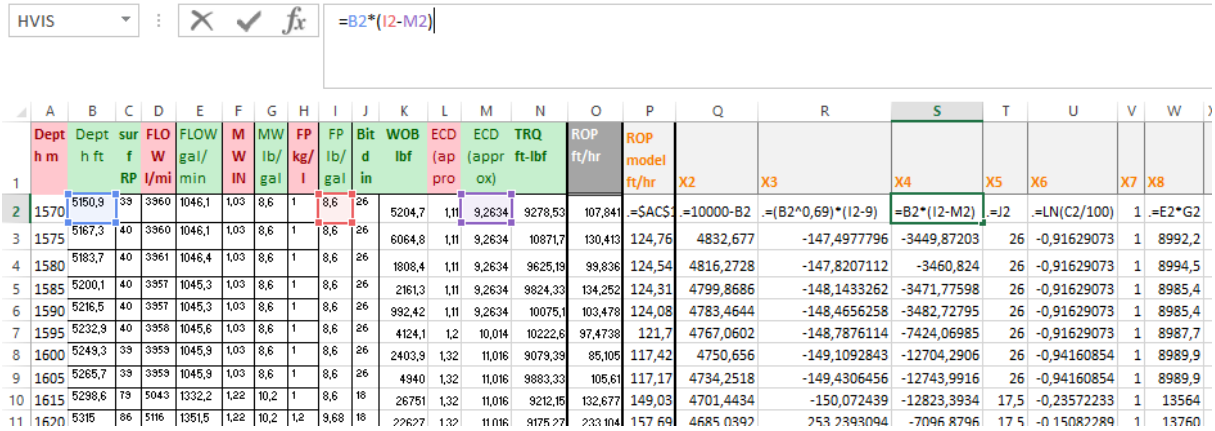

	A	B	C	D	E	F	G	H	I	J	K	L	M	N	O	P	Q	R	S	T	U	V	W
1	Depth m	Depth ft	surf RP	FLOW l/min	FLOW gal/min	MW IN	MW lb/gal	FP kg/l	FP lb/gal	Bit d in	WOB lbf	ECD (apro	ECD (approx)	TRQ ft-lbf	ROP ft/hr	ROP model ft/hr	X2	X3	X4	X5	X6	X7	X8
2	1570	5150,9	39	3960	1046,1	1,03	8,6	1	8,6	26	5204,7	1,11	9,2634	9278,53	107,841	.=$AC$1	.=10000-B2	.=(B2^0,69)*(I2-9)	=B2*(I2-M2)	.=J2	.=LN(C2/100)	1	.=E2*G2
3	1575	5167,3	40	3960	1046,1	1,03	8,6	1	8,6	26	6064,8	1,11	9,2634	10871,7	130,413	124,76	4832,677	-147,4977796	-3449,87203	26	-0,91629073	1	8992,2
4	1580	5183,7	40	3961	1046,4	1,03	8,6	1	8,6	26	1808,4	1,11	9,2634	9625,19	99,836	124,54	4816,2728	-147,8207112	-3460,824	26	-0,91629073	1	8994,5
5	1585	5200,1	40	3957	1045,3	1,03	8,6	1	8,6	26	2161,3	1,11	9,2634	9824,33	134,252	124,31	4799,8686	-148,1433262	-3471,77598	26	-0,91629073	1	8985,4
6	1590	5216,5	40	3957	1045,3	1,03	8,6	1	8,6	26	992,42	1,11	9,2634	10075,1	103,478	124,08	4783,4644	-148,4656258	-3482,72795	26	-0,91629073	1	8985,4
7	1595	5232,9	40	3958	1045,6	1,03	8,6	1	8,6	26	4124,1	1,2	10,014	10222,6	97,4738	121,7	4767,0602	-148,7876114	-7424,06985	26	-0,91629073	1	8987,7
8	1600	5249,3	39	3959	1045,9	1,03	8,6	1	8,6	26	2403,9	1,32	11,016	9079,39	85,105	117,42	4750,656	-149,1092843	-12704,2906	26	-0,94160854	1	8989,9
9	1605	5265,7	39	3959	1045,9	1,03	8,6	1	8,6	26	4940	1,32	11,016	9883,33	105,61	117,17	4734,2518	-149,4306456	-12743,9916	26	-0,94160854	1	8989,9
10	1615	5298,6	79	5043	1332,2	1,22	10,2	1	8,6	18	26751	1,32	11,016	9212,15	132,677	149,03	4701,4434	-150,072439	-12823,3934	17,5	-0,23572233	1	13564
11	1620	5315	86	5116	1351,5	1,22	10,2	1,2	9,68	18	22627	1,32	11,016	9175,27	233,104	157,69	4685,0392	253,2393094	-7096,8796	17,5	-0,15082289	1	13760

Figure 11: Bourgoyne & Young's model drilling effects calculated in Microsoft Excel

With drilling data obtained from the wells it is possible to compute most of the drilling effects ($x_{1\text{-}8}$). However, alterations are necessary as not all data required was available. Drilling effects $x_{1\text{-}3}$ and x_6 are calculated without alterations. Only one of the two groups of wells has sufficient ECD values available needed to compute x_4. The other group of wells have to simply discard this effect. Effect of bit diameter and bit weight (x_5) was altered to only be an effect of bit diameter with equation 3.8. The effect of tooth wear (x_7) was not available. X_8 is simplified to equation 3.9, removing the apparent viscosity and bit nozzle diameter as the data was not available.

$$x_5 = d_{bit} \tag{3.8}$$

$$x_8 = \rho q \tag{3.9}$$

With the drilling effects computed as accurately as possible, the belonging coefficients can be calculated. For the multiple regression method, this is done by regression data analysis, where the X-area input is the drilling effects $x_{1\text{-}8}$. Y-area is the natural logarithm of observed ROP. The coefficients are then applied to the drilling effects of neighboring wells with equation 3.7 to predict the natural logarithm of ROP (figure 12). By applying the exponential on the natural logarithm of ROP, the ROP is found. For the least square method, the coefficients are designed by use of Solver Add-inn to minimize the sum of error squared found by equation 3.5. These coefficients are also so implemented in equation 3.7 for neighboring well data, to predict the ROP. Both overall procedures are shown in figure 13.

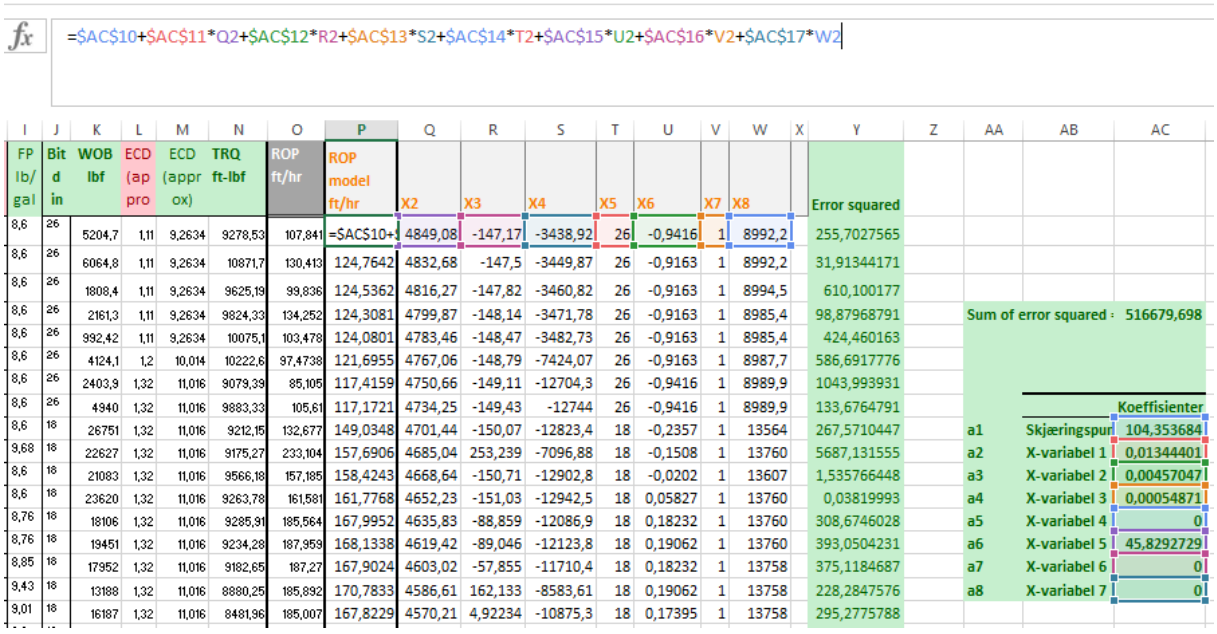

=$AC$10+$AC$11*Q2+$AC$12*R2+$AC$13*S2+$AC$14*T2+$AC$15*U2+$AC$16*V2+$AC$17*W2

FP lb/gal	Bit d in	WOB lbf	ECD (apro	ECD (approx)	TRQ ft-lbf	ROP ft/hr	ROP model ft/hr	X2	X3	X4	X5	X6	X7	X8	Error squared
8,6	26	5204,7	1,11	9,2634	9278,53	107,841	=$AC$10+	4849,08	-147,17	-3438,92	26	-0,9416	1	8992,2	255,7027565
8,6	26	6064,8	1,11	9,2634	10871,7	130,413	124,7642	4832,68	-147,5	-3449,87	26	-0,9163	1	8992,2	31,91344171
8,6	26	1808,4	1,11	9,2634	9625,19	99,836	124,5362	4816,27	-147,82	-3460,82	26	-0,9163	1	8994,5	610,100177
8,6	26	2161,3	1,11	9,2634	9824,33	134,252	124,3081	4799,87	-148,14	-3471,78	26	-0,9163	1	8985,4	98,87968791
8,6	26	992,42	1,11	9,2634	10075,1	103,478	124,0801	4783,46	-148,47	-3482,73	26	-0,9163	1	8985,4	424,460163
8,6	26	4124,1	1,2	10,014	10222,6	97,4738	121,6955	4767,06	-148,79	-7424,07	26	-0,9163	1	8987,7	586,6917776
8,6	26	2403,9	1,32	11,016	9079,39	85,105	117,4159	4750,66	-149,11	-12704,3	26	-0,9416	1	8989,9	1043,993931
8,6	26	4940	1,32	11,016	9883,33	105,61	117,1721	4734,25	-149,43	-12744	26	-0,9416	1	8989,9	133,6764791
8,6	18	26751	1,32	11,016	9212,15	132,677	149,0348	4701,44	-150,07	-12823,4	18	-0,2357	1	13564	267,5710447
9,68	18	22627	1,32	11,016	9175,27	233,104	157,6906	4685,04	253,239	-7096,88	18	-0,1508	1	13760	5687,131555
8,6	18	21083	1,32	11,016	9566,18	157,185	158,4243	4668,64	-150,71	-12902,8	18	-0,0202	1	13607	1,535766448
8,6	18	23620	1,32	11,016	9263,78	161,581	161,7768	4652,23	-151,03	-12942,5	18	0,05827	1	13760	0,03819993
8,76	18	18106	1,32	11,016	9285,91	185,564	167,9952	4635,83	-88,859	-12086,9	18	0,18232	1	13760	308,6746028
8,76	18	19451	1,32	11,016	9234,28	187,959	168,1338	4619,42	-89,046	-12123,8	18	0,19062	1	13760	393,0504231
8,85	18	17952	1,32	11,016	9182,65	187,27	167,9024	4603,02	-57,855	-11710,4	18	0,18232	1	13758	375,1184687
9,43	18	13188	1,32	11,016	8880,25	185,892	170,7833	4586,61	162,133	-8583,61	18	0,19062	1	13758	228,2847576
9,01	18	16187	1,32	11,016	8481,96	185,007	167,8229	4570,21	4,92234	-10875,3	18	0,17395	1	13758	295,2775788

Sum of error squared : 516679,698

		Koeffisienter
a1	Skjæringspur	104,353684
a2	X-variabel 1	0,01344401
a3	X-variabel 2	0,00457047
a4	X-variabel 3	0,00054871
a5	X-variabel 4	0
a6	X-variabel 5	45,8292729
a7	X-variabel 6	0
a8	X-variabel 7	0

Figure 12: Applying coefficients to the drilling effects to produce ROP with equation 3.7

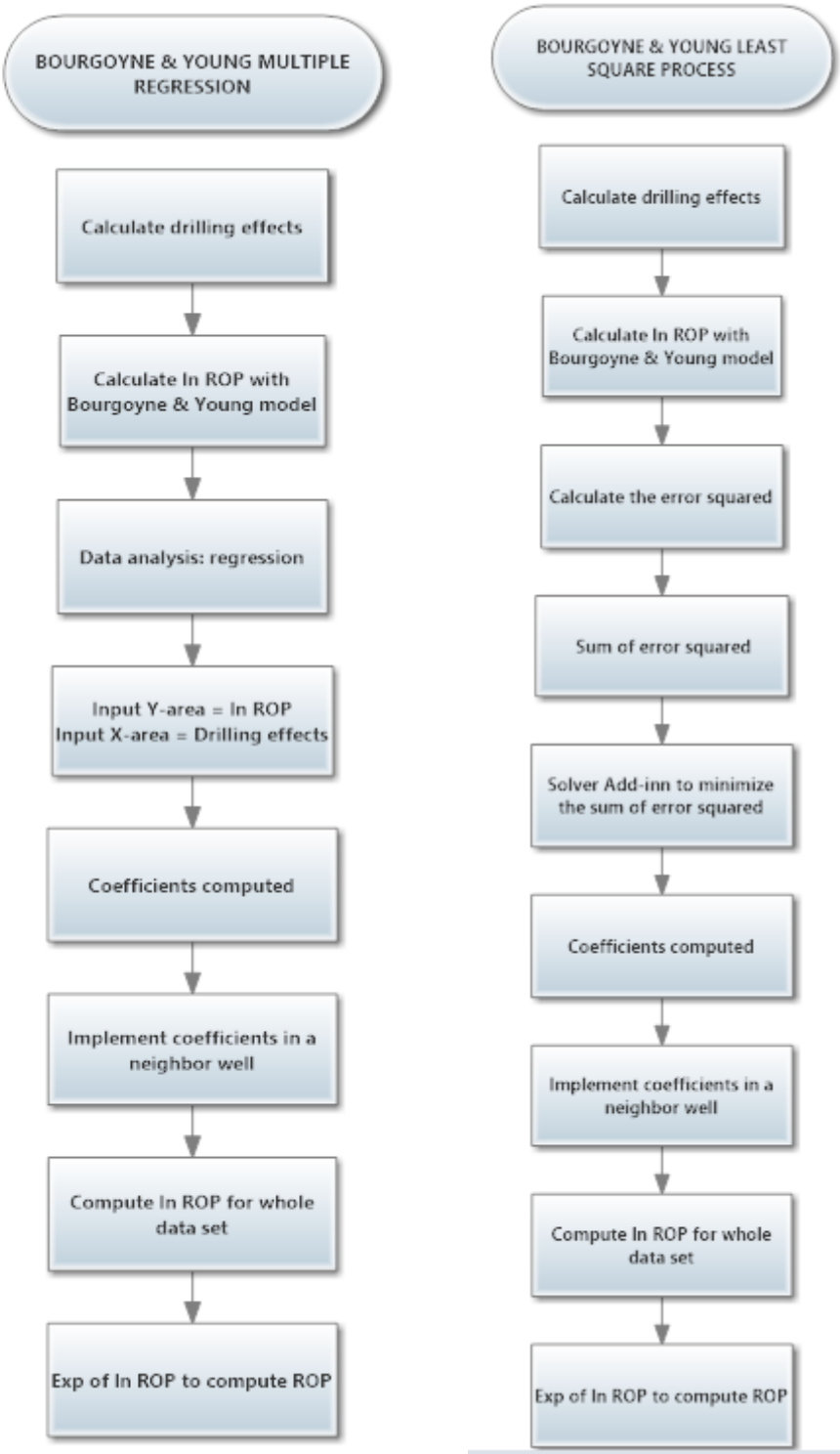

Figure 13: Multiple regression and least square with Bourgoyne & Young's model procedure flowcharts

3.4 D-exponent

The d-exponent normalizes the ROP by taking into account the effects of drillability on the drilling parameters. This drillability d-exponent is given by equation 2.28. A corrected d-exponent value can also be utilized, established by equation 2.29. This corrected d-exponent requires ECD values, which are not available for all wells analyzed in this thesis. Additionally the correction is allegedly without a thorough theoretical basis [58]. Therefore, the normal d-exponent is further developed in this thesis to predict ROP values.

With equation 2.28 as the basis, a technique is developed in this thesis to use the d-exponents of a close-by well to compute ROP. It is assumed that the drillability is correlative within close-by wells. D-exponent values are calculated for a well, with the use of equation 2.28 (figure 14). These d-exponent values are then implemented and used in the close-by wells. Equation 2.28 is developed into equation 3.10, to be able to produce ROP values from d-exponent values from neighboring wells (figure 15). The procedure for this technique is shown in figure 16.

Equation 2.28 → $log\left(\frac{R}{60N}\right) = d * \log\left(\frac{12WOB}{1000d_B}\right)$

→ $\log R - \log 60N = d * log\left(\frac{12WOB}{1000d_B}\right)$ → $\log R = d * log\left(\frac{12WOB}{1000d_B}\right) + \log(60N)$ →

$$R = 10^{d*\log\left(\frac{12WOB}{1000d_B}\right)+\log(60N)} \quad (3.10)$$

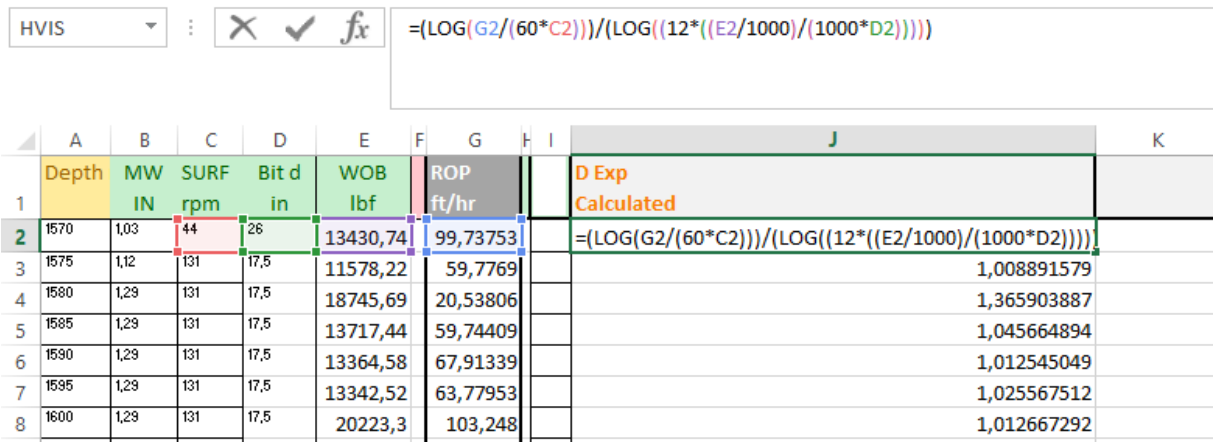

	A	B	C	D	E	F	G	H	I	J	K
1	Depth	MW IN	SURF rpm	Bit d in	WOB lbf		ROP ft/hr			D Exp Calculated	
2	1570	1,03	44	26	13430,74		99,73753			=(LOG(G2/(60*C2)))/(LOG((12*((E2/1000)/(1000*D2)))))	
3	1575	1,12	131	17,5	11578,22		59,7769			1,008891579	
4	1580	1,29	131	17,5	18745,69		20,53806			1,365903887	
5	1585	1,29	131	17,5	13717,44		59,74409			1,045664894	
6	1590	1,29	131	17,5	13364,58		67,91339			1,012545049	
7	1595	1,29	131	17,5	13342,52		63,77953			1,025567512	
8	1600	1,29	131	17,5	20223,3		103,248			1,012667292	

Figure 14: D-exponents calculated in Microsoft Excel

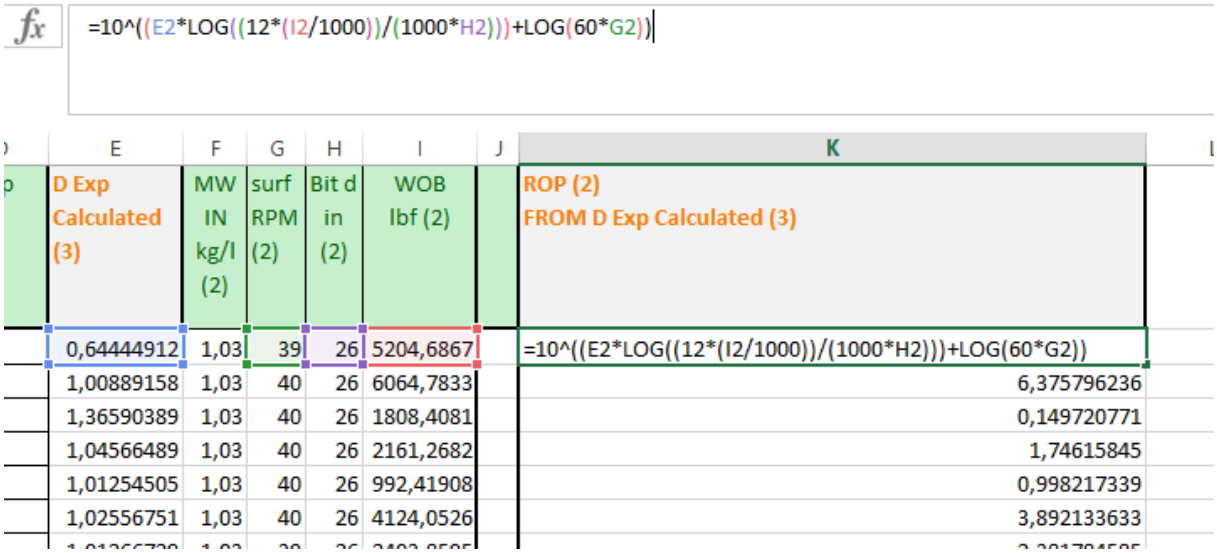

Figure 15: ROP calculated by d-exponents in Microsoft Excel

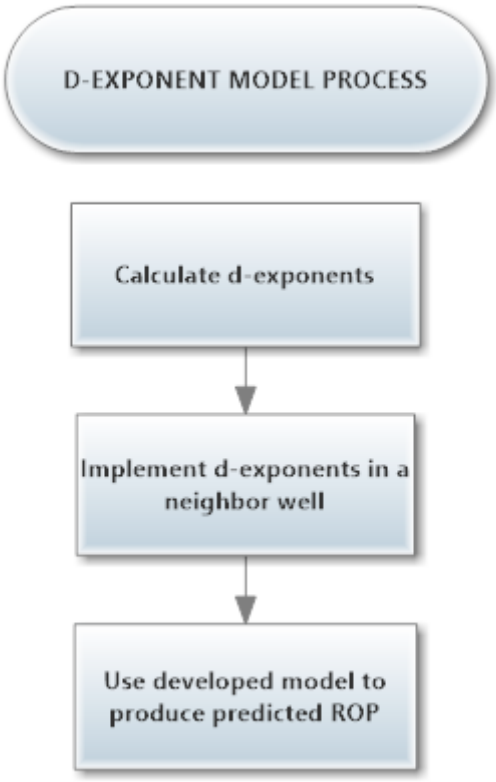

Figure 16: D-exponent model procedure flowchart

3.5 MSE

MSE is the work or energy required to drill a certain amount of rock. This factor was introduced by Teale and can be expressed by equation 3.11. The MSE model is further developed in this thesis to be able to produce ROP values.

$$MSE = \frac{4\,WOB}{1000\,\pi\,D^2} + \frac{480\,RPM\,T}{1000\,ROP\,D^2} \tag{3.11}$$

Where MSE: Mechanical specific energy [Kpsi], WOB: Weight on bit [lbs], D: Bit diameter [in] and T: Torque [ft-lb].

Equation 3.11 is used as the basis to develop a technique in this thesis to use MSE values from a close-by well to compute ROP. It is assumed that the work or energy required to drill a certain amount of rock is correlative within close-by wells. The MSE values are calculated for a well, with the use of equation 3.11 as shown in figure 17. These MSE values are then implemented and used in the close-by wells. Equation 3.11 is developed into equation 3.12, to be able to produce ROP values from MSE computed values from neighboring wells as shown in figure 18. The MSE technique procedure is shown in figure 19.

Equation 3.11 → $MSE * 1000\,D^2 = \frac{4\,WOB}{\pi} + \frac{480\,RPM\,T}{ROP}$

→ $\frac{480\,RPM\,T}{ROP} = MSE\,1000\,D^2 - \frac{4\,WOB}{\pi}$ → $\frac{1}{ROP} = \frac{MSE\,1000\,D^2 - \frac{4\,WOB}{\pi}}{480\,RPM\,T}$ →

$$ROP = \left[\frac{MSE\,1000\,D^2 - \frac{4\,WOB}{\pi}}{480\,RPM\,T}\right]^{-1} \tag{3.12}$$

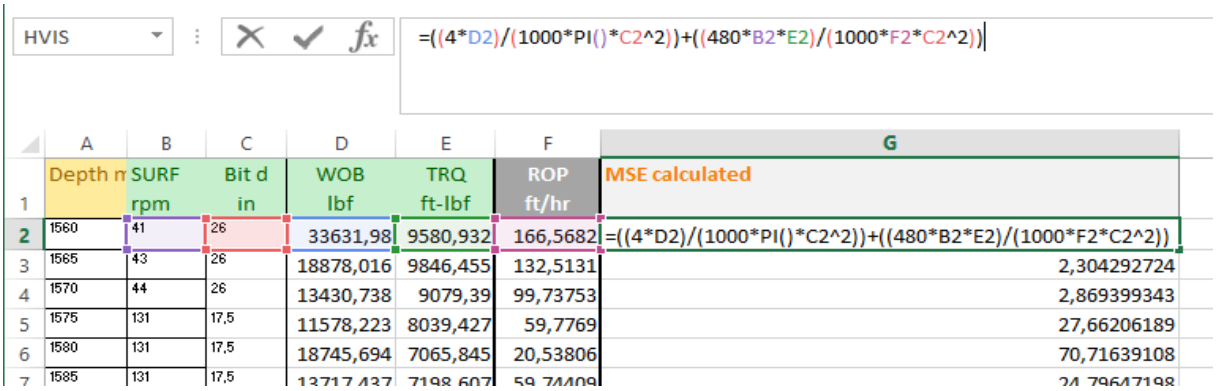

Figure 17: MSE calculated in Microsoft Excel

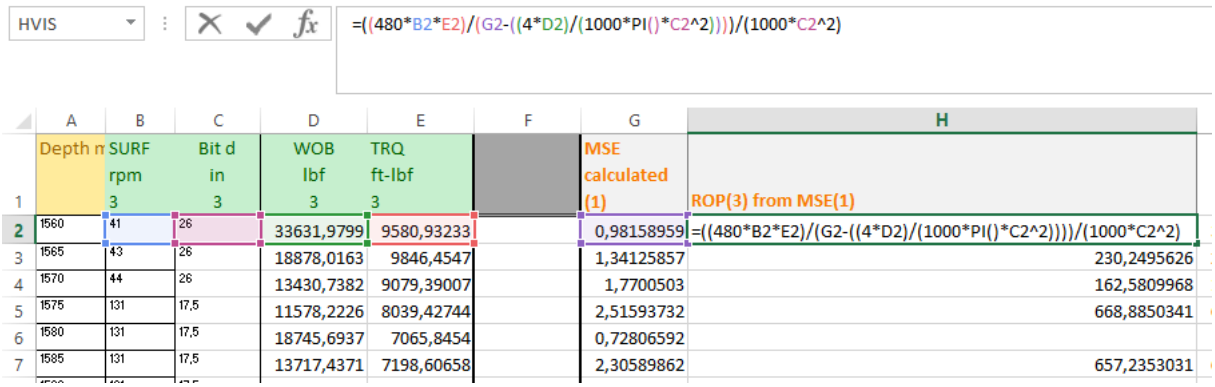

Figure 18: ROP calculated by MSE in Microsoft Excel

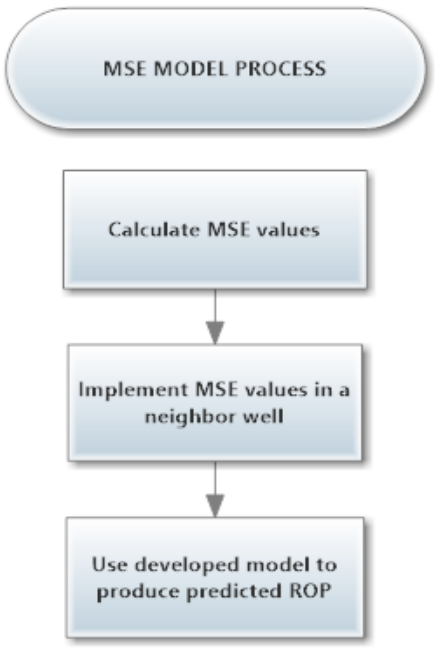

Figure 19: MSE model procedure flowchart

4 ROP MODELLING ANALYSIS

Analysis of the rate of penetration modelling done is conducted in this thesis to better evaluate the results. Using methods within Microsoft Excel, a valid analysis of the results has been successfully produced. The analysis focuses on how well the modelling of ROP correlates with the actual ROP. Two analytical methods are developed in this thesis. With the collaboration of these, it may be possible to select the preferable modelling of the ROP.

The data used in this analysis originates only from the results in this thesis. Only the values of observed and predicted ROP, in addition to the measured depth is implemented in the analysis. By use of statistical essentials such as average and percentages, the analysis provides a clear overview of the results. Comparable overall results are presented, where each method has one average result from all the wells for statistical purposes. This organization is shown in figure 20. Every well has different sets of two neighboring well coefficients applied for the different implemented methods. These results are therefore sorted by the specific method used, and are the analysis of that method with coefficients. In figure 20, "Multiple Regression Coefficients" is the average analysis result of multiple regression technique with the use of coefficients from neighboring wells applied for all wells. "Least Square Coefficients" is the same for least square technique. Both are also presented with the inclusion of Bourgoyne and Young model as "Least Square B&Y Coefficients" and "Multiple Regression B&Y Coefficients". These methods are also included where the coefficients are used on the originating well. For these results, they are only denoted with the method name and are color-coded yellow. The remaining "D-EXP" and "MSE" are averaged results of drillability d-exponent model technique and MSE model technique implemented in all wells.

=F4/$S$4

	E	F	G	H	I	J	K	L	M	N	O	P	Q	R	S
		Multiple Regression	Multiple Regression Coefficients	Least Square	Least Square Coefficients	Least Square B&Y	Least Square B&Y Coefficients	D-EXP	MSE	Multiple Regression B&Y Coefficients	Multiple Regression B&Y				
	deviation:	0,03143802	9,41694129	0,19702731	1,16554984	0,82982064	1,47678006	3,63173413	1,73813529	2,67140672	0,54531936		Average drilling time		13,3149
	% deviation:	=F4/$S$4	0,70724945	0,01479753	0,08753739	0,0623228	0,11091201	0,27275756	0,13054082	0,20063318	0,04095564				
		Multiple Regression	Multiple Regression Coefficients	Least Square	Least Square Coefficients	Least Square B&Y	Least Square B&Y Coefficients	D-EXP	MSE	Multiple Regression B&Y Coefficients	Multiple Regression B&Y				
	deviation:	0,786219033	6,26998571	0,4433712	5,81315276	3,03229195	8,36766666	12,3012475	5,12201525	3,08188924	1,48795292		Average drilling time		37,6786
	% deviation:	0,020866451	0,166407	0,01176718	0,15428253	0,08047779	0,22207997	0,3264782	0,13593957	0,08179411	0,03949064				
	deviation	0,408828527	7,8434635	0,32019925	3,4893513	1,93105629	4,92222336	7,96649081	3,43007527	2,87664798	1,01663614		Average drilling time		25,4967
	% deviation:	0,016034535	0,30762602	0,01255843	0,13685475	0,07573735	0,19305298	0,31245124	0,13452991	0,11282411	0,03987317				

Figure 20: Analysis organization (by field)

4.1 Plot comparison

The analysis by plot comparison aims to identify how well the predicted ROP plot corresponds to the plot of observed ROP. Producing identical plots is highly unlikely, however within a specific margin is achievable. A method is therefore implemented to identify how much of the predicted ROP plot retains within certain margins of the observed plot. Two appropriate margins are selected and used to give a practical analysis.

The selected margins in this thesis are 5 % and 10 % deviation of the observed ROP plot. A margin of 5 % is chosen as it may be considered as very close and a statistical insignificant difference. Values within a deviation of 0 to +/- 5 % are included in this margin. A second margin is introduced to identify plots that are still comparable, but may lack the utmost similar values. This margin is stretched to include 0 to +/- 10 % deviation of the observed ROP plot. Figure (21) presents an example of 5 % and 10 % deviation margins around a target plot. Although the “ROP modelled” plot stays near the “ROP” plot, only limited parts of it manages to plot within the margins. This demonstrates how demanding the margins selected are.

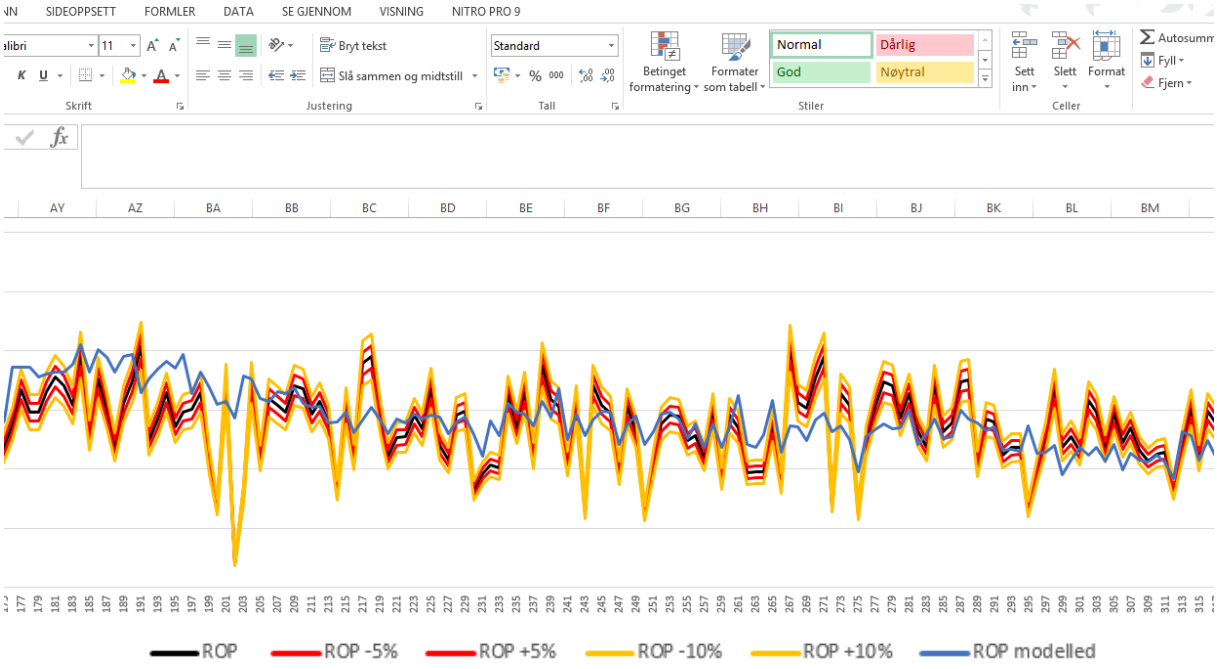

Figure 21: Plot showing 5% and 10% deviation limits

In order to identify the amount of a plot that is within a margin, a method is introduced. This method gives the percentages of the plot within the margin. An increase in the percent of a plot within the margins increases the validity of the method used to generate that plot. To attain the percentages of the plot within the margins, equation 4.1 is created. The equation is applied on all ROP modelled data plots. The equation generates "1" values if the ROP predicted plot is within the given boundaries, and "0" values if not. Finding the average of the resulting values will generate the percentage of plot within the margins, as shown in figure 23. Figure 22 shows how equation 4.1 may be implemented for boundaries of 5 %. Equation 4.1 simply states that if the predicted ROP is between –X % ROP and +X % ROP a value of "1" is generated, if not "0" is generated. In figure 22 "HVIS" is used as this is the Norwegian equivalent to "IF".

$$IF\left(\left(ROP_{predicted}\right) = MEDIAN\left((ROP_{-X\%}):(ROP_{+X\%})\right); 1; 0 \right) \quad \text{.....(4.1)}$$

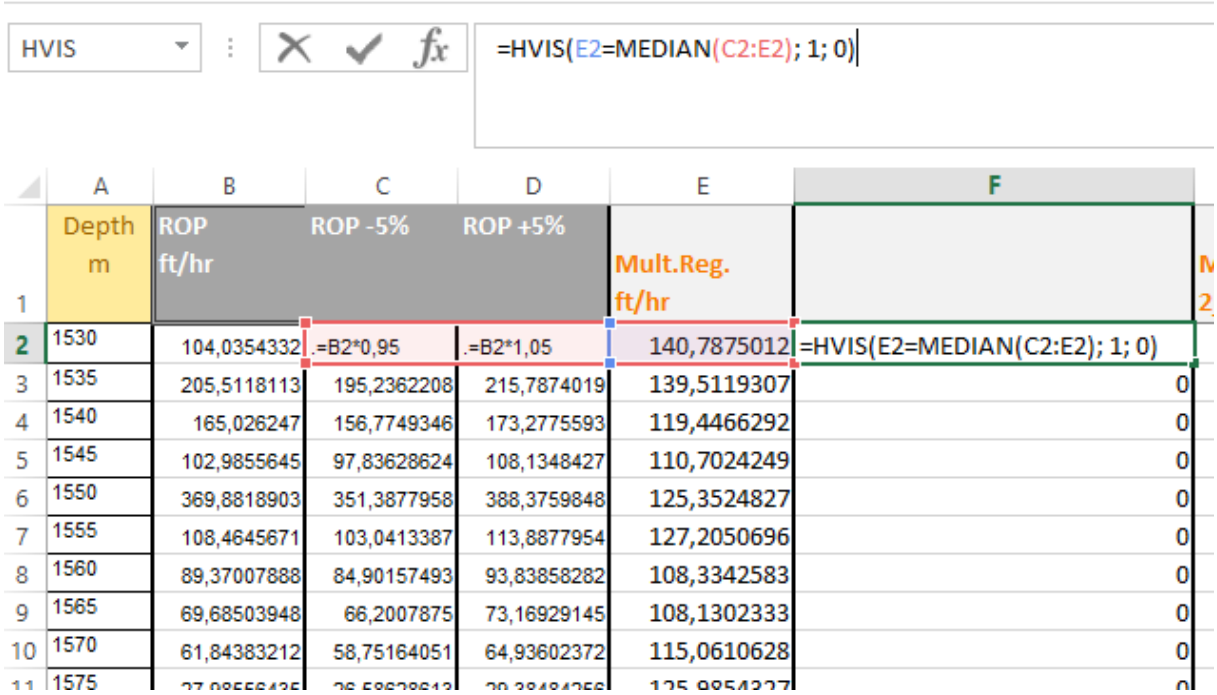

HVIS | =HVIS(E2=MEDIAN(C2:E2); 1; 0)

	A	B	C	D	E	F
1	Depth m	ROP ft/hr	ROP -5%	ROP +5%	Mult.Reg. ft/hr	
2	1530	104,0354332	.=B2*0,95	.=B2*1,05	140,7875012	=HVIS(E2=MEDIAN(C2:E2); 1; 0)
3	1535	205,5118113	195,2362208	215,7874019	139,5119307	0
4	1540	165,026247	156,7749346	173,2775593	119,4466292	0
5	1545	102,9855645	97,83628624	108,1348427	110,7024249	0
6	1550	369,8818903	351,3877958	388,3759848	125,3524827	0
7	1555	108,4645671	103,0413387	113,8877954	127,2050696	0
8	1560	89,37007888	84,90157493	93,83858282	108,3342583	0
9	1565	69,68503948	66,2007875	73,16929145	108,1302333	0
10	1570	61,84383212	58,75164051	64,93602372	115,0610628	0
11	1575					

Figure 22: Equation 4.1 applied in Microsoft Excel

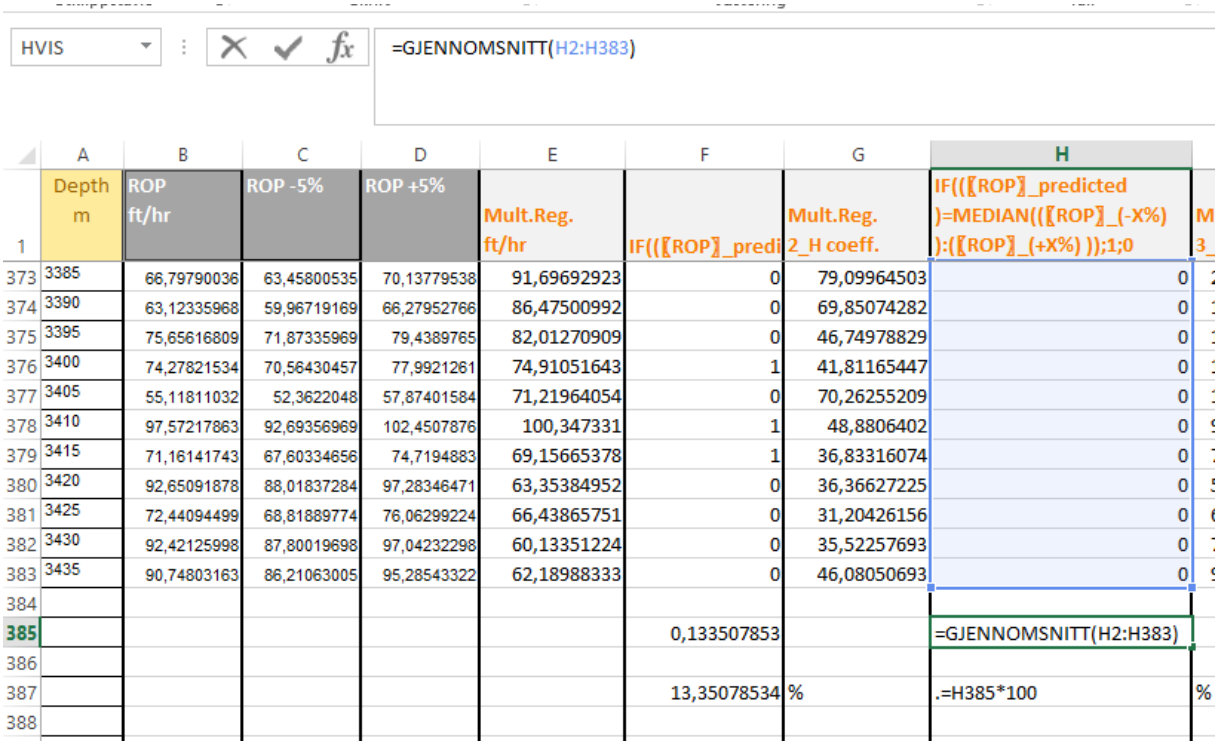

HVIS | =GJENNOMSNITT(H2:H383)

	A	B	C	D	E	F	G	H	
1	Depth m	ROP ft/hr	ROP -5%	ROP +5%	Mult.Reg. ft/hr	IF(([ROP]_predi	Mult.Reg. 2_H coeff.	IF(([ROP]_predicted)=MEDIAN(([ROP]_(-X%)):([ROP]_(+X%)));1;0	M 3_
373	3385	66,79790036	63,45800535	70,13779538	91,69692923	0	79,09964503	0	
374	3390	63,12335968	59,96719169	66,27952766	86,47500992	0	69,85074282	0	
375	3395	75,65616809	71,87335969	79,4389765	82,01270909	0	46,74978829	0	
376	3400	74,27821534	70,56430457	77,9921261	74,91051643	1	41,81165447	0	
377	3405	55,11811032	52,3622048	57,87401584	71,21964054	0	70,26255209	0	
378	3410	97,57217863	92,69356969	102,4507876	100,347331	1	48,8806402	0	
379	3415	71,16141743	67,60334656	74,7194883	69,15665378	1	36,83316074	0	
380	3420	92,65091878	88,01837284	97,28346471	63,35384952	0	36,36627225	0	
381	3425	72,44094499	68,81889774	76,06299224	66,43865751	0	31,20426156	0	
382	3430	92,42125998	87,80019698	97,04232298	60,13351224	0	35,52257693	0	
383	3435	90,74803163	86,21063005	95,28543322	62,18988333	0	46,08050693	0	
384									
385						0,133507853		=GJENNOMSNITT(H2:H383)	
386									
387						13,35078534	%	.=H385*100	%
388									

Figure 23: Finding the average percentage of plot within 5/10 % of ROP in Microsoft Excel

This process is applied for all generated plots of the ROP in each well. The data is first grouped by each well, and then wells are grouped by their field. Figure 24 presents the organization of

data with the wells grouped together within a field. Here it is easy to view the performance of each set of coefficients on each neighboring well. Additionally, the combined performance of each set of coefficients and methods can be organized as shown in figure 25.

Wells 6305											
1	Mult.Reg. ft/hr	Mult.Reg. 1_H coeff.	Mult.Reg. 2_H coeff.	Mult.Reg. 3_H coeff.	Least Squared ft/hr	LeastSquare 1_H coeff.	LeastSquared 2_H coeff.	LeastSquare 3_H coeff.	LS B&Y ft/hr	LS-B&Y 1_H coeff
	0,1335079		0,0706806	0,0209424	0,1649215		0,10209424	0,12565445	0,16492147	
2	Mult.Reg. ft/hr	Mult.Reg. 1_H coeff.	Mult.Reg. 2_H coeff.	Mult.Reg. 3_H coeff.	Least Squared ft/hr	LeastSquare 1_H coeff.	LeastSquare 2_H coeff.	LeastSquare 3_H coeff.	LS B&Y ft/hr	LS-B&Y 1_H coeff
	0,1308901	0,0890052		0,0287958	0,1361257	0,11518325		0,11780105	0,13874346	0,123036
3	Mult.Reg. ft/hr	Mult.Reg. 1_H coeff.	Mult.Reg. 2_H coeff.	Mult.Reg. 3_H coeff.	Least Squared ft/hr	LeastSquare 1_H coeff.	LeastSquare 2_H coeff.	LeastSquare 3_H coeff.	LS B&Y ft/hr	LS-B&Y 1_H coeff
	0,117801	0,0680628	0,0628272		0,078534	0,07853403	0,05759162		0,08115183	0,115183

Figure 24: Plot analysis organization (by well)

METHODS COMPARED		MULT.REG.				LEAST SQR				LS B&Y				
		0				0				0				
		0,382199				0,3795812				0,38482				
		0,382199				0,3795812				0,38482				
COEFF. COMPARED	1H		Mult.Reg. 1_H coeff.				Least Square 1_H coeff.				LS-B&Y 1_H coeff.			D Exp 1_H D-Exp
			0				0				0			0
			0,157068				0,1937173				0,2382199			0,11518325
			0,157068				0,1937173				0,2382199			0,11518325
Average:			0,078534				0,0968586				0,1191099			0,05759162
COEFF. COMPARED	2H			Mult.Reg. 2_H coeff.				Least Square 2_H coeff.				LS-B&Y 2_H coeff.		D Exp 2_H I
				0				0				0		
				0,1335079				0,1596859				0,2041885		0,1
				0,1335079				0,1596859				0,2041885		0,1
Average:				0,0667539				0,0798429				0,1020942		0,0
COEFF. COMPARED	3H				Mult.Reg. 3_H coeff.				Least Square 3_H coeff.				LS-B&Y 3_H coeff.	
					0				0				0	
					0,0497382				0,243455				0,2303665	
					0,0497382				0,243455				0,2303665	
Average:					0,0248691				0,121728				0,1151832	

Figure 25: Plot analysis organization (by coefficient set)

Finally, all results with corresponding margins are organized by the method. Where the results of coefficients applied in neighboring wells from the same method are combined. First within each field as in figure 26, then all wells together as in figure 27.

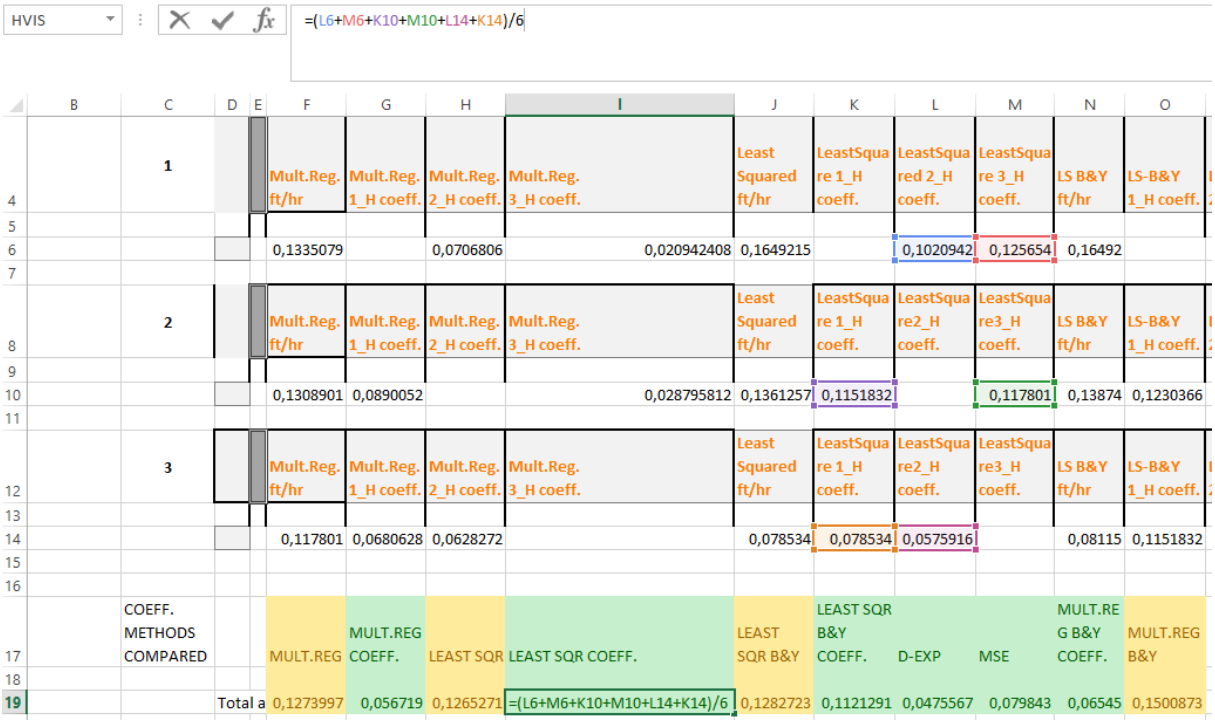

Figure 26: Plot nalysis organization (by each field)

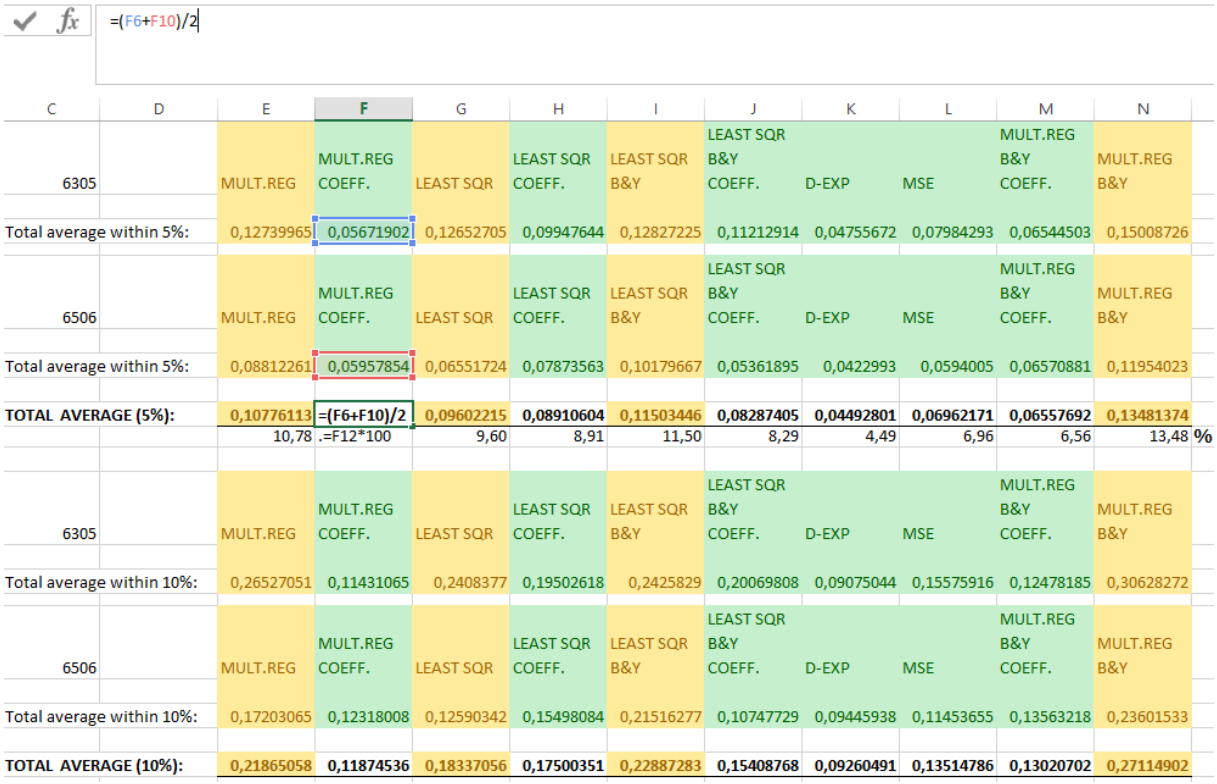

C	D	E	F	G	H	I	J	K	L	M	N
6305		MULT.REG	MULT.REG COEFF.	LEAST SQR	LEAST SQR COEFF.	LEAST SQR B&Y	LEAST SQR B&Y COEFF.	D-EXP	MSE	MULT.REG B&Y COEFF.	MULT.REG B&Y
Total average within 5%:		0,12739965	0,05671902	0,12652705	0,09947644	0,12827225	0,11212914	0,04755672	0,07984293	0,06544503	0,15008726
6506		MULT.REG	MULT.REG COEFF.	LEAST SQR	LEAST SQR COEFF.	LEAST SQR B&Y	LEAST SQR B&Y COEFF.	D-EXP	MSE	MULT.REG B&Y COEFF.	MULT.REG B&Y
Total average within 5%:		0,08812261	0,05957854	0,06551724	0,07873563	0,10179667	0,05361895	0,0422993	0,0594005	0,06570881	0,11954023
TOTAL AVERAGE (5%):		**0,10776113**	**=(F6+F10)/2**	**0,09602215**	**0,08910604**	**0,11503446**	**0,08287405**	**0,04492801**	**0,06962171**	**0,06557692**	**0,13481374**
		10,78	.=F12*100	9,60	8,91	11,50	8,29	4,49	6,96	6,56	13,48 %
6305		MULT.REG	MULT.REG COEFF.	LEAST SQR	LEAST SQR COEFF.	LEAST SQR B&Y	LEAST SQR B&Y COEFF.	D-EXP	MSE	MULT.REG B&Y COEFF.	MULT.REG B&Y
Total average within 10%:		0,26527051	0,11431065	0,2408377	0,19502618	0,2425829	0,20069808	0,09075044	0,15575916	0,12478185	0,30628272
6506		MULT.REG	MULT.REG COEFF.	LEAST SQR	LEAST SQR COEFF.	LEAST SQR B&Y	LEAST SQR B&Y COEFF.	D-EXP	MSE	MULT.REG B&Y COEFF.	MULT.REG B&Y
Total average within 10%:		0,17203065	0,12318008	0,12590342	0,15498084	0,21516277	0,10747729	0,09445938	0,11453655	0,13563218	0,23601533
TOTAL AVERAGE (10%):		**0,21865058**	**0,11874536**	**0,18337056**	**0,17500351**	**0,22887283**	**0,15408768**	**0,09260491**	**0,13514786**	**0,13020702**	**0,27114902**

Figure 27: Plot analysis organization (overall)

4.2 Time comparison

The analysis by time comparison aims to investigate how well the total drilling time of the estimated ROP compares with the actual drilling time derived from the observed ROP. This analysis promotes methods that might not estimate ROP plots well, but can still determine a good overall drilling time estimate. Results of this analysis simply state the amount and percentages of time deviation of the predicted ROP time.

ROP modelling results are given as rate of penetration in feet per hour. As the amount of feet or depth drilled is also available, it is simple to derive the time or hours drilled by equation 4.2. Initially all predicted ROP results are averaged for each method tested on each well, as in figure 28. These ROP values are then used in the equation 4.2 together with the depth interval for the ROP values. As a result, predicted time for each method is revealed (figure 29).

$$time_{drilled} = \frac{depth_{drilled}}{ROP} \tag{4.2}$$

HVIS | =GJENNOMSNITT(E2:E383)

	A	B	C	D	E	F	G
1	Depth m	Depth ft	ROP ft/hr	Mult.Reg. ft/hr	Multiple Regression 2_H coeff.	Mult.Reg. 3_H coeff.	LeastSquar ft/hr
371	3375	11072,835	31,33202105	91,87156531	117,2427448	381,4281195	114,6963
372	3380	11089,2392	55,7086615	102,229589	95,28272964	311,9616059	114,4569
373	3385	11105,6434	66,79790036	91,69692923	79,09964503	230,3976693	114,9929
374	3390	11122,0476	63,1233597	86,47500992	69,85074282	188,8652718	114,9470
375	3395	11138,4518	75,6561681	82,01270909	46,74978829	124,4802999	114,7172
376	3400	11154,856	74,2782153	74,91051643	41,81165447	108,8538099	114,7172
377	3405	11171,2602	55,1181103	71,21964054	70,26255209	183,7859337	113,9208
378	3410	11187,6644	97,5721786	100,347331	48,8806402	97,88374201	118,8845
379	3415	11204,0686	71,1614174	69,15665378	36,83316074	73,18955381	112,174
380	3420	11220,4728	92,6509188	63,35384952	36,36627225	58,82807634	112,1895
381	3425	11236,877	72,440945	66,43865751	31,20426156	63,90101345	112,1895
382	3430	11253,2812	92,42126	60,13351224	35,52257693	72,92728842	112,1895
383	3435	.=A383*3,28084	90,7480316	62,18988333	46,08050693	98,93565613	112,1895
384							
385	1905	.=SUMMER(B383-B2)	154,822405	155,4078207	=GJENNOMSNITT(E2:E383)	49,98418515	155,51
386							
387							
388							
389							

Figure 28: Predicted ROP averaged in Microsoft Excel

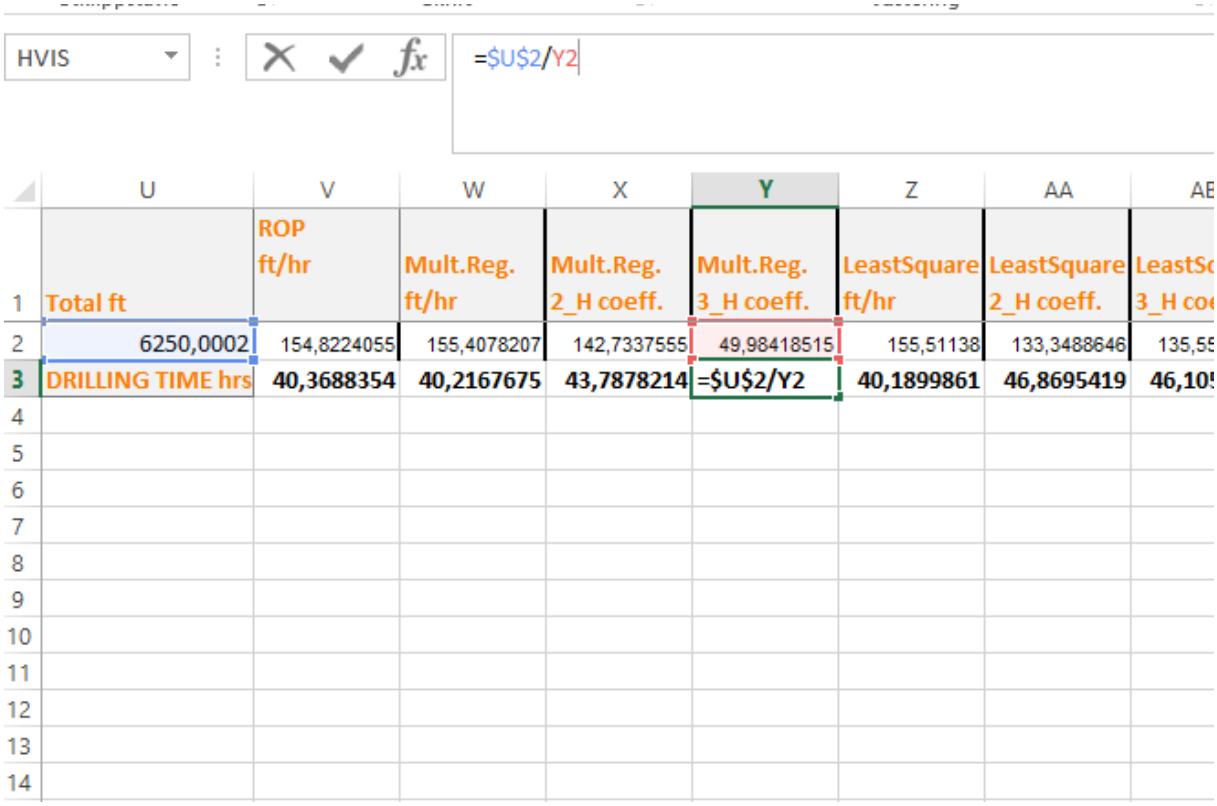

Figure 29: Equation 4.2 applied in Microsoft Excel

These data are then organized with the wells grouped by their field as shown in figure 30. Here the deviation from the actual drilling time is also computed. Further to this the combined estimates of each method and sets of coefficients within the wells of each field are organized as presented in figure 31. By organizing the data in such ways, it is easier to determine if the method's results are consistent. One method may have six results giving just a satisfactory average result, when in fact it has five very good results and one unfortunate weak. Further investigation may strengthen the reliability of such a method.

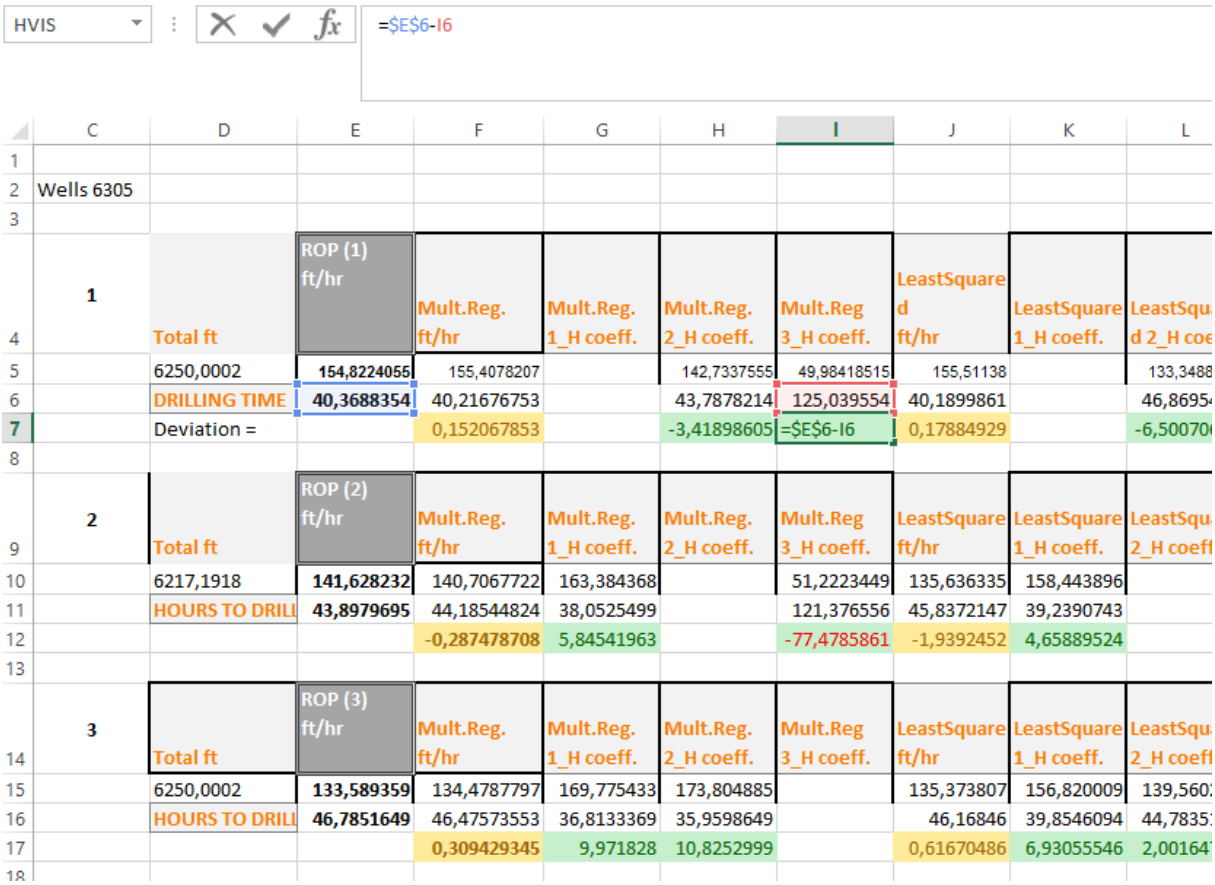

	C	D	E	F	G	H	I	J	K	L
1										
2	Wells 6305									
3										
4	1	Total ft	ROP (1) ft/hr	Mult.Reg. ft/hr	Mult.Reg. 1_H coeff.	Mult.Reg. 2_H coeff.	Mult.Reg 3_H coeff.	LeastSquared ft/hr	LeastSquare 1_H coeff.	LeastSqu d 2_H coe
5		6250,0002	154,8224055	155,4078207		142,7337555	49,98418515	155,51138		133,3488
6		DRILLING TIME	40,3688354	40,21676753		43,7878214	125,039554	40,1899861		46,8695
7		Deviation =		0,152067853		-3,41898605	=$E$6-I6	0,17884929		-6,50070
8										
9	2	Total ft	ROP (2) ft/hr	Mult.Reg. ft/hr	Mult.Reg. 1_H coeff.	Mult.Reg. 2_H coeff.	Mult.Reg 3_H coeff.	LeastSquare ft/hr	LeastSquare 1_H coeff.	LeastSqu 2_H coef
10		6217,1918	141,628232	140,7067722	163,384368		51,2223449	135,636335	158,443896	
11		HOURS TO DRILL	43,8979695	44,18544824	38,0525499		121,376556	45,8372147	39,2390743	
12				-0,287478708	5,84541963		-77,4785861	-1,9392452	4,65889524	
13										
14	3	Total ft	ROP (3) ft/hr	Mult.Reg. ft/hr	Mult.Reg. 1_H coeff.	Mult.Reg. 2_H coeff.	Mult.Reg 3_H coeff.	LeastSquare ft/hr	LeastSquare 1_H coeff.	LeastSqu 2_H coef
15		6250,0002	133,589359	134,4787797	169,775433	173,804885		135,373807	156,820009	139,560
16		HOURS TO DRILL	46,7851649	46,47573553	36,8133369	35,9598649		46,16846	39,8546094	44,7835
17				0,309429345	9,971828	10,8252999		0,61670486	6,93055546	2,00164
18										

Figure 30: Time analysis organization (by well)

	C	D	E	F	G	H	I	J	K	L	M
20	METHODS COMPARED		TOTAL ROP	MULT.REG.				LEAST SQR			
21			430,039996	430,5933727				426,521522			
22			131,05197	130,8779513				132,195661			
23				0,17401849				-1,14369105			
24											
25	COEFF. COMPARED	1H	TOTAL 1H ROP		Mult.Reg. 1_H coeff.				LeastSquare 1_H coeff.		
26			275,217591		333,1598				315,263905		
27			90,6831344		74,8658868				79,0936837		
28					15,8172476				11,5894507		
29		Average:			7,90862381				5,79472535		
30	COEFF. COMPARED	2H	TOTAL 2H ROP			Mult.Reg. 2_H coeff.				LeastSquare 2_H coeff.	
31			288,411765			316,538641				272,909143	
32			87,1540003			79,7476864				91,6530596	
33						7,40631388				-4,49905932	
34		Average:				3,70315694				-2,24952966	
35	COEFF. COMPARED	3H	TOTAL 3H ROP				Mult.Reg. 3_H coeff.				LeastSquare 3_H coeff.
36			296,450637				101,20653				273,667283
37			84,2668049				246,416109				91,1221902
38							-162,149304				-6,85538527
39		Average:					-81,0746522				-3,42769263

Figure 31: Time analysis organization (by coefficient set)

Finally, all results are averaged by the method. Where the results of coefficients applied in neighboring wells are combined to one average for each method. First within each field as in figure 32, then all wells together as in figure 33. In the final results also the percentages deviation from the actual drilling time is calculated. This gives a more realistic and comparable evaluation of the results.

HVIS =(-H7-I7+G12-I12+G17+H17)/6

	C	D	E	F	G	H	I	J	K	L	M	N
4	1	Total ft	ROP (1) ft/hr	Mult.Reg. ft/hr	Mult.Reg. 1_H coeff.	Mult.Reg. 2_H coeff.	Mult.Reg 3_H coeff.	LeastSquared ft/hr	LeastSquare 1_H coeff.	LeastSquare d 2_H coeff.	LeastSquare 3_H coeff.	LS B&Y ft/hr
5		6250,0002	154,8224055	155,4078207		142,7337555	49,98418515	155,51138		133,3488646	135,5582036	148,6
6		DRILLING TIME	40,3688354	40,21676753		43,7878214	125,0395536	40,1899861		46,8695419	46,1056582	42,05
7		Deviation =		0,152067853		-3,41898605	-84,6707183	0,17884929		-6,50070652	-5,7368228	-1,689
8												
9	2	Total ft	ROP (2) ft/hr	Mult.Reg. ft/hr	Mult.Reg. 1_H coeff.	Mult.Reg. 2_H coeff.	Mult.Reg 3_H coeff.	LeastSquare ft/hr	LeastSquare 1_H coeff.	LeastSquare 2_H coeff.	LeastSquare 3_H coeff.	LS B&Y ft/hr
10		6217,1918	141,628232	140,7067722	163,384368		51,22234493	135,636335	158,443896		138,10908	135,1
11		HOURS TO DRILL	43,8979695	44,18544824	38,0525499		121,3765556	45,8372147	39,2390743		45,016532	45,99
12				-0,287478708	5,84541963		-77,4785861	-1,9392452	4,65889524		-1,11856247	-2,097
13												
14	3	Total ft	ROP (3) ft/hr	Mult.Reg. ft/hr	Mult.Reg. 1_H coeff.	Mult.Reg. 2_H coeff.	Mult.Reg 3_H coeff.	LeastSquare ft/hr	LeastSquare 1_H coeff.	LeastSquare 2_H coeff.	LeastSquare 3_H coeff.	LS B&Y ft/hr
15		6250,0002	133,589359	134,4787797	169,775433	173,804885		135,373807	156,820009	139,560279		122,1
16		HOURS TO DRILL	46,7851649	46,47573553	36,8133369	35,9598649		46,16846	39,8546094	44,7835177		51,16
17				0,309429345	9,971828	10,8252999		0,61670486	6,93055546	2,00164721		-4,380
18												
19	COEFF. METHODS COMPARED			MULT.REG	MULT.REG COEFF.	LEAST SQR	LEAST SQR COEFF.	LEAST SQR B&Y	LEAST SQR B&Y COEFF.	D-EXP	MSE	MULT.F B&Y COEFF.
20												
21		Total average deviation:		0,249658635	=(-H7-I7+G12	0,91159979	4,491198284	2,72250874	4,8450791	13,0864647	4,60698631	8,764

Figure 32: Time analysis organization (by field)

HVIS =(F4+F9)/2

	C	D	E	F	G	H	I	J	K	L	M	N	O	P	Q	R	S
2	6305	COEFF. METHODS COMPARED		Multiple Regression	Multiple Regression Coefficients	Least Square	Least Square Coefficients	Least Square B&Y	Least Square B&Y Coefficients	D-EXP	MSE	Multiple Regression B&Y Coefficients	Multiple Regression B&Y				
4		6305 average deviation:		0,24965864	32,0351397	0,9116	4,49119828	2,7225	4,8450791	13,086	4,61	8,76445803	1,7891056		Average actual drilling hrs		43,68
6			% deviation:	.=F4/$$4	0,73333823	0,0209	0,10281108	0,0623	0,11091201	0,2996	0,11	0,20063318	0,0409556				
7	6506	COEFF. METHODS COMPARED		Multiple Regression	Multiple Regression Coefficients	Least Square	Least Square Coefficients	Least Square B&Y	Least Square B&Y Coefficients	D-EXP	MSE	Multiple Regression B&Y Coefficients	Multiple Regression B&Y				
9		6506 average deviation:		2,58155442	21,8574419	1,4546	20,325637	9,9485	27,4529755	40,358	25,4	10,2813329	4,8817354		Average actual drilling hrs		.=G20
11			% deviation:	.=F9/$$9	.=G9/$$9	.=H9/$$	.=I9/$$9	.=J9/$$	.=K9/$$9	.=L9/$$	.=M9/	.=N9/$$9	.=O9/$$9				
13	ALL	Total average deviation		=(F4+F9)/2	26,9462908	1,1831	12,4084176	6,3355	16,1490273	26,722	15	**9,52289546**	3,3354205			Total average	83,65
15			% deviation:	.=F13/$$13	0,32212848	0,0141	0,14833599	0,0757	0,19305298	0,3195	0,18	0,11384112	0,0398732				
16			**%**	.=F15*100	32,21	1,41	14,83	7,57	19,31	31,95	17,92	11,38	3,99		**%**		
18	Actual drilling hrs		well 6506-1:	135,076229													
19			well 6506-2:	107,136787	Average 6506 wells drilling hrs												
20			well 6506-3:	128,639542	**.=GJENNOMSNITT(F18:F20)**			Total average drilling hrs									
21			well 6305-1:	40,3688354				**83,651**									
22			well 6305-2:	43,8979695	Average 6305 wells drilling hrs												
23			well 6305-3:	46,7851649	**43,6839899**												

Figure 33: Time analysis organization (overall)

5 RESULTS & DISCUSSION

This part presents the results and discussion. The results are presented by plots of the modelled ROP. The plots of the modelled ROP by use of neighboring well coefficients or values are colored grey. In all the plots, the actual ROP plot accompanies the modelled ROP plot. This actual ROP is considered the reference plot and colored blue. For all plots in this thesis, the y-axis has ROP values in feet per hour and the x-axis represents depth in meters. Interpreting the coefficients by themselves is determined unnecessary, because there is limited correlation between the sets of coefficients within the same field area. If anything, the coefficient sets differ vastly from each other. The hypothesis is however that the coefficient sets will be applicable in the close-by wells.

Sections 5.1-5.4 are results derived from obtaining and implementing coefficients from neighboring wells to determine a prediction for the ROP. The resulting ROP prediction by use of these coefficients are available on the following pages. The first resulting plots are from testing the coefficients in their originating well. These modelled ROP plots are colored orange. Further on the main results are displayed, where the coefficients are implemented for their neighboring wells.

Sections 5.5 and 5.6 are the results from application of specific values from neighboring wells to determine a prediction for the ROP. These specific values are first compared with the corresponding values in the well they are to be used in. The hypothesis is that these close-by wells will have correlating values. The resulting ROP predictions by use of the specific neighboring values are then calculated. Also here the modelled ROP plot is colored grey, while the actual ROP is colored blue.

Outcomes from the analysis of the results are presented in sections 5.7 and 5.8. Both plot compared and time compared analysis of the results are displayed in percentages. This provides relatable and comparable results for determining the validity of the different methods. Analysis of the results from each method from each well applied on each of its neighboring wells is provided.

5.1 Multiple Regression

The results from using the multiple regression technique are available in this section. Calculated coefficients of each of the six wells are presented in tables 1 to 6.

6305-7-D-1	*Coefficients*
Intercept	-87,8750911
X-variabel 1	-0,2997981
X-variabel 2	0,02531424
X-variabel 3	-82,0078713
X-variabel 4	315,856596
X-variabel 5	-5,0084196
X-variabel 6	0,00121308
X-variabel 7	-0,00305867

1

6305-7-D-2	*Coefficients*
Intercept	18,2763422
X-variabel 1	-0,65968705
X-variabel 2	-0,00296188
X-variabel 3	168,446659
X-variabel 4	86,3563993
X-variabel 5	0,38438467
X-variabel 6	0,00205784
X-variabel 7	-0,01081484

2

6305-7-D-3	*Coefficients*
Intercept	2288,2085
X-variabel 1	-3,23373879
X-variabel 2	0,05697566
X-variabel 3	-1095,01162
X-variabel 4	448,861118
X-variabel 5	-52,8164771
X-variabel 6	0,00323162
X-variabel 7	-0,03220143

3

6506-11-A-1	*Coefficients*
Intercept	670,362834
X-variabel 1	0,76194104
X-variabel 2	-0,00792429
X-variabel 3	-241,033258
X-variabel 4	110,6011
X-variabel 5	-14,1680233
X-variabel 6	-0,00147219
X-variabel 7	-0,0096805

4

6506-11-A-2	*Coeffiscents*
Intercept	-789,452774
X-variabel 1	0,31511465
X-variabel 2	0,10800635
X-variabel 3	71,970428
X-variabel 4	272,192212
X-variabel 5	3,45475488
X-variabel 6	-0,00254154
X-variabel 7	0,00341641

5

6506-11-A-3	*Coefficients*
Intercept	-6,35211543
X-variabel 1	0,02780985
X-variabel 2	0,06638021
X-variabel 3	-212,639471
X-variabel 4	278,840407
X-variabel 5	-7,76867542
X-variabel 6	-0,00140094
X-variabel 7	0,00183274

6

Figures 34 to 39 show the resulting ROP plots from implementing the coefficients in their originating well. The Ormen Lange wells are presented in figures 34 through 36. Overall the method seems to compute the ROP well. Well 6305/7-D-1 is clearly the most accurate, while well 6305/7-D-3 appear to poorly compare in several sections of its plot.

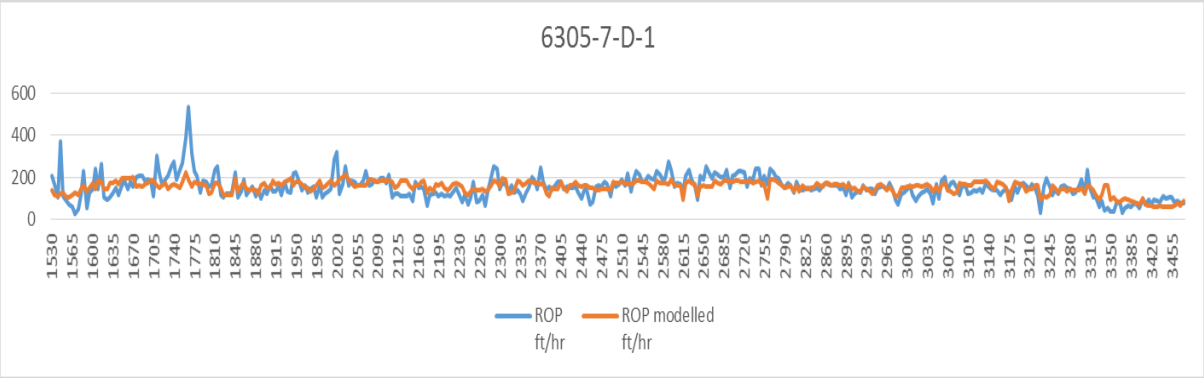

Figure 34: Multiple regression method in well 6305/7-D-1

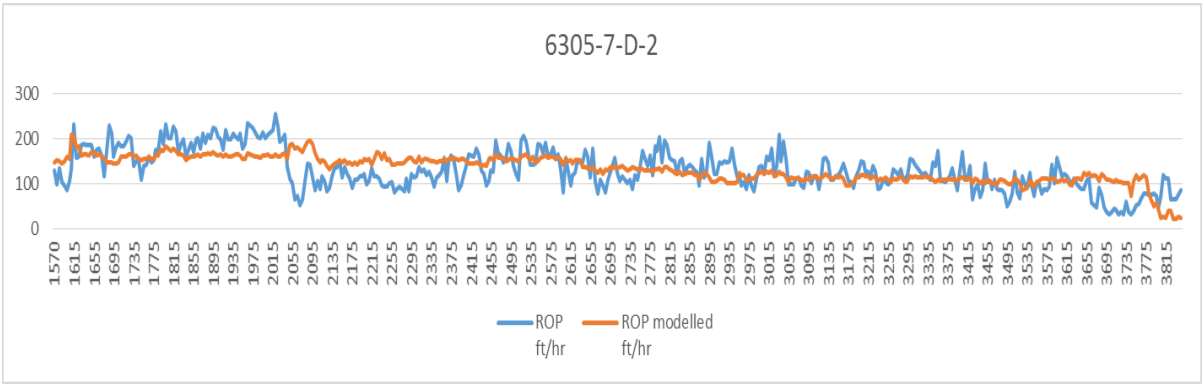

Figure 35: Multiple regression method in well 6305/7-D-2

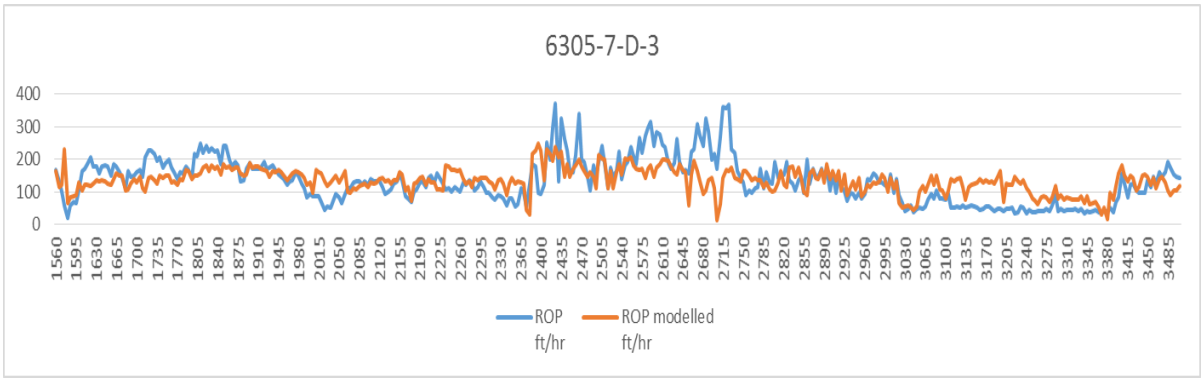

Figure 36: Multiple regression method in well 6305/7-D-3

Figures 37 to 39 are the Morvin field wells. Like the Ormen Lange wells, the method models the ROP fairly well. Results vary also here between the wells. Wells 6506/11-A-1 and 6506/11-A-3 appear as the most accurate, and do very well in computing the ROP. Well 6506/11-A-2 result is noticeably poorer, but the plots seem to correlate well in some sections.

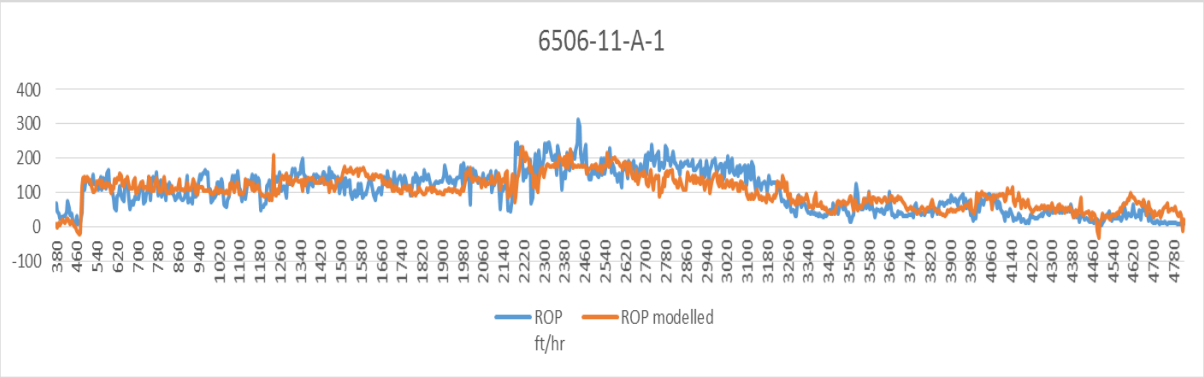

Figure 37: Multiple regression method in well 6506/11-A-1

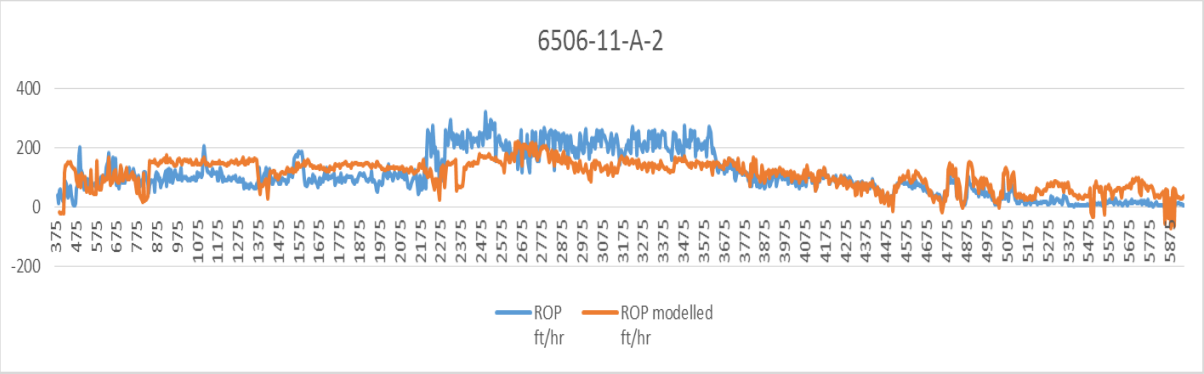

Figure 38: Multiple regression method in well 6506/11-A-2

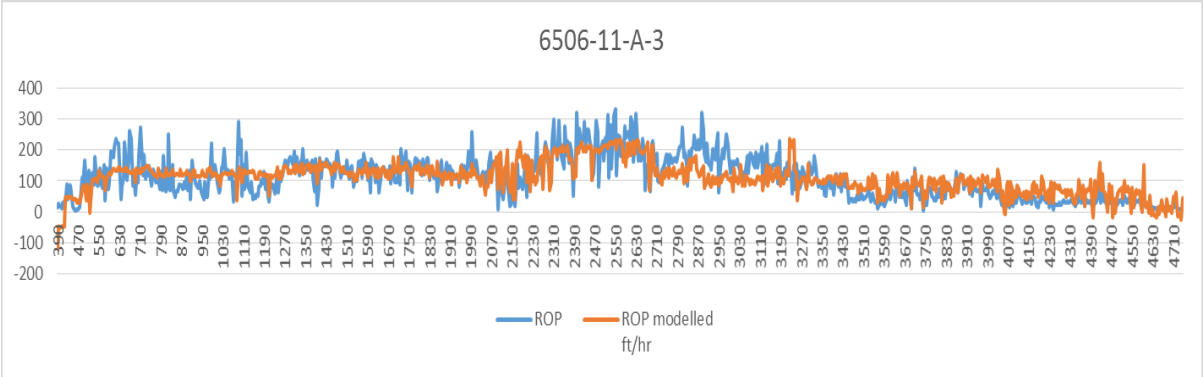

Figure 39: Multiple regression method in well 6506/11-A-3

The following plots are those of most interest for this thesis. Shown here is the plotted results of ROP predicted by coefficients applied from close-by wells. The Ormen Lange wells are first presented. Well 6305/7-D-1 plots are shown in figures 40 and 41. Figure 40 has the predicted ROP by use of coefficients from well 6305/7-D-2. The predicted ROP here seems relatively well modelled, although it deviates in a few sections. In figure 41, the ROP is modelled by coefficients from well 6305/7-D-3. Here the ROP clearly looks poorly modelled. The predicted plot is parallel with the actual ROP in most of the plot, but deviates significantly.

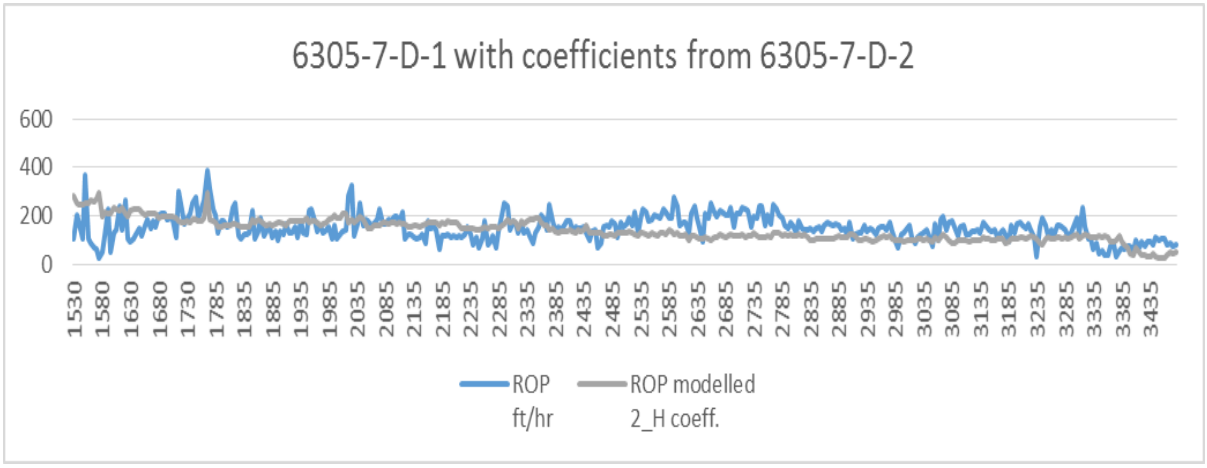

Figure 40: Multiple regression - 6305/7-D-1 with coefficients from 6305/7-D-2

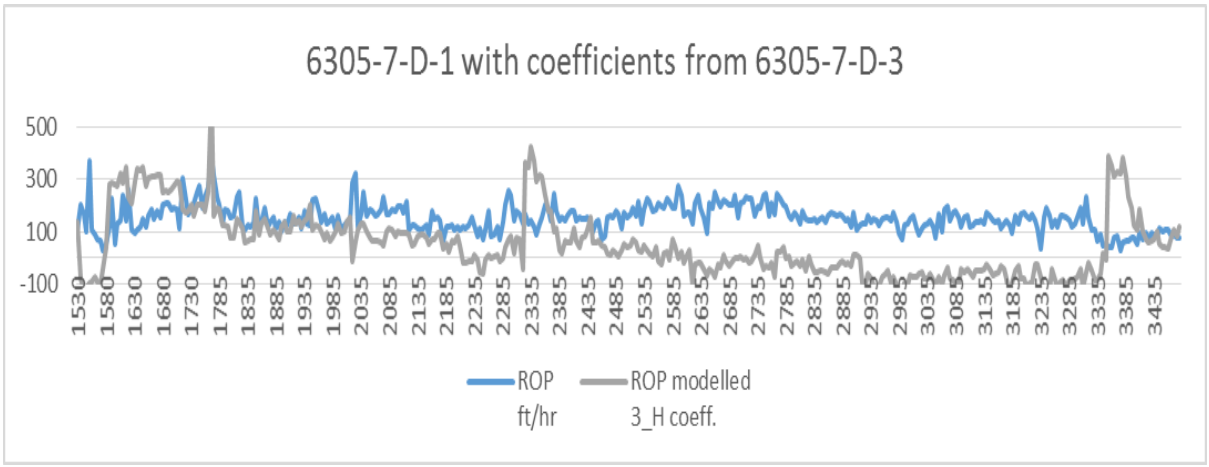

Figure 41: Multiple regression - 6305/7-D-1 with coefficients from 6305/7-D-3

Well 6305/7-D-2 with coefficients applied from neighboring wells is presented in figures 42 and 43. Figure 42 show the plot of ROP predicted by well 6305/7-D-1 coefficients. Well 6305/7-D-1 coefficients appear to produce a good ROP prediction plot. The modelled ROP plot deviates to some degree over large parts, but appears to stay parallel with the actual ROP. ROP modelled by well 6305/7-D-3 coefficients is displayed in figure 43. Again, coefficients from well 6305/7-D-3 produces a clearly deviating ROP prediction. Similar is the large deviation over the same area, as well as managing to maintain parallel with the actual ROP in large sections.

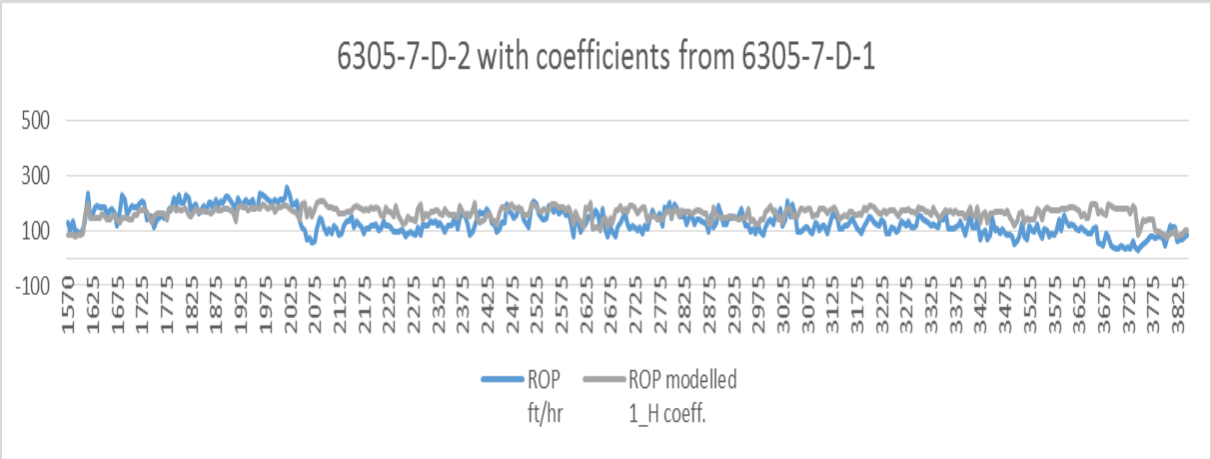

Figure 42: Multiple regression - 6305/7-D-2 with coefficients from 6305/7-D-1

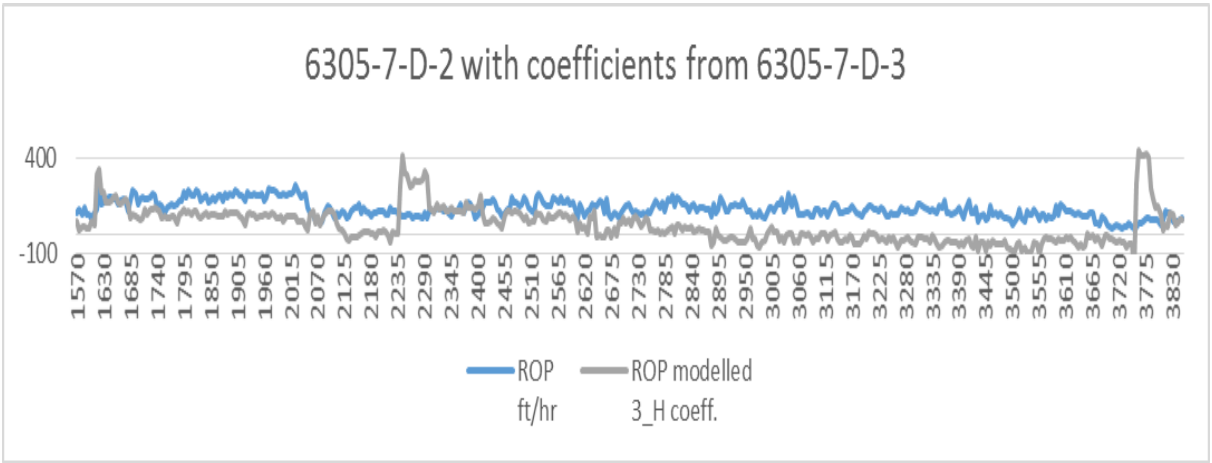

Figure 43: Multiple regression - 6305/7-D-2 with coefficients from 6305/7-D-3

Figures 44 and 45 presents well 6305/7-D-3 with coefficients applied from neighboring wells. Coefficients from well 6305/7-D-1 is used to model the ROP in figure 44. In figure 45, the ROP is modelled with coefficients from well 6305/7-D-2. In both figures, the ROP looks poorly modelled and they deviate similarly.

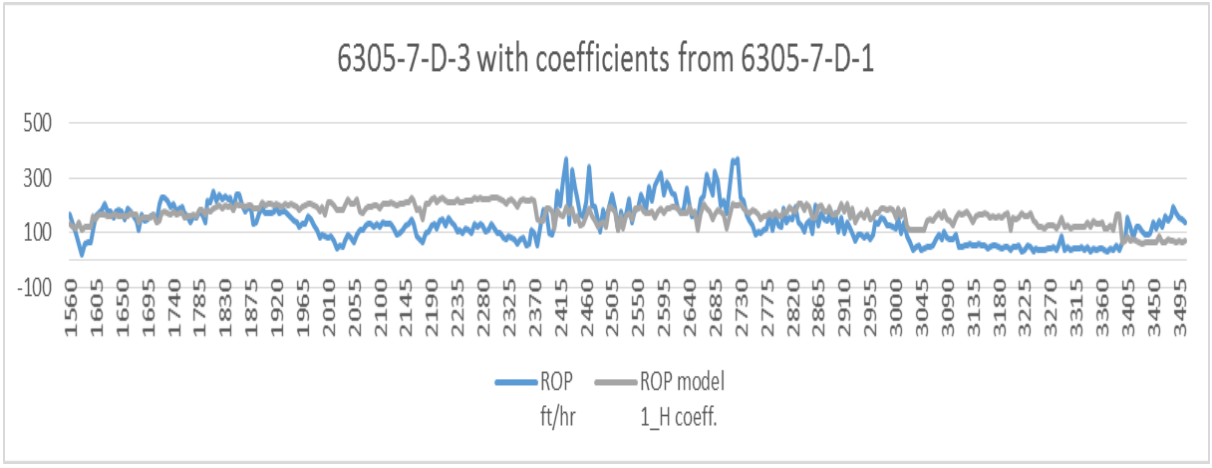

Figure 44: Multiple regression - 6305/7-D-3 with coefficients from 6305/7-D-1

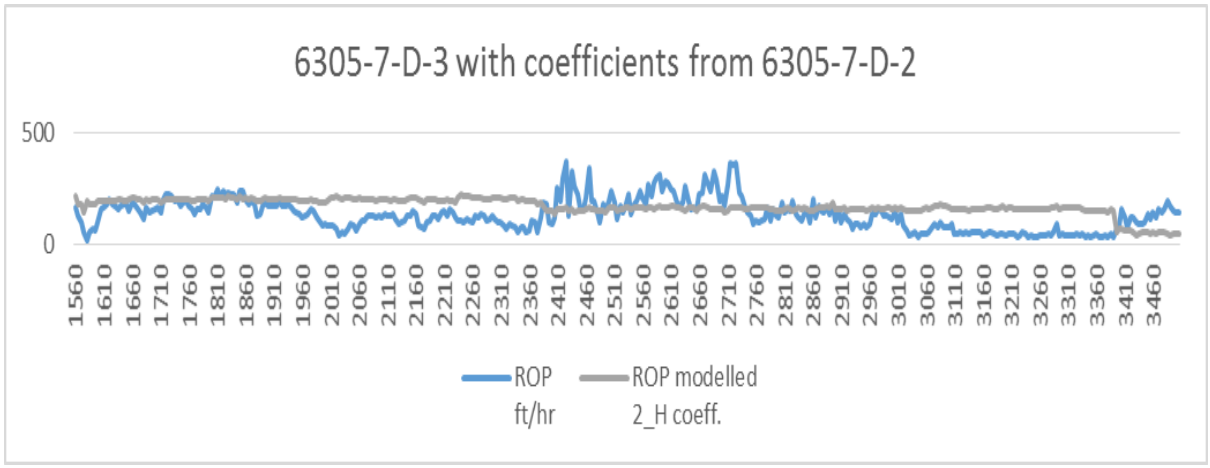

Figure 45: Multiple regression - 6305/7-D-3 with coefficients from 6305/7-D-2

The following figures show plots from the Morvin field wells. ROP plots of well 6506/11-A-1 with neighboring coefficients applied are displayed in figures 46 and 47. Figure 46 plots ROP modelled by well 6506/11-A-2 coefficients. In figure 47, the ROP is modelled by well 6506/11-A-3 coefficients. The results appear similar for both sets of coefficients, both in deviation and form. However, the coefficients from well 6506/11-A-3 seem to give better results. The predicting plots show weakness particularly around 2200 to 3200 meters depth.

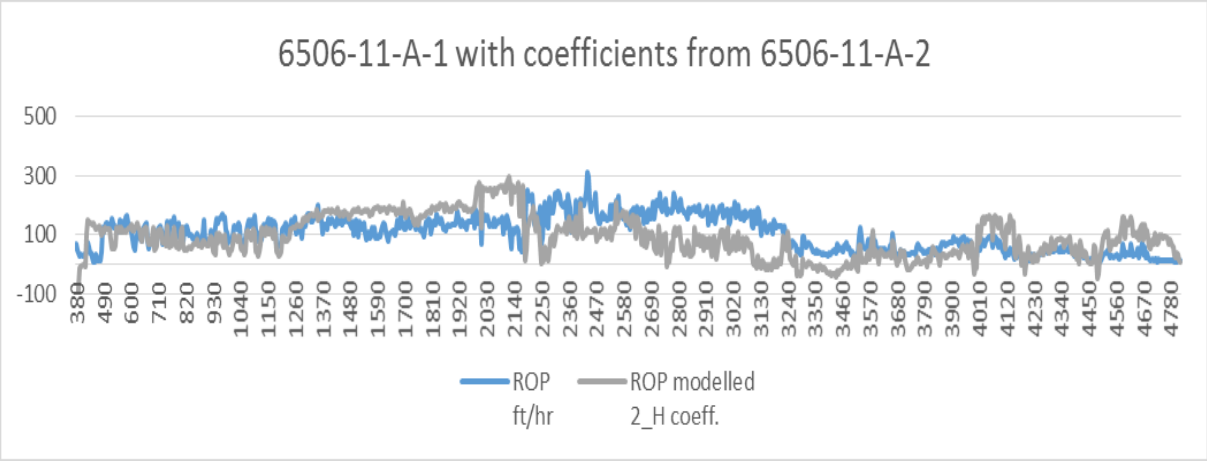

Figure 46: Multiple regression - 6506/11-A-1 with coefficients from 6506/11-A-2

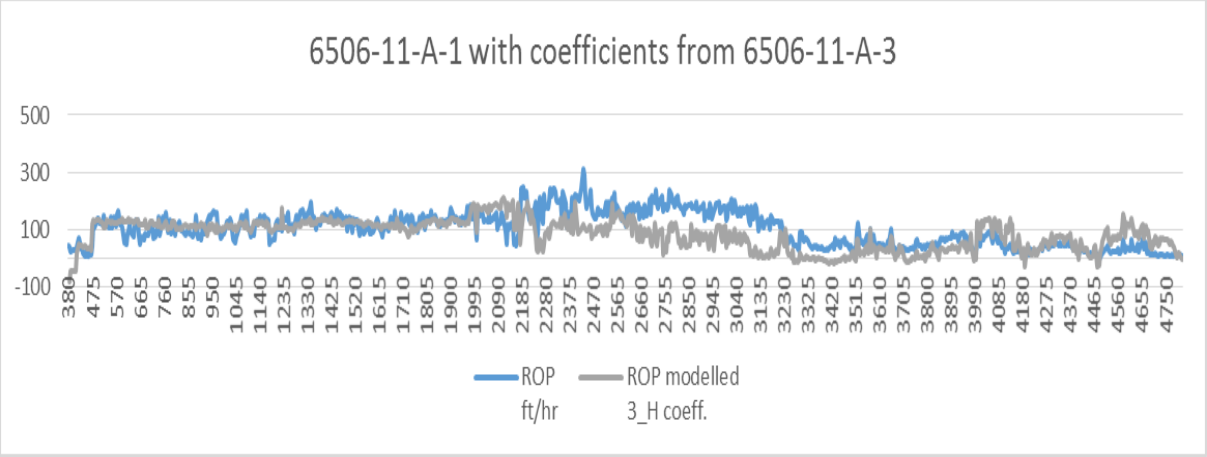

Figure 47: Multiple regression - 6506/11-A-1 with coefficients from 6506/11-A-3

Well 6305/7-D-2 with coefficients applied from neighboring wells is presented in figures 48 and 49. Figure 48 shows the plot of the ROP predicted by well 6506/11-A-1 coefficients. The plot of the ROP predicted by well 6506/11-A-3 coefficients is displayed in figure 49. Both plots provide similar looking results. The vast deviations are around 2300 to 3600 meters and from 5200 meters depths. ROP prediction by coefficients from well 6506/11-A-3 provides seemingly better results than from well 6506/11-A-1. The deviation from the reference plot looks lesser, and parts of the plots appear impressively correlative.

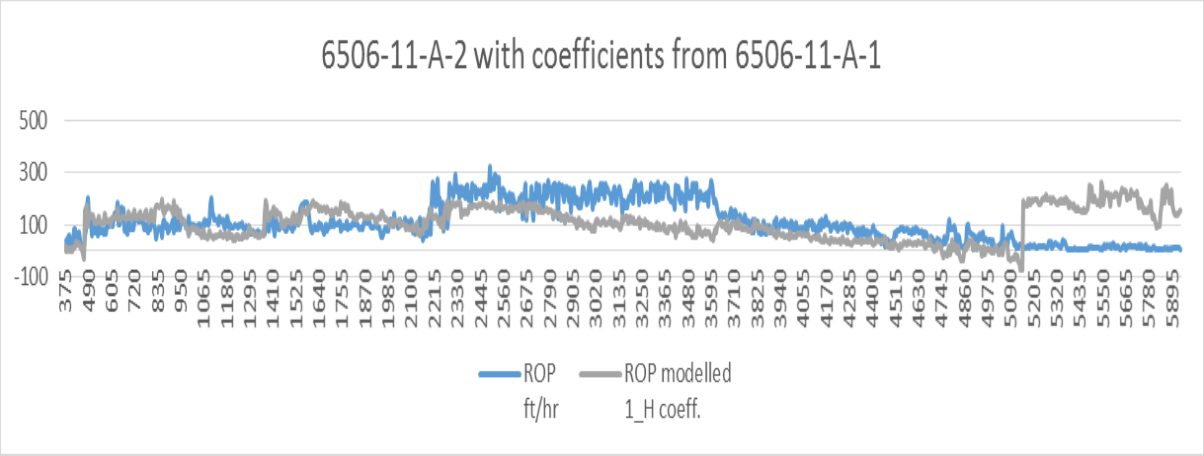

Figure 48: Multiple regression - 6506/11-A-2 with coefficients from 6506/11-A-1

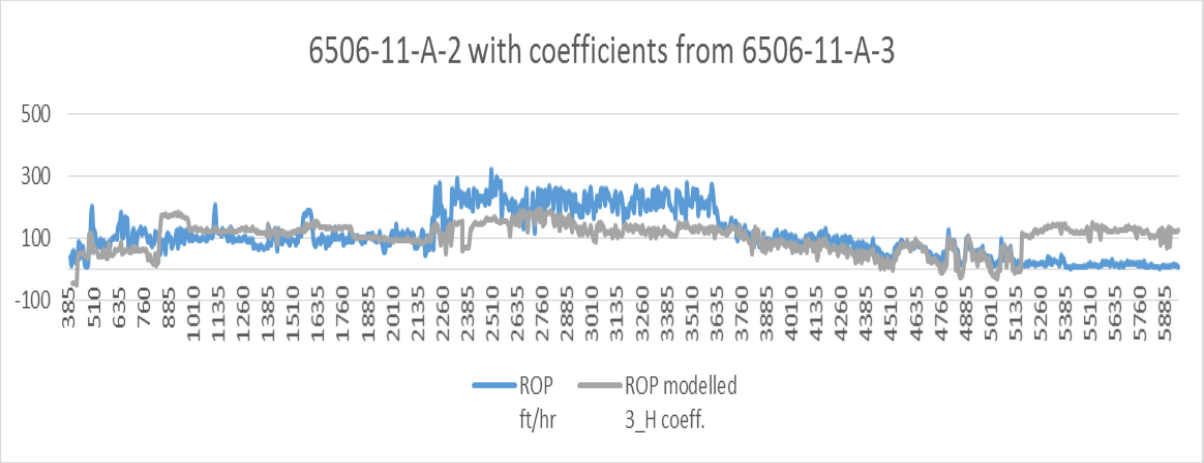

Figure 49: Multiple regression - 6506/11-A-2 with coefficients from 6506/11-A-3

To complete the results of the multiple regression technique in this thesis are the 6506/11-A-3 plots of modelled ROP from coefficients of close-by wells shown below. Figure 50 shows the ROP predicted from well 6506/11-A-1 coefficients. The overall plot appears very good and only has a few places where the plot deviates noticeably. Impressively, the plot of ROP predicted by well 6506/11-A-2 coefficients in figure 51 seems even better. This plot looks correlative to the actual ROP, with very small areas of minor deviation.

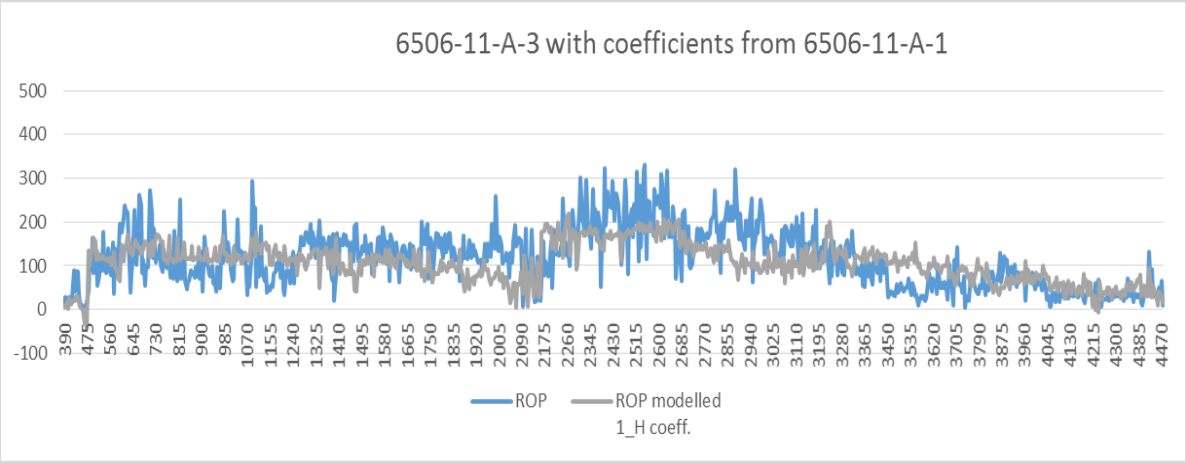

Figure 50: Multiple regression - 6506/11-A-3 with coefficients from 6506/11-A-1

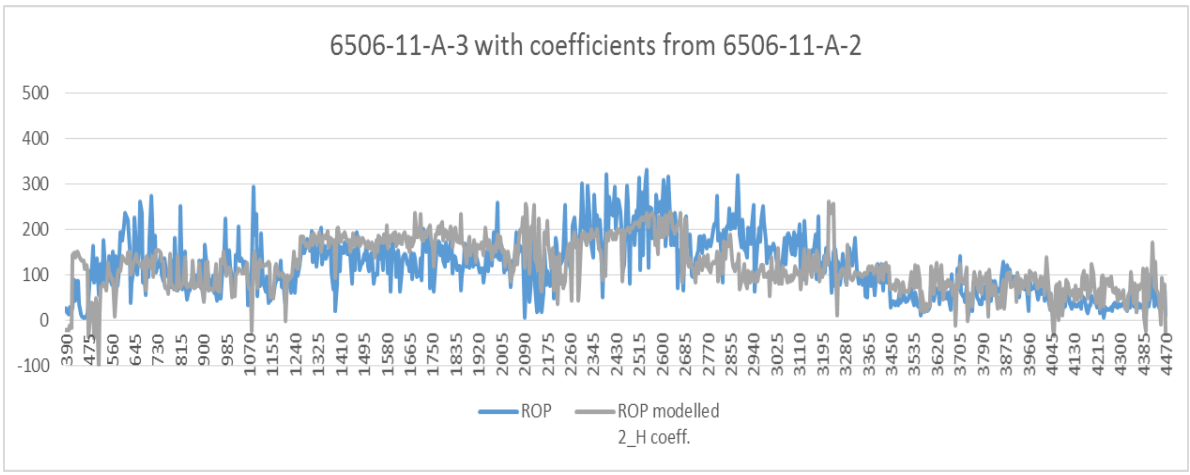

Figure 51: Multiple regression - 6506/11-A-3 with coefficients from 6506/11-A-2

5.2 Least Square

The results from using the least square technique are available in this section. Calculated coefficients of each of the six wells are presented in tables 7 to 12.

6305-7-D-1	*Coefficients*
Intercept	0
X-variabel 1	0
X-variabel 2	0,01531515
X-variabel 3	0
X-variabel 4	74,55941
X-variabel 5	0
X-variabel 6	0
X-variabel 7	0

7

6305-7-D-2	*Coefficients*
Intercept	0
X-variabel 1	0
X-variabel 2	0,02782357
X-variabel 3	0
X-variabel 4	0
X-variabel 5	0,19918447
X-variabel 6	0,0006707
X-variabel 7	0

8

6305-7-D-3	*Coefficients*
Intercept	0
X-variabel 1	0
X-variabel 2	0
X-variabel 3	0
X-variabel 4	113,612045
X-variabel 5	0
X-variabel 6	0
X-variabel 7	0

9

6506-11-A-1	*Coefficients*
Intercept	1,12082582
X-variabel 1	0,25031291
X-variabel 2	4,3756E-05
X-variabel 3	0
X-variabel 4	35,3949705
X-variabel 5	1,99406704
X-variabel 6	0
X-variabel 7	0

10

6506-11-A-2	*Coefficients*
Intercept	0
X-variabel 1	0
X-variabel 2	0
X-variabel 3	0
X-variabel 4	116,425757
X-variabel 5	0
X-variabel 6	0
X-variabel 7	0

11

6506-11-A-3	*Coefficients*
Intercept	0
X-variabel 1	0
X-variabel 2	0,0119807
X-variabel 3	0
X-variabel 4	57,3868209
X-variabel 5	0
X-variabel 6	0
X-variabel 7	0

12

Figures 52 to 57 show resulting ROP plots from implementing the coefficients in their originating well. The Ormen Lange wells are presented in figures 52 to 54. Wells 6305/7-D-1 and 6305/7-D-2 appears to have good results, where maybe the most accurate results are found with well 6305/7-D-1. Well 6305/7-D-3 results seems to suffer from having a large variation in the actual ROP. As the least square attempts to minimize the difference between the actual and predicted values, often a levelled prediction is computed. Especially when the actual values varies vastly.

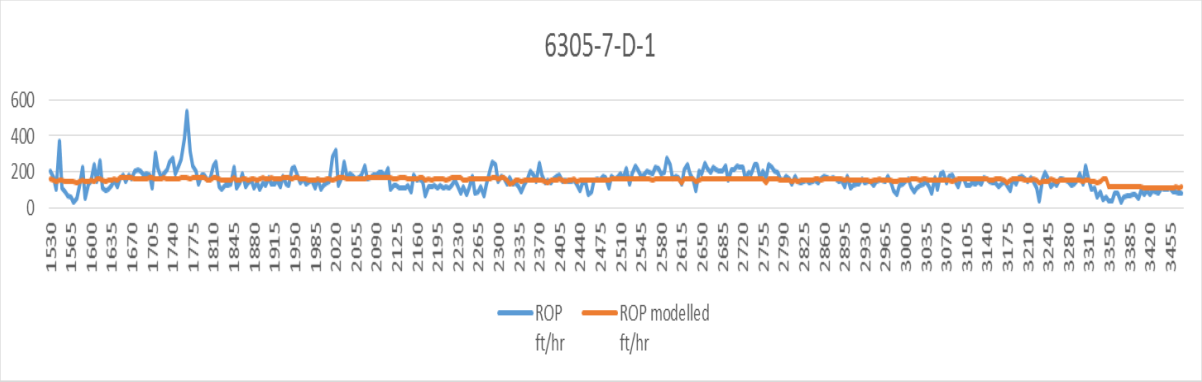

Figure 52: Least square method in well 6305/7-D-1

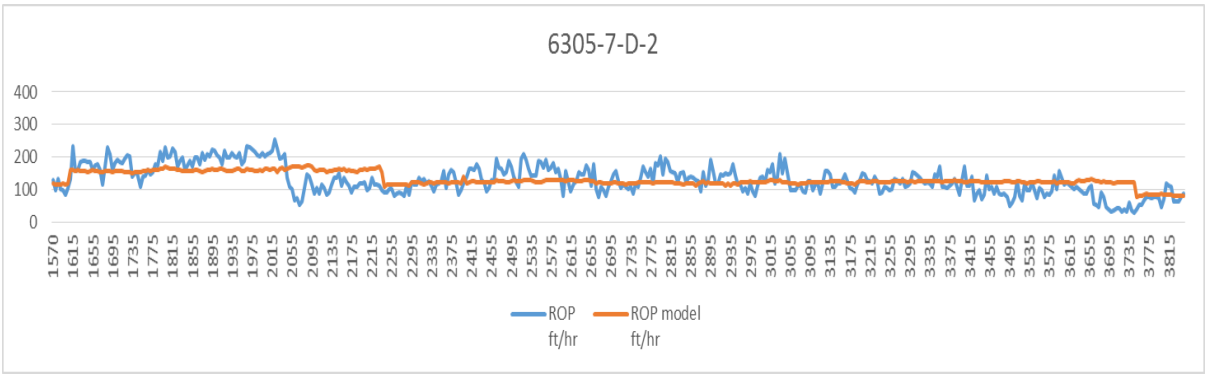

Figure 53: Least square method in well 6305/7-D-2

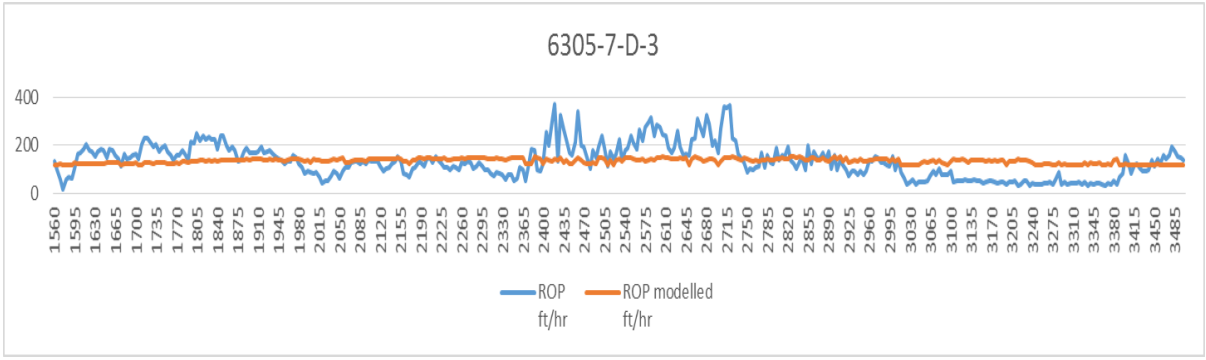

Figure 54: Least square method in well 6305/7-D-3

Figures 55 to 57 are the Morvin field wells. The results for the Morvin field wells appears not as good as in the Ormen Lange field wells. All the wells here compute good-looking results for most of the first 2000 meters. Well 6506/11-A-1 seems to correlates particularly well with its modelled ROP in this area. As all the predicted plots then maintain fairly levelled, the varying actual ROP values results in clear deviations.

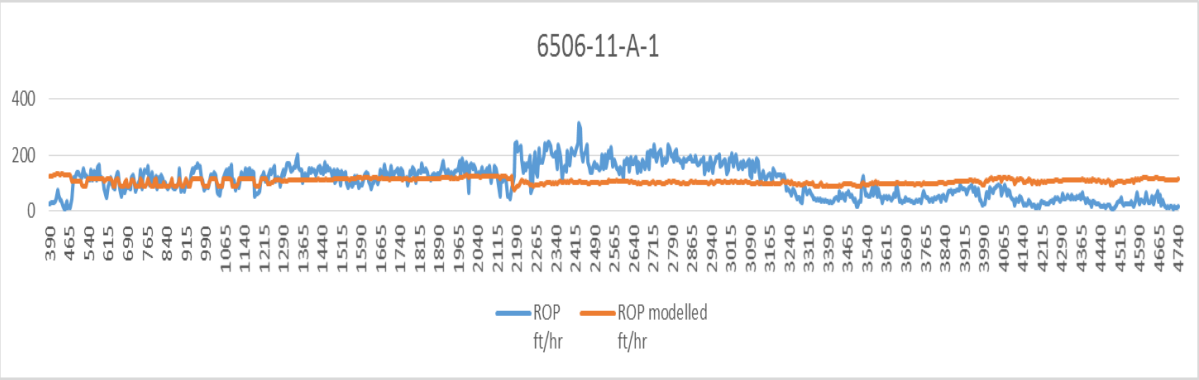

Figure 55: Least square method in well 6506/11-A-1

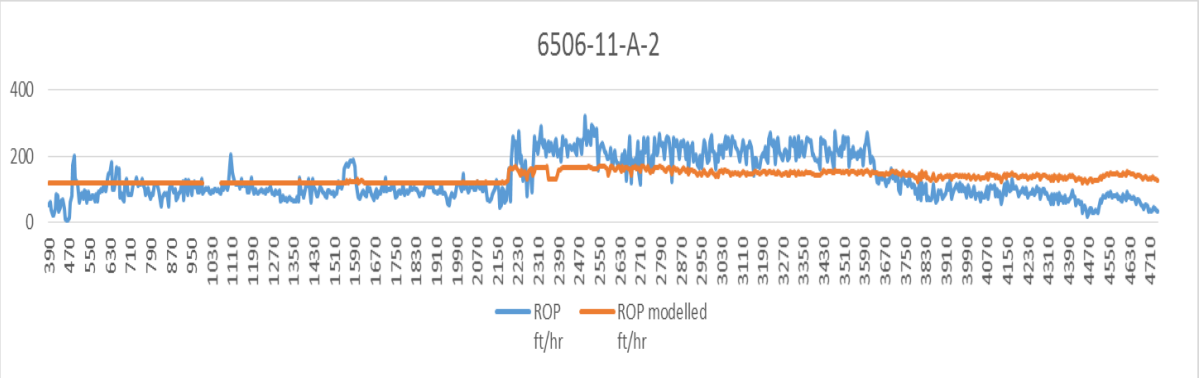

Figure 56: Least square method in well 6506/11-A-2

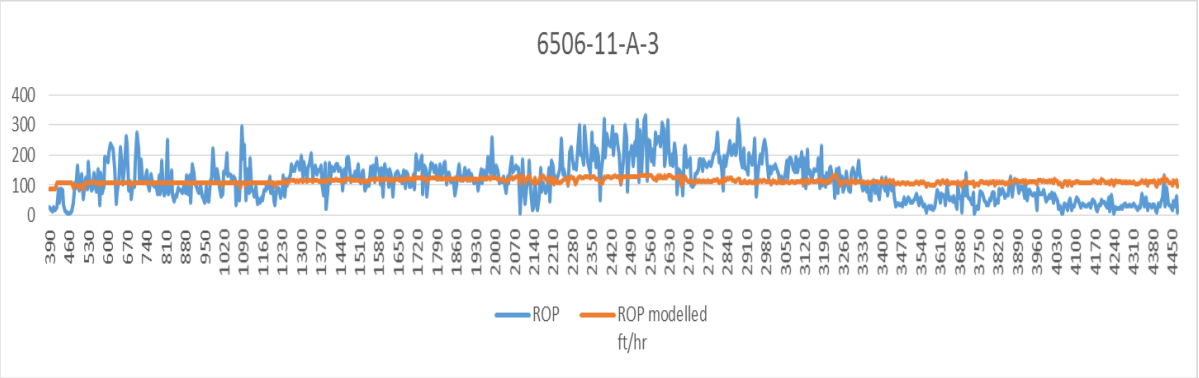

Figure 57: Least square method in well 6506/11-A-3

On the following pages, the plotted results of ROP predicted by coefficients applied from close-by wells are shown. The Ormen Lange wells are first presented. Well 6305/7-D-1 plots are shown in figures 58 and 59. Figure 58 has the predicted ROP by use of coefficients from well 6305/7-D-2. In figure 59, the ROP is modelled by coefficients from well 6305/7-D-3. Both modelled plots appear like adequate results. Well 6305/7-D-3 plots better around the middle of the plot, while well 6305/7-D-2 coefficients correlates better to the actual ROP at the end.

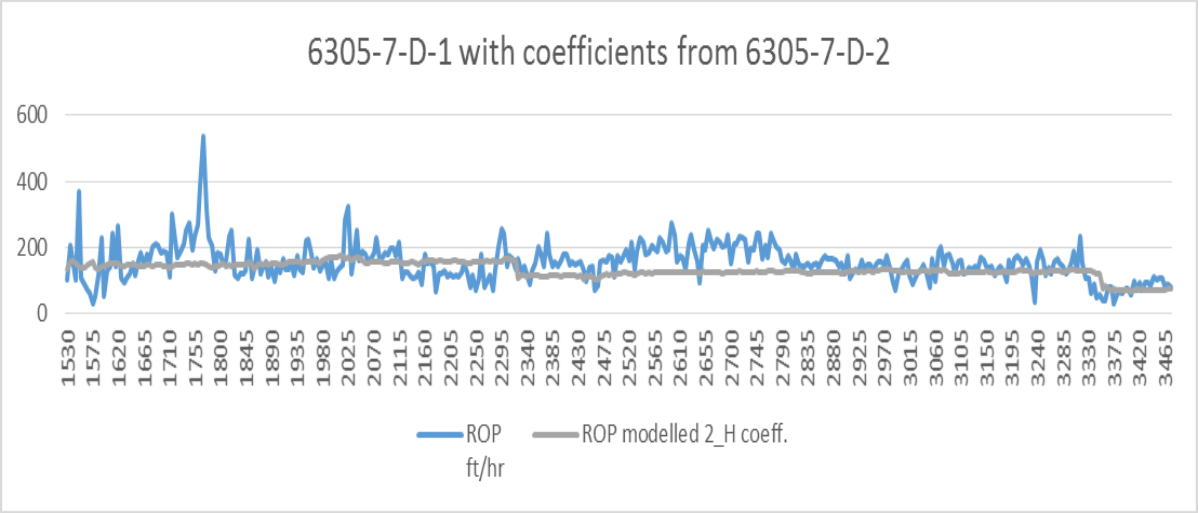

Figure 58: Least square - 6305/7-D-1 with coefficients from 6305/7-D-2

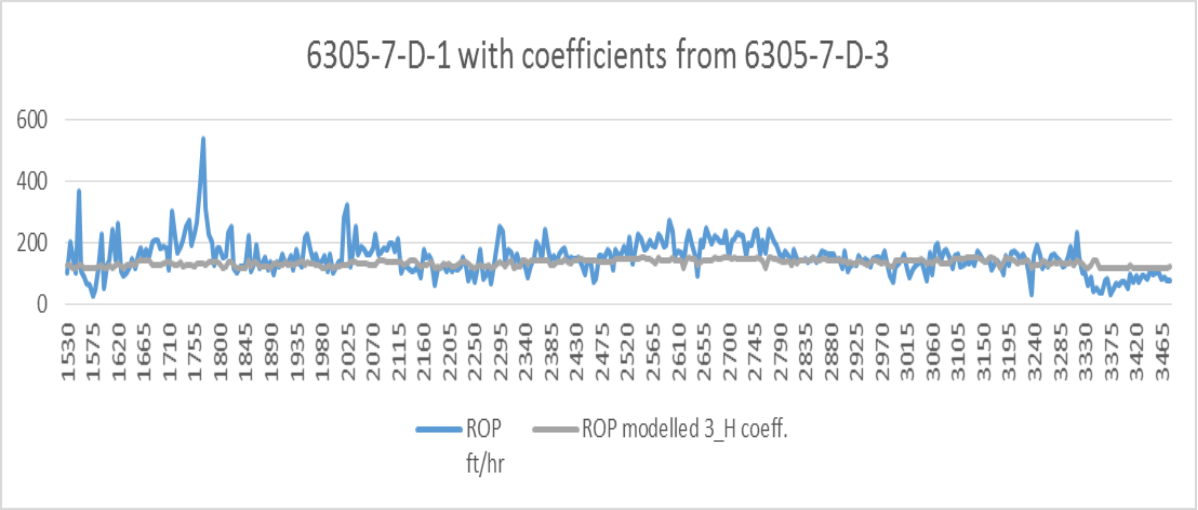

Figure 59: Least square - 6305/7-D-1 with coefficients from 6305/7-D-3

Well 6305/7-D-2 with coefficients applied from neighboring wells is presented in figures 60 and 61. Figure 60 shows the plot of ROP predicted by well 6305/7-D-1 coefficients. This plot manages to stay in proximity of the actual values, but does not look ideal. ROP modelled by well 6305/7-D-3 coefficients is displayed in figure 61. This plot appears to correlate very well for the most parts.

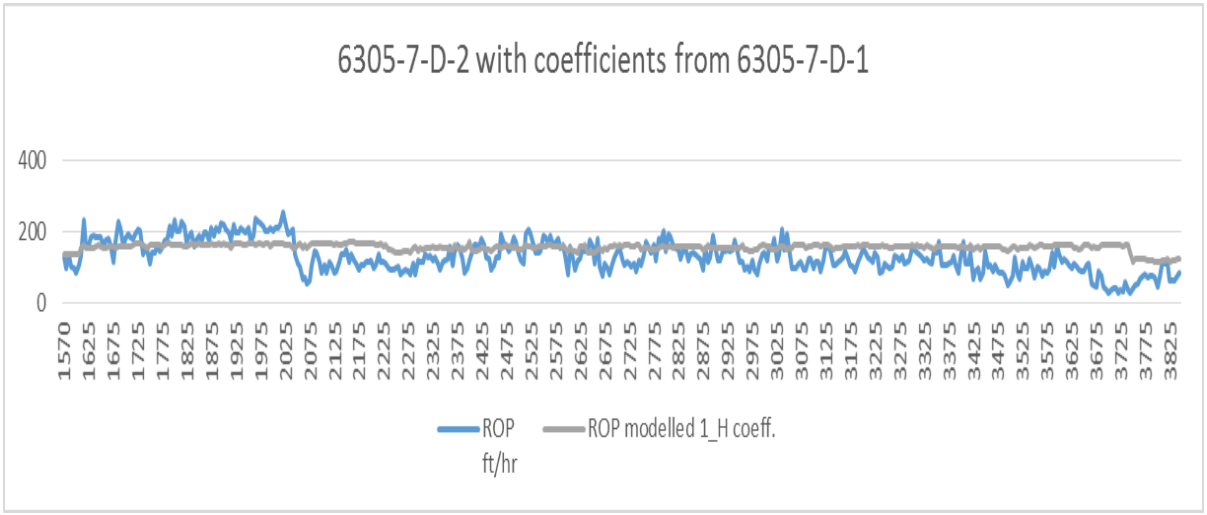

Figure 60: Least square - 6305/7-D-2 with coefficients from 6305/7-D-1

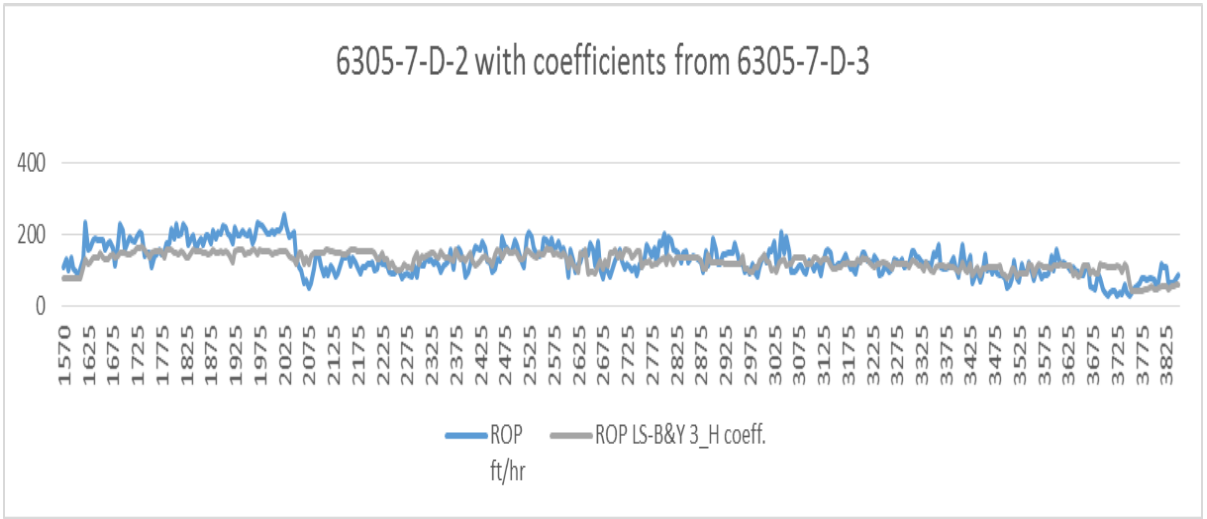

Figure 61: Least square - 6305/7-D-2 with coefficients from 6305/7-D-3

Figures 62 and 63 presents well 6305/7-D-3 with coefficients applied from neighboring wells. Coefficients from well 6305/7-D-1 are used to model ROP as shown in figure 62. In figure 63, ROP is modelled with coefficients from well 6305/7-D-2. In both figures, the ROP does not look well modelled and they deviate similarly. The coefficients from the neighboring wells produce similar results as the coefficients from the well, seen in figure 54. They are not very different from the results from the multiple regression technique in figures 62 and 63.

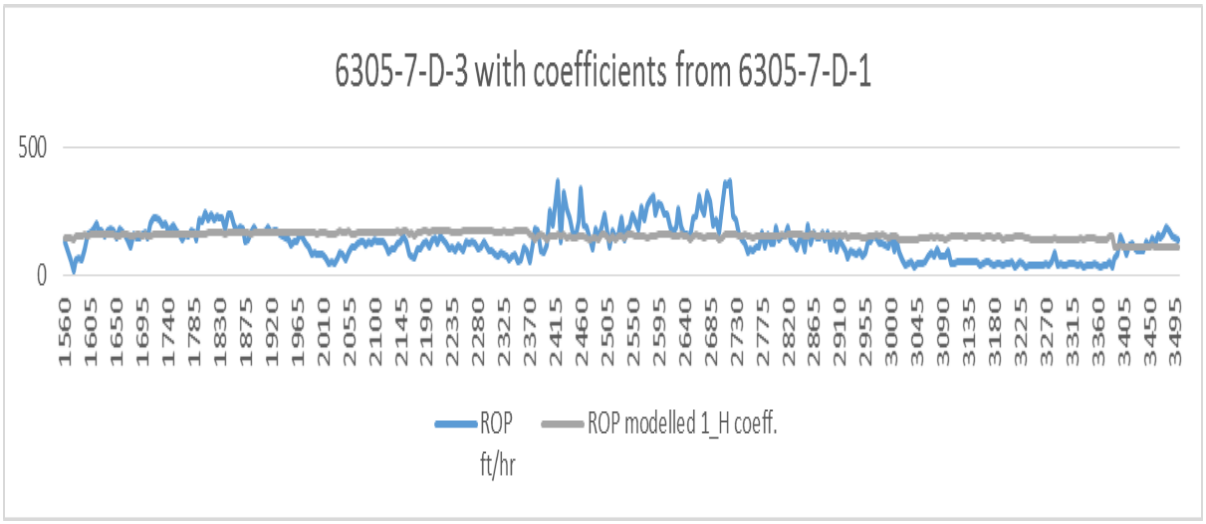

Figure 62: Least square - 6305/7-D-3 with coefficients from 6305/7-D-1

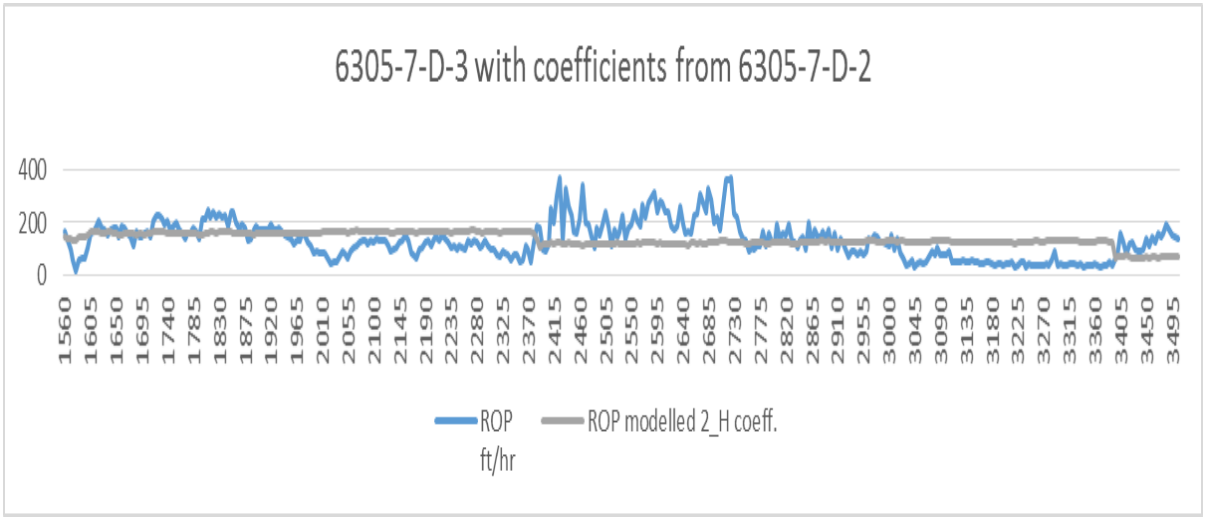

Figure 63: Least square - 6305/7-D-3 with coefficients from 6305/7-D-2

The following figures are plots from the Morvin field wells. ROP plots of well 6506/11-A-1 with neighboring coefficients applied are displayed in figures 64 and 65. Figure 64 plots the ROP modelled by well 6506/11-A-2 coefficients. This plot appears initially good, but deviates more with depth. In figure 65, the ROP is modelled by well 6506/11-A-3 coefficients. The modelled ROP plot by the well's own coefficients is also included here. It shows how closely the predicted ROP plots are, and thereby how correlative the use of coefficients can be. Even though the coefficients by themselves are not comparable.

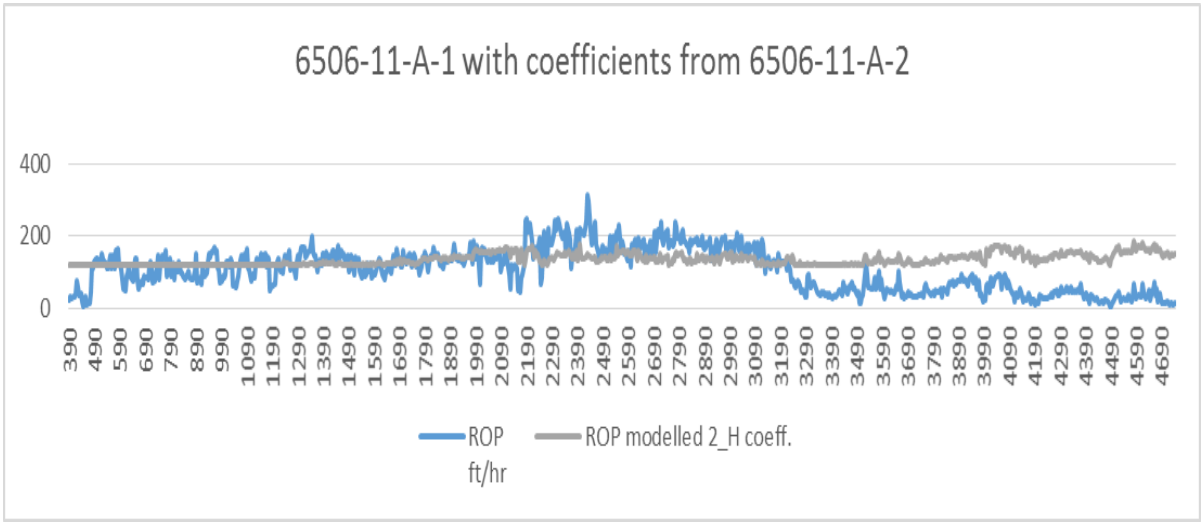

Figure 64: Least square - 6506/11-A-1 with coefficients from 6506/11-A-2

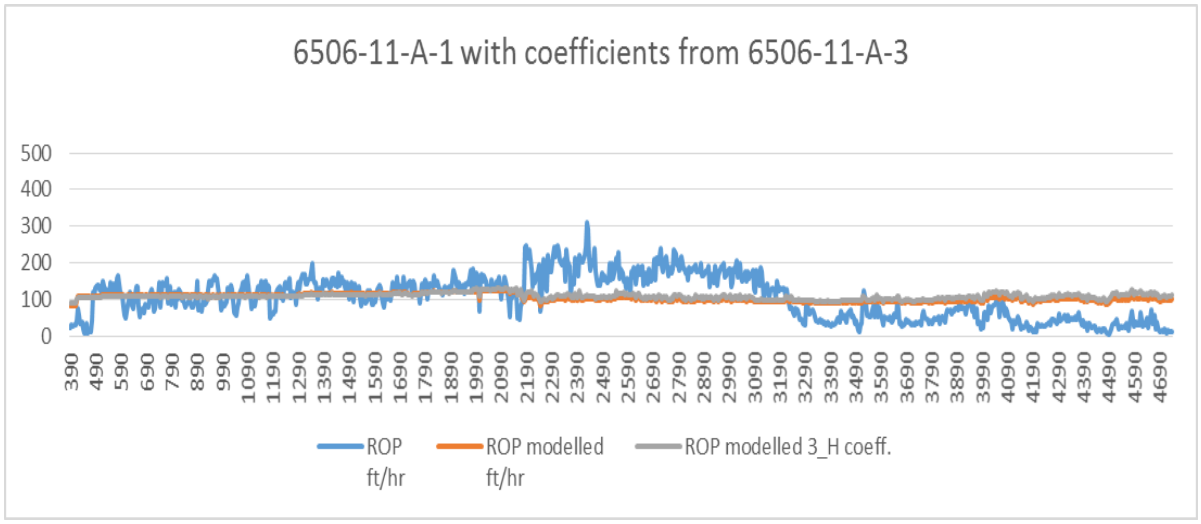

Figure 65: Least square - 6506/11-A-1 with coefficients from 6506/11-A-3

Well 6506/11-A-2 with coefficients applied from neighboring wells is presented in figures 66 and 67. Figure 66 show the plot of ROP predicted by well 6506/11-A-1 coefficients. Plot of ROP predicted by well 6506/11-A-3 coefficients is displayed in figure 67. Both of these wells also have the plot by coefficients originating from the actual wells. In these wells, the coefficient sets appear to produce almost identical plots. The result of the plots seems on the other hand only adequate. There is an especially large deviation in the middle of the plot, where the actual ROP experienced high values.

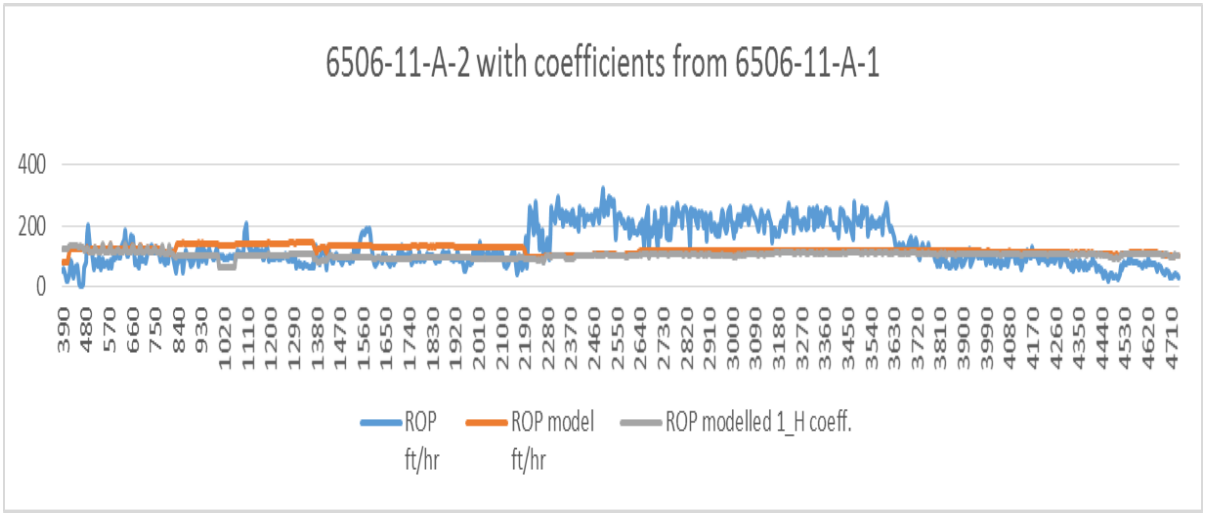

Figure 66: Least square - 6506/11-A-2 with coefficients from 6506/11-A-1

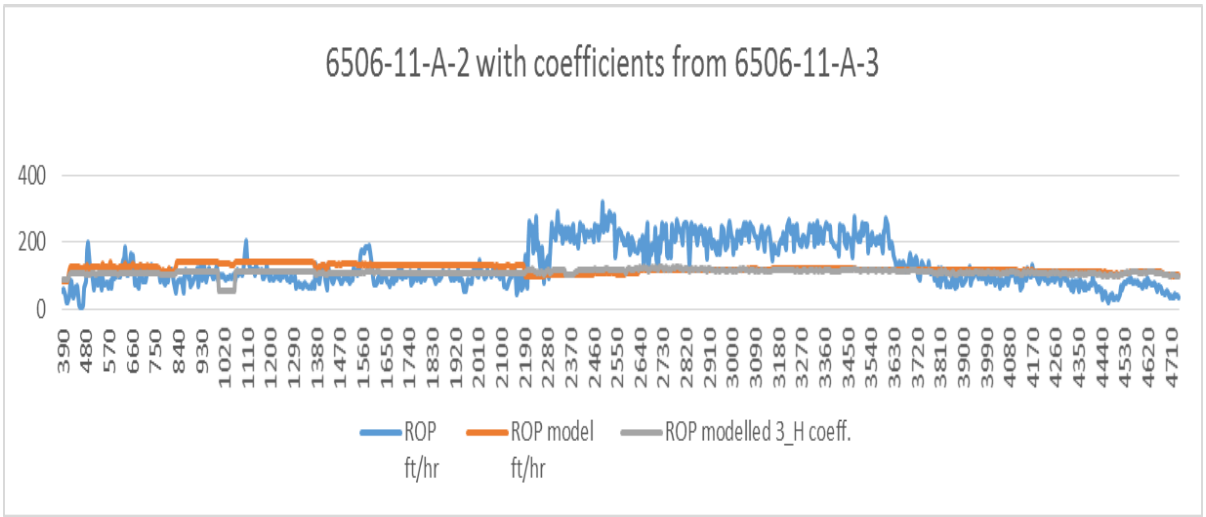

Figure 67: Least square - 6506/11-A-2 with coefficients from 6506/11-A-3

To complete the results from the least square technique in this thesis is the 6506/11-A-3 plots of modelled ROP from coefficients of close-by wells. Figure 68 shows the ROP predicted from well 6506/11-A-1 coefficients. This plot looks fairly level and stays in proximity of the actual plot in the first half of the plot. The last half of the plot has significant deviations of the results. ROP predicted from well 6506/11-A-2 coefficients in figure 69 appears to show better results. This plot manages to correlate quite well until it deviates vastly towards the end of the plot. Actual ROP values vary frequently and by large values, making it challenging to evaluate the predicted plot.

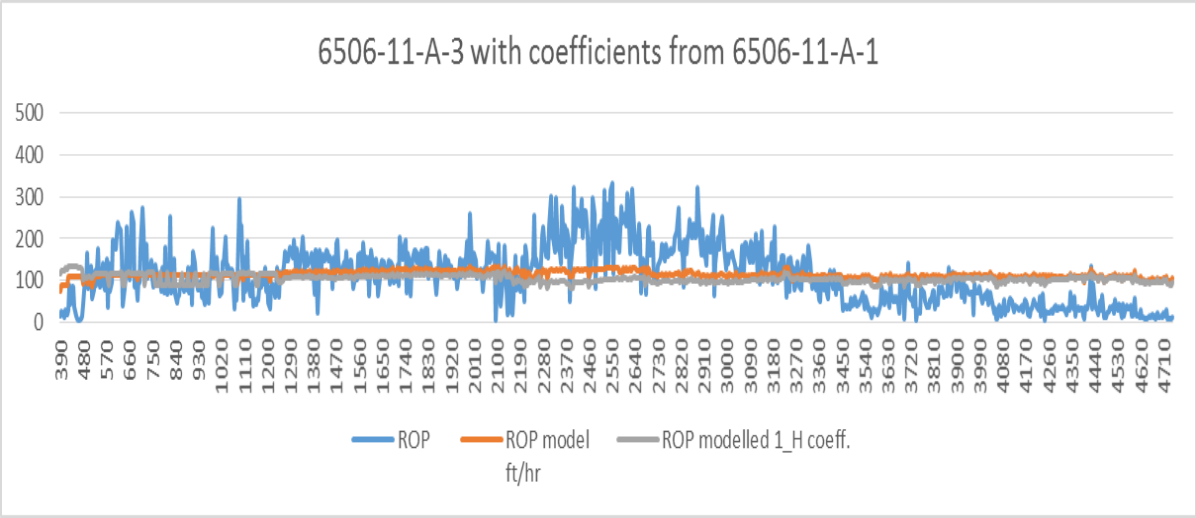

Figure 68: Least square - 6506/11-A-3 with coefficients from 6506/11-A-1

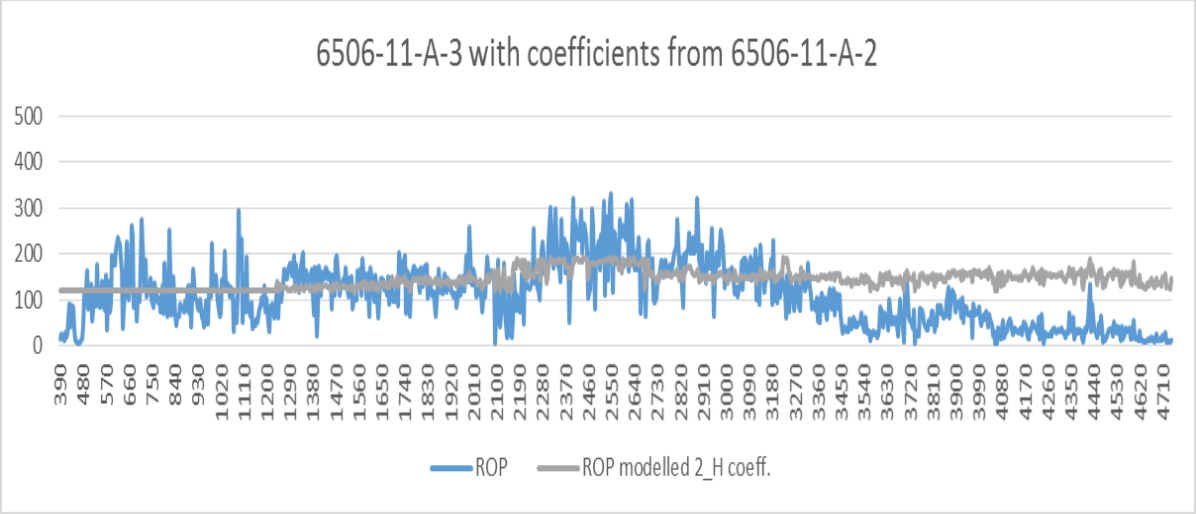

Figure 69: Least square - 6506/11-A-3 with coefficients from 6506/11-A-2

5.3 Multiple Regression with Bourgoyne & Young's Model

The results from using the multiple regression technique with Bourgoyne and Young's model are available in this section. Calculated coefficients of each of the six wells are presented in tables 13 to 18. These coefficients are the first sets to be close to comparable. Still, the main reason why all sets within each field have zero for the same coefficients is that the values they are to interact with are constant.

6305-7-D-1	*Coefficients*
Intercept	1,04726151
X-variabel 1	0,00040102
X-variabel 2	0,00251851
X-variabel 3	-0,00012836
X-variabel 4	-0,03233096
X-variabel 5	0,038008
X-variabel 6	0
X-variabel 7	6,4984E-05

13

6305-7-D-2	*Coefficients*
Intercept	4,69687645
X-variabel 1	0,00020906
X-variabel 2	0,00040947
X-variabel 3	-1,6252E-05
X-variabel 4	0,00362551
X-variabel 5	0,519272
X-variabel 6	0
X-variabel 7	-6,7247E-05

14

6305-7-D-3	*Coefficients*
Intercept	8,01596241
X-variabel 1	0,0004574
X-variabel 2	0,00047156
X-variabel 3	4,857E-06
X-variabel 4	-0,20741642
X-variabel 5	-0,98914419
X-variabel 6	0
X-variabel 7	-7,3597E-05

15

6506-11-A-1	*Coefficients*
Intercept	7,66199056
X-variabel 1	0,00032889
X-variabel 2	0,00040226
X-variabel 3	0
X-variabel 4	-0,17022179
X-variabel 5	0,24352929
X-variabel 6	0
X-variabel 7	-9,9799E-05

16

6506-11-A-2	*Coefficients*
Intercept	5,70009583
X-variabel 1	5,1787E-05
X-variabel 2	0,0002469
X-variabel 3	0
X-variabel 4	-0,06616008
X-variabel 5	0,58949979
X-variabel 6	0
X-variabel 7	-4,6391E-05

17

6506-11-A-3	*Coefficients*
Intercept	6,79545902
X-variabel 1	0,00034113
X-variabel 2	0,00057759
X-variabel 3	0
X-variabel 4	-0,14899919
X-variabel 5	1,17436476
X-variabel 6	0
X-variabel 7	-8,8636E-05

18

Figures 70 to 75 show the resulting ROP plots from implementing the coefficients in their originating well. The Ormen Lange wells are presented in figures 70 to 72. Wells 6305/7-D-1 and 6305/7-D-2 appear to give good results as in the plain multiple regression method. In well 6305/7-D -3 however, the coefficients seem to correlate far better with the actual ROP.

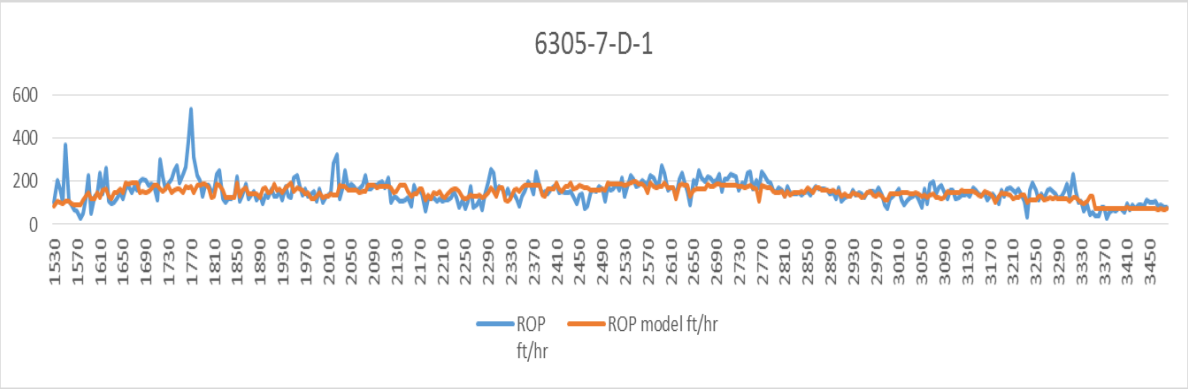

Figure 70: Multiple regression with Bourgoyne & Young's model in well 6305/7-D-1

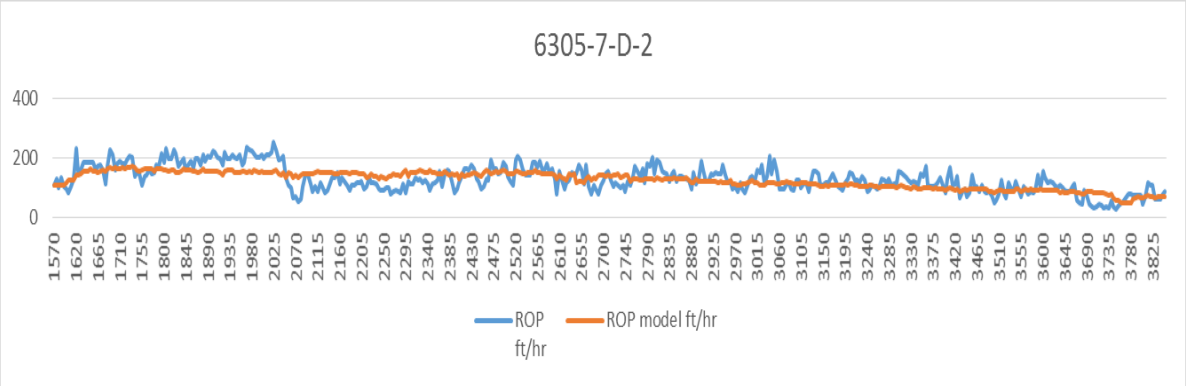

Figure 71: Multiple regression with Bourgoyne & Young's model in well 6305/7-D-2

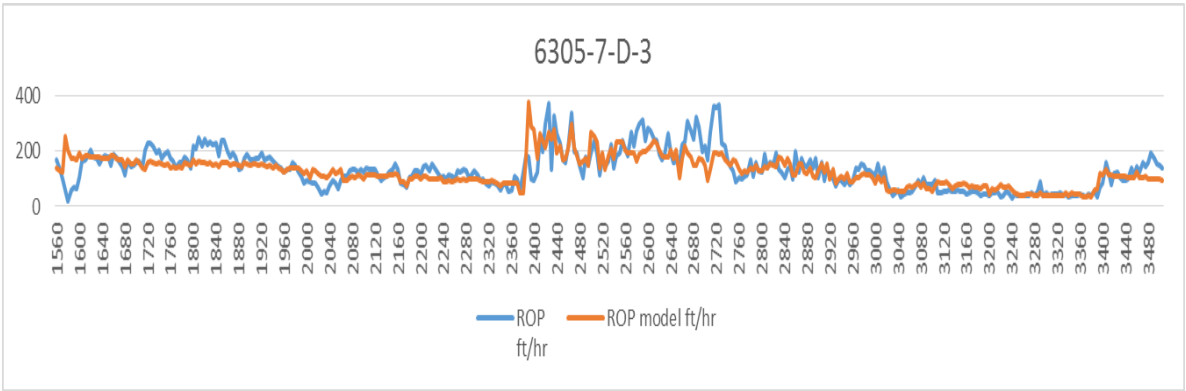

Figure 72: Multiple regression with Bourgoyne & Young's model in well 6305/7-D-3

Figures 73 to 75 are the Morvin field wells. Well 6506/11-A-2 is the only plot that noticeably seem to improve compared to the plain multiple regression results. Still, all the results appear to model the ROP very well.

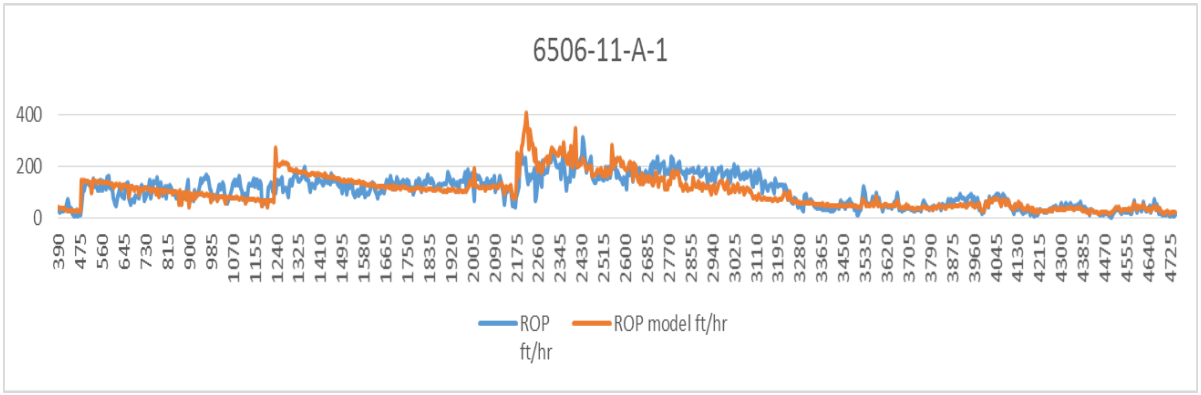

Figure 73: Multiple regression with Bourgoyne & Young's model in well 6506/11-A-1

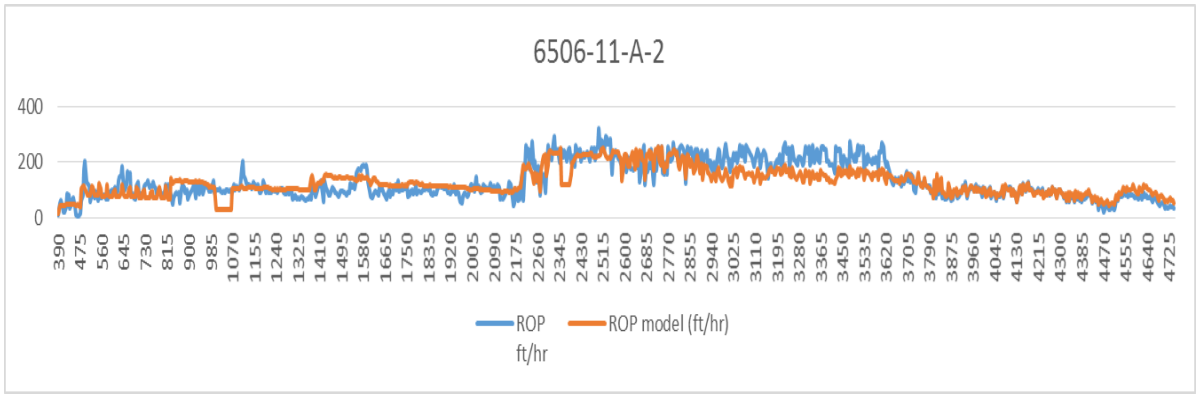

Figure 74: Multiple regression with Bourgoyne & Young's model in well 6506/11-A-2

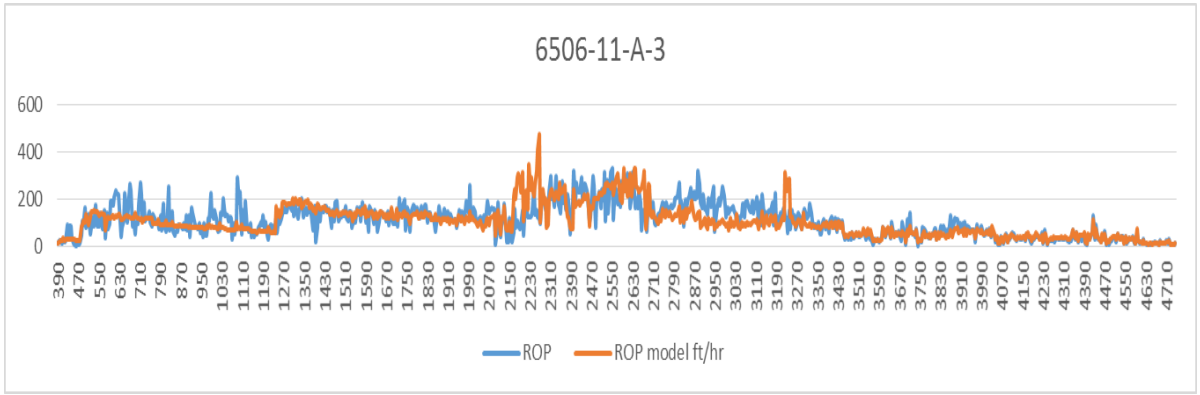

Figure 75: Multiple regression with Bourgoyne & Young's model in well 6506/11-A-3

Shown here are the plotted results of the ROP predicted by coefficients applied from close-by wells. The Ormen Lange wells are first presented. Well 6305/7-D-1 plots are shown in figures 76 and 77. Figure 76 has the predicted ROP by use of coefficients from well 6305/7-D-2. In figure 77, the ROP is modelled by coefficients from well 6305/7-D-3. The ROP predicted by coefficients from well 6305/7-D-3 appears to have massive improvements by using the Bourgoyne & Young's model in computing coefficients with multiple regression. See figure 41 for reference.

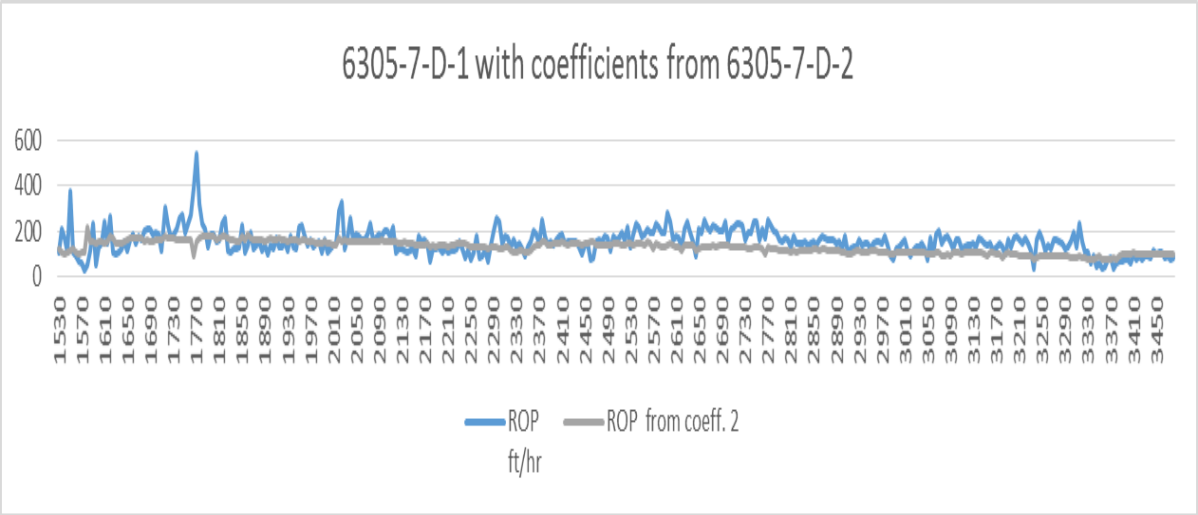

Figure 76: Multiple regression with Bourgoyne & Young's model - 6305/7-D-1 with coefficients from 6305/7-D-2

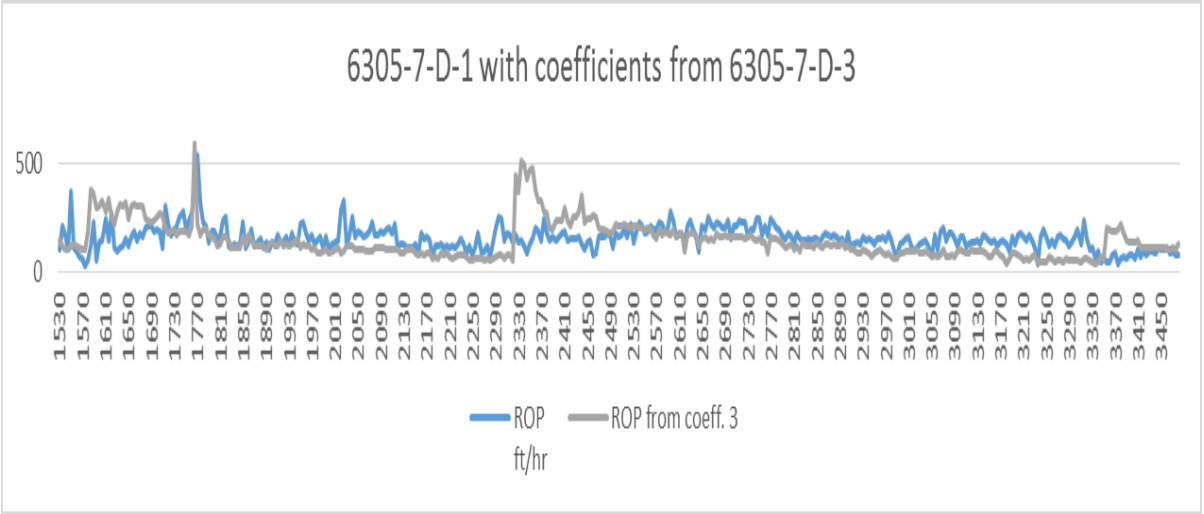

Figure 77: Multiple regression with Bourgoyne & Young's model - 6305/7-D-1 with coefficients from 6305/7-D-3

Well 6305/7-D-2 with coefficients applied from neighboring wells is presented in figures 78 and 79. Figure 78 shows the plot of ROP predicted by well 6305/7-D-1 coefficients. ROP modelled by well 6305/7-D-3 coefficients is displayed in figure 79. The results vary with the two sets of coefficients used in this well. Use of coefficients from well 6305/7-D-1 produce largely deviating results, unlike in the plain multiple regression method for this well. However, where the well 6305/7-D-3 coefficients are applied the results are significantly better.

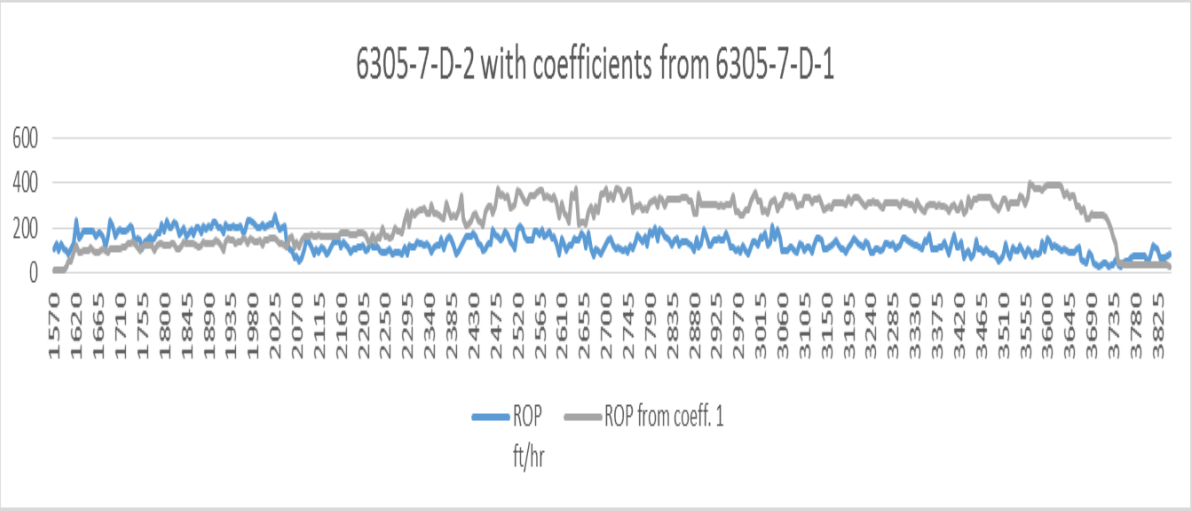

Figure 78: Multiple regression with Bourgoyne & Young's model - 6305/7-D-2 with coefficients from 6305/7-D-1

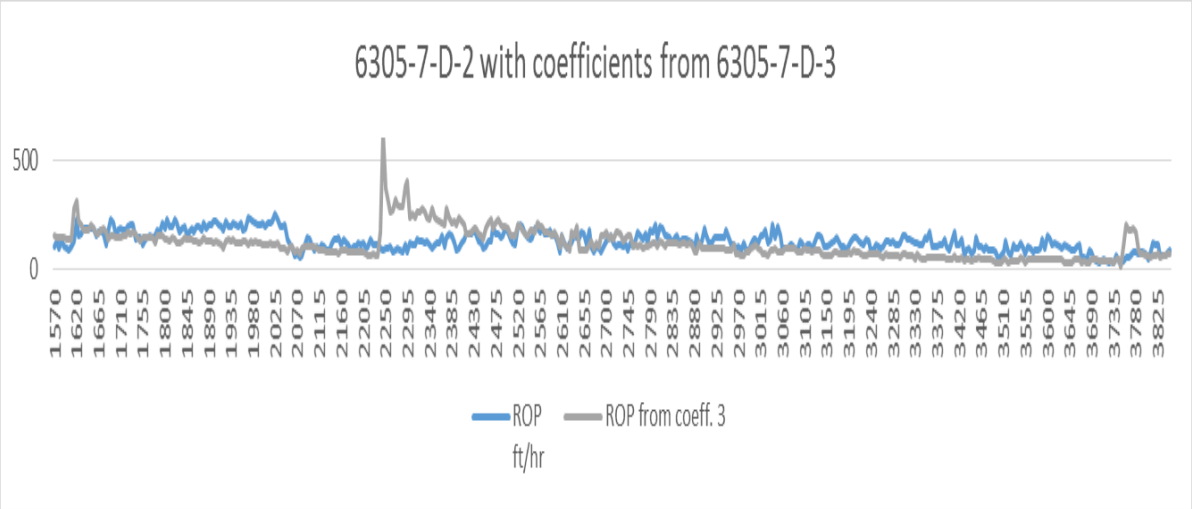

Figure 79: Multiple regression with Bourgoyne & Young's model - 6305/7-D-2 with coefficients from 6305/7-D-3

Figures 80 and 81 present well 6305/7-D-3 with coefficients applied from neighboring wells. Coefficients from well 6305/7-D-1 are used to model ROP in figure 80. In figure 81, the ROP is modelled with coefficients from well 6305/7-D-2. Similarly as in the plain multiple regression, the modelled ROP does not provide good results for coefficients applied in this well.

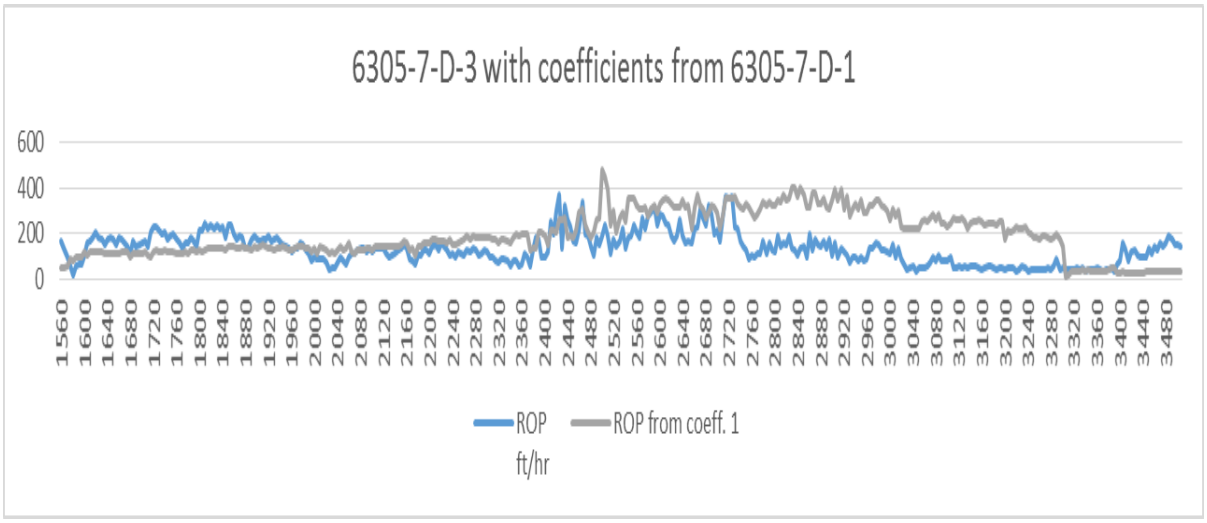

Figure 80: Multiple regression with Bourgoyne & Young's model - 6305/7-D-3 with coefficients from 6305/7-D-1

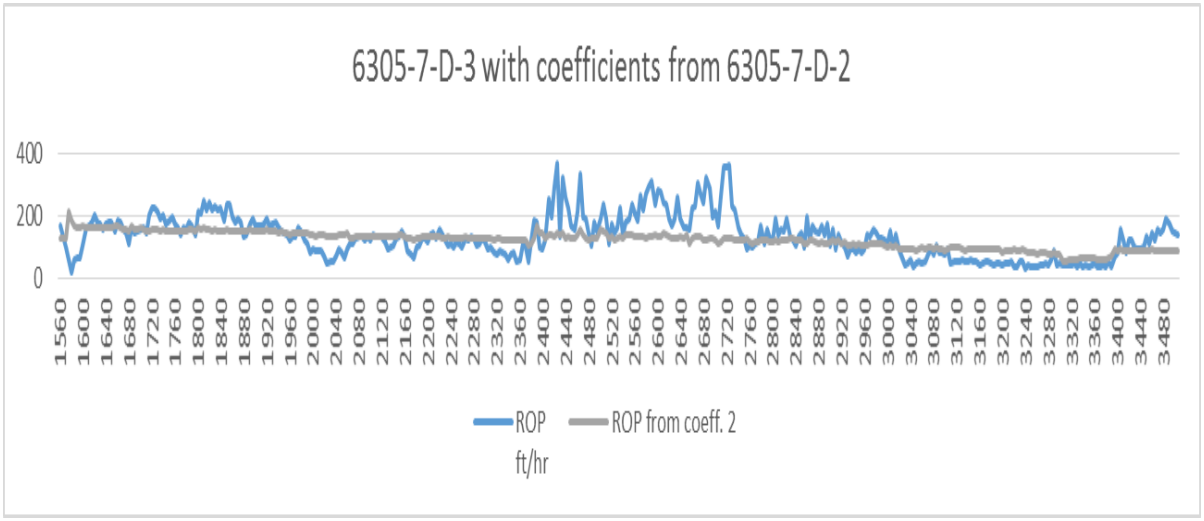

Figure 81: Multiple regression with Bourgoyne & Young's model - 6305/7-D-3 with coefficients from 6305/7-D-2

The following figures are plots from the Morvin field wells. ROP modelled plots of well 6506/11-A-1 with neighboring coefficients applied are displayed in figures 82 and 83. Figure 82 plots ROP modelled by well 6506/11-A-2 coefficients. In figure 83, the ROP is modelled by well 6506/11-A-3 coefficients. Results from this well appear neither better nor worse than the results by use of only multiple regression. Both sets of results seem adequate, with the results from well 6506/11-A-3 coefficients looking more correlative to the actual ROP.

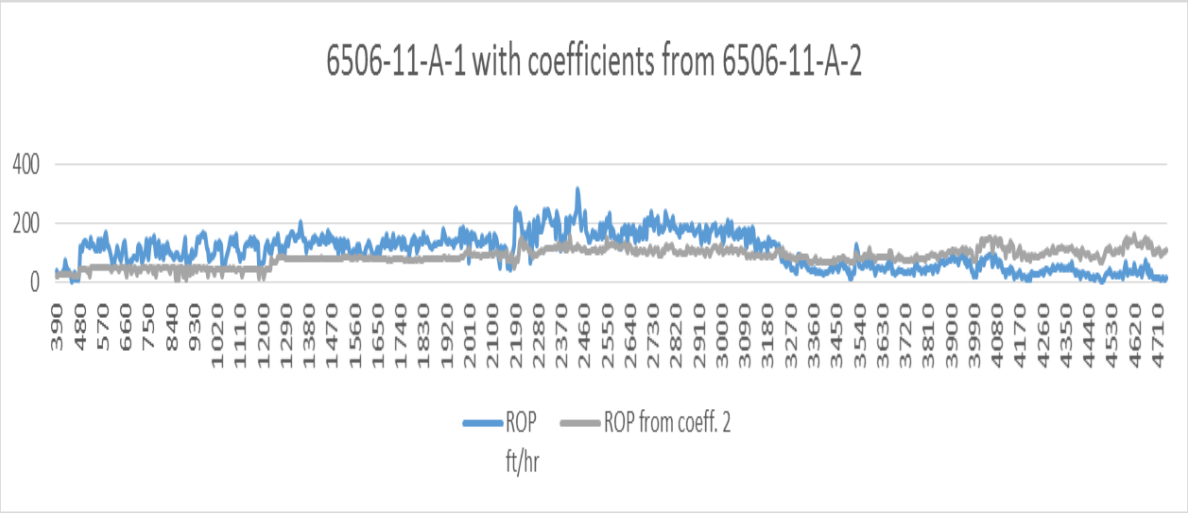

Figure 82: Multiple regression with Bourgoyne & Young's model - 6506/11-A-1 with coefficients from 6506/11-A-2

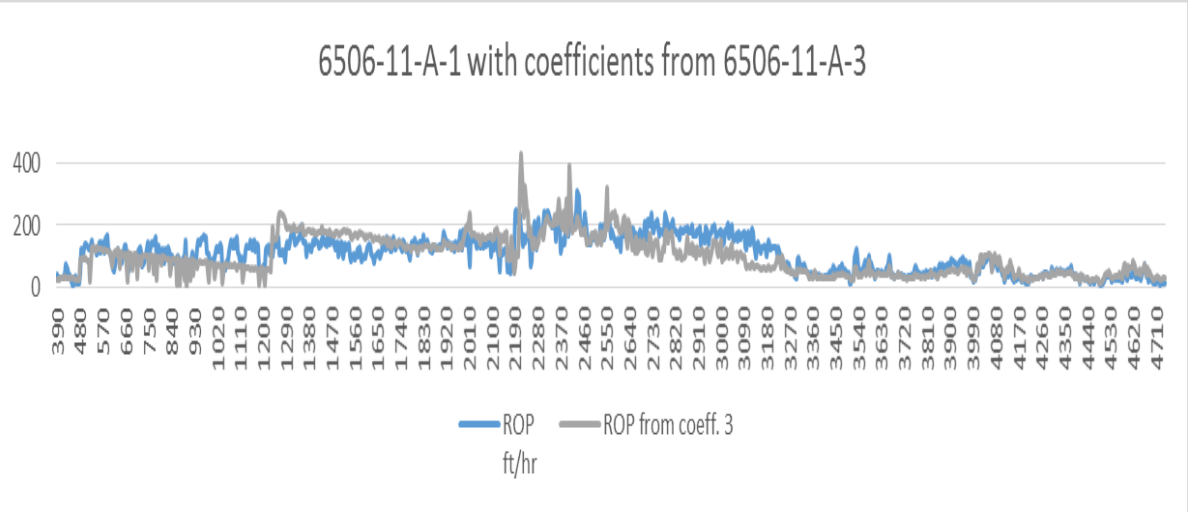

Figure 83: Multiple regression with Bourgoyne & Young's model - 6506/11-A-1 with coefficients from 6506/11-A-3

Well 6506/11-A-2 with coefficients applied from neighboring wells is presented in figures 84 and 85. Figure 84 shows the plot of the ROP predicted by well 6506/11-A-1 coefficients. The plot of the ROP predicted by well 6506/11-A-3 coefficients is displayed in figure 85. These plots appear by far as the most deviating results.

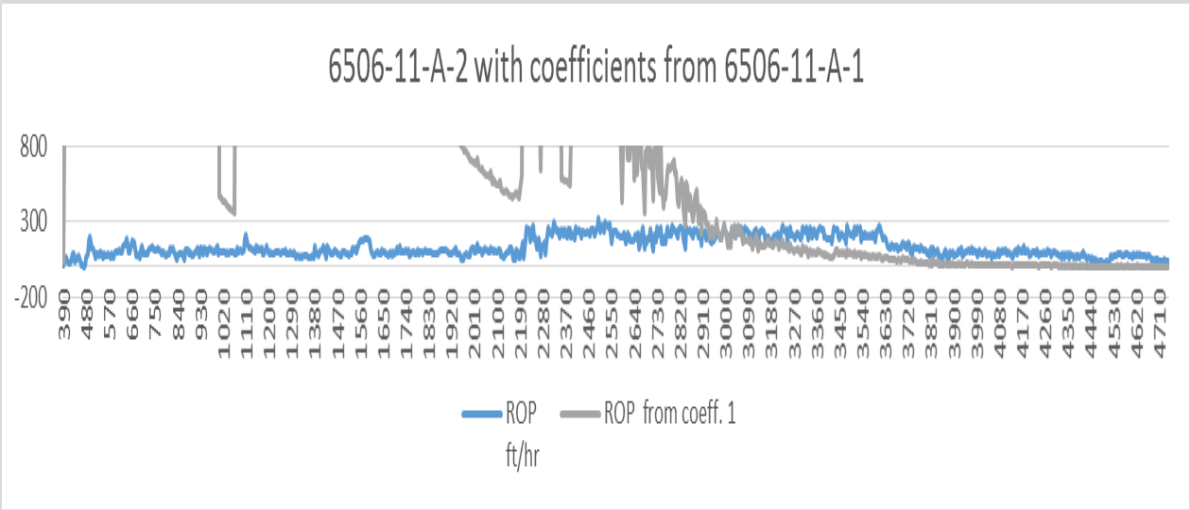

Figure 84: Multiple regression with Bourgoyne & Young's model - 6506/11-A-2 with coefficients from 6506/11-A-1

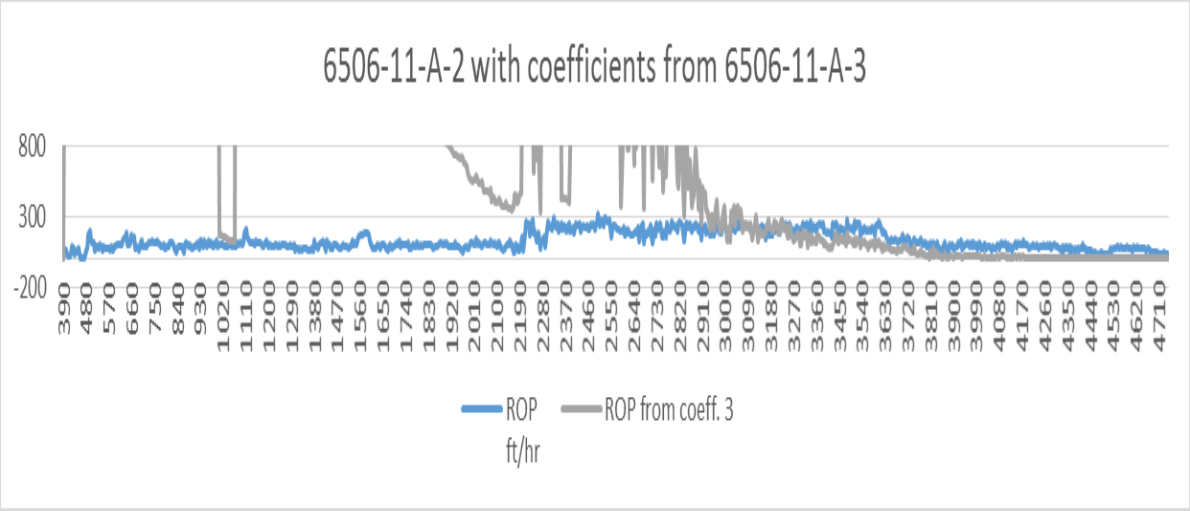

Figure 85: Multiple regression with Bourgoyne & Young's model - 6506/11-A-2 with coefficients from 6506/11-A-3

To complete the results of the multiple regression technique with Bourgoyne & Young's model in this thesis the 6506/11-A-3 plots of ROP modelled from coefficients of close-by wells are presented here. Figure 86 show the ROP predicted from well 6506/11-A-1 coefficients. This plot correlates well with the actual ROP. Well 6506/11-A-2 coefficients are displayed in figure 87. This plot appear to have worsen from the use of plain multiple regressions, by noticeably deviating over large parts of the plot.

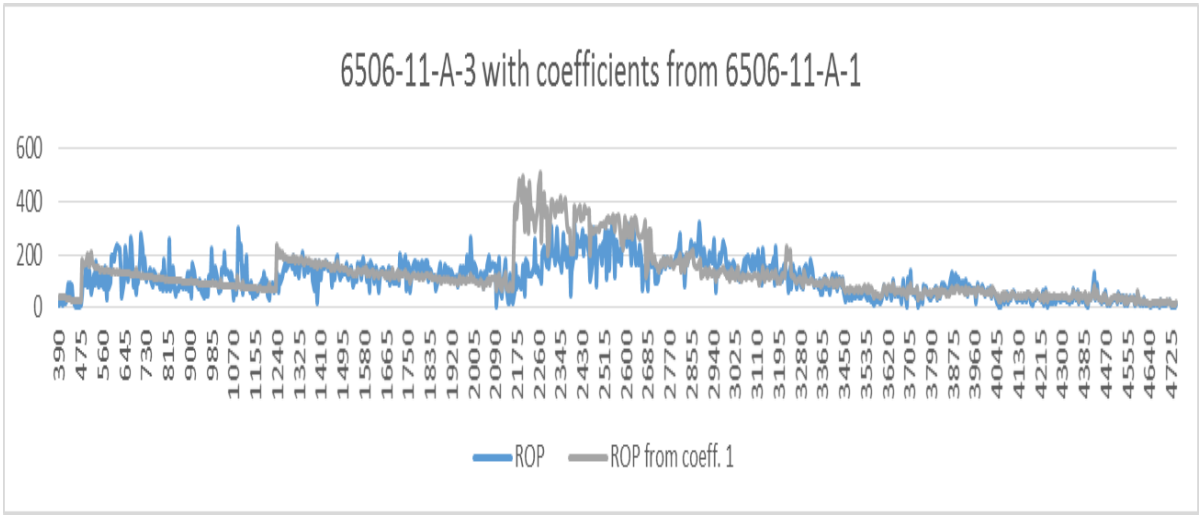

Figure 86: Multiple regression with Bourgoyne & Young's model - 6506/11-A-3 with coefficients from 6506/11-A-1

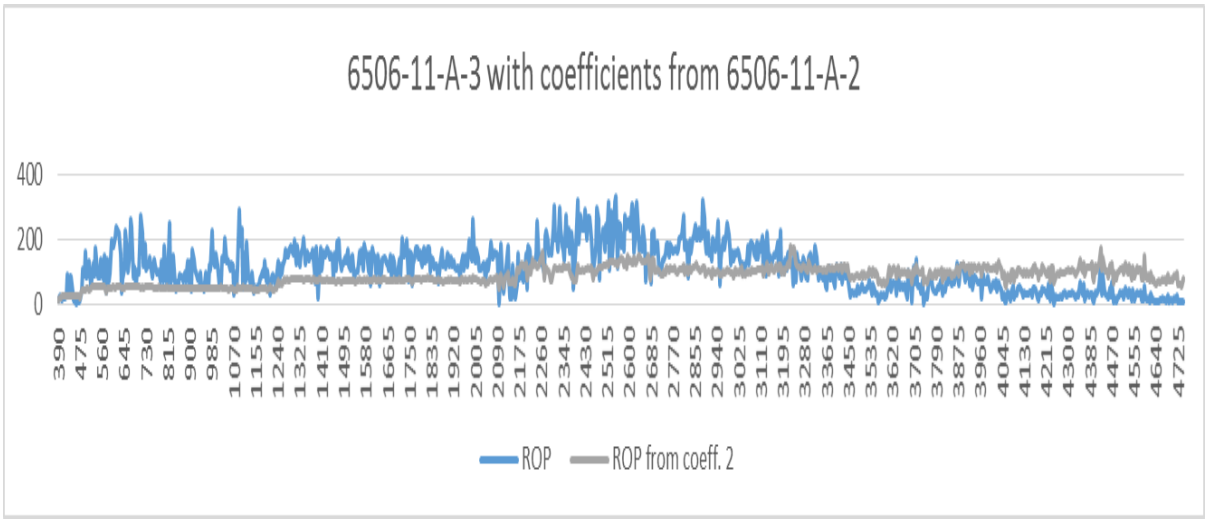

Figure 87: Multiple regression with Bourgoyne & Young's model - 6506/11-A-3 with coefficients from 6506/11-A-2

5.4 Least Square with Bourgoyne & Young's Model

The results from using the least square technique with Bourgoyne and Young's model are available in this section. Calculated coefficients for each of the six wells are presented in tables 19 to 24.

6305-7-D-1	*Coefficients*
Intercept	2,16186292
X-variabel 1	9,4388E-05
X-variabel 2	0,00043157
X-variabel 3	0
X-variabel 4	0
X-variabel 5	0,25840718
X-variabel 6	2,25218612
X-variabel 7	8,0918E-06

19

6305-7-D-2	*Coefficients*
Intercept	4,45334395
X-variabel 1	0,0001293
X-variabel 2	0,00012888
X-variabel 3	0
X-variabel 4	0
X-variabel 5	0,36318188
X-variabel 6	0
X-variabel 7	0

20

6305-7-D-3	*Coefficients*
Intercept	0,04883496
X-variabel 1	0,00013349
X-variabel 2	0,00037065
X-variabel 3	0
X-variabel 4	0
X-variabel 5	0,48274846
X-variabel 6	4,18560799
X-variabel 7	0

21

6506-11-A-1	*Coefficients*
Intercept	0,04289576
X-variabel 1	0,00013918
X-variabel 2	0,00025041
X-variabel 3	0,00102158
X-variabel 4	0
X-variabel 5	0,30624914
X-variabel 6	3,11749218
X-variabel 7	7,7026E-05

22

6506-11-A-2	*Coefficients*
Intercept	1,36523342
X-variabel 1	7,2948E-05
X-variabel 2	0,00069895
X-variabel 3	0,00037711
X-variabel 4	0
X-variabel 5	0,24184414
X-variabel 6	1,36523637
X-variabel 7	0,00011708

23

6506-11-A-3	*Coefficients*
Intercept	0,09219548
X-variabel 1	0,00019387
X-variabel 2	0,00080278
X-variabel 3	0,00038018
X-variabel 4	0
X-variabel 5	0,32045484
X-variabel 6	2,09057107
X-variabel 7	0,00010949

24

Figures 88 to 93 show the resulting ROP plots from implementing the coefficients in their originating well. The Ormen Lange wells are presented in figures 88 to 90. Wells 6305/7-D-1 and 6305/7-D-2 has good results, and as with the previous methods well 6305/7-D-3 has far less accurate predicting results. Well 6305/7-D-1 prediction appears to correlates very well with the actual ROP.

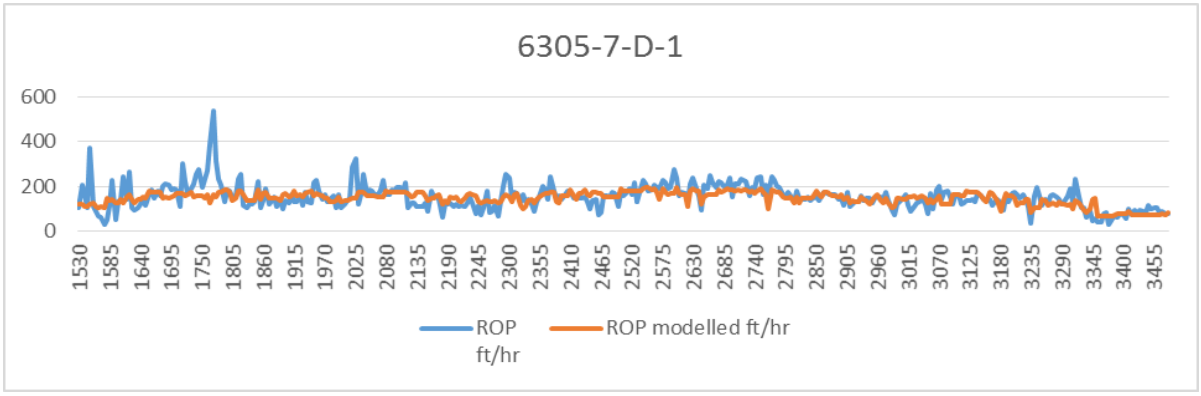

Figure 88: Least square with Bourgoyne & Young's model in well 6305/7-D-1

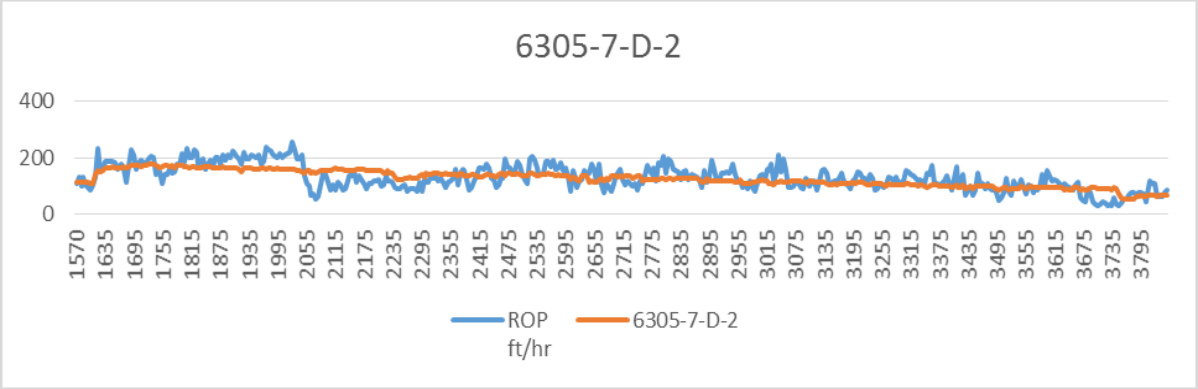

Figure 89: Least square with Bourgoyne & Young's model in well 6305/7-D-2

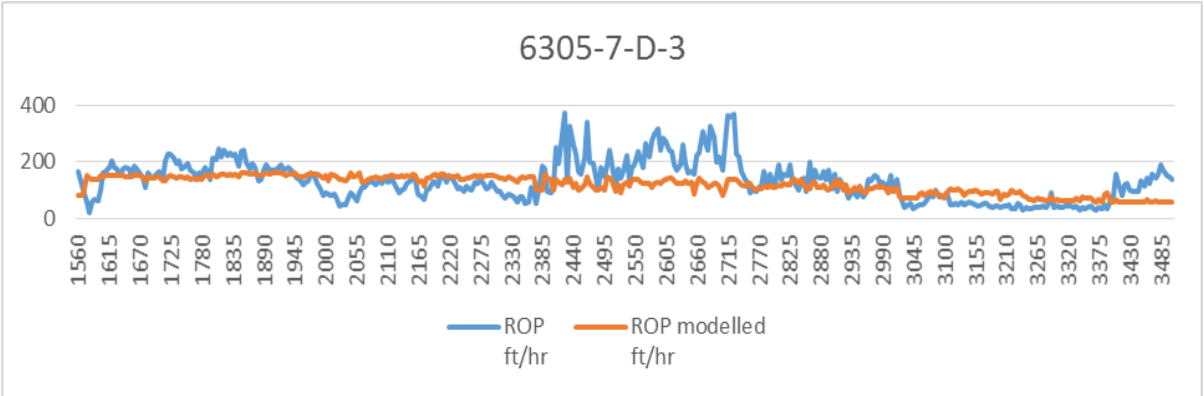

Figure 90: Least square with Bourgoyne & Young's model in well 6305/7-D-3

Figures 91 to 93 are the Morvin field wells. Well 6506/11-A-1 prediction does not differ much from the plain least square prediction in figure 55. Wells 6506/11-A-2 and 6506/11-A-3 predictions however have a clear and impressive improvement with the Bourgoyne and Young's model. These plots are far more correlative with the actual ROP.

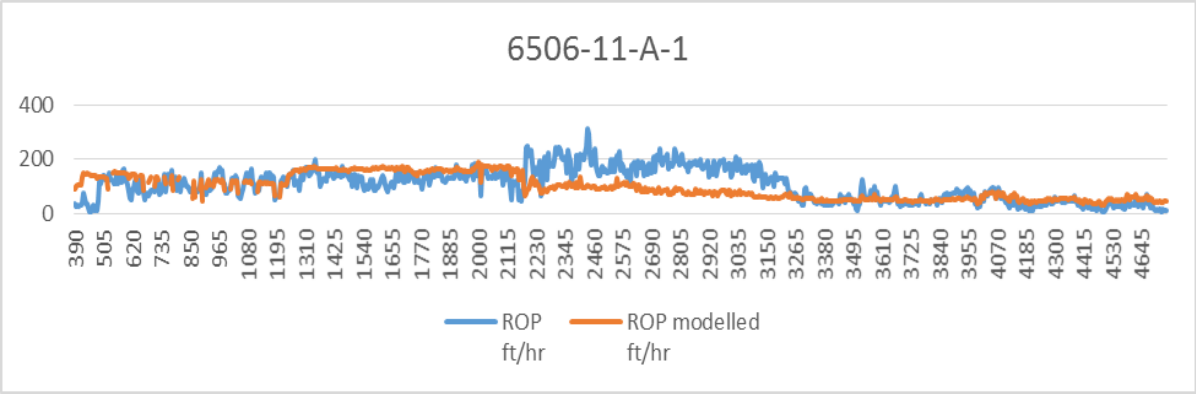

Figure 91: Least square with Bourgoyne & Young's model in well 6506/11-A-1

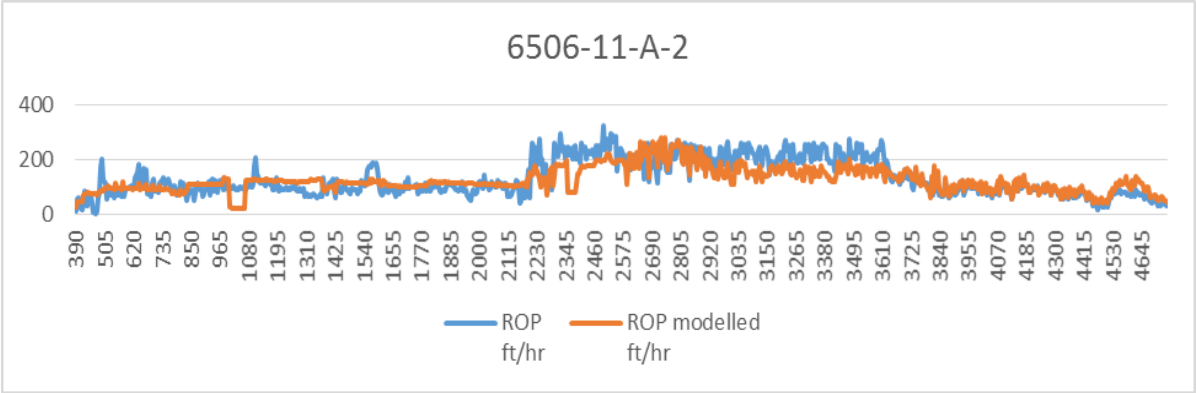

Figure 92: Least square with Bourgoyne & Young's model in well 6506/11-A-2

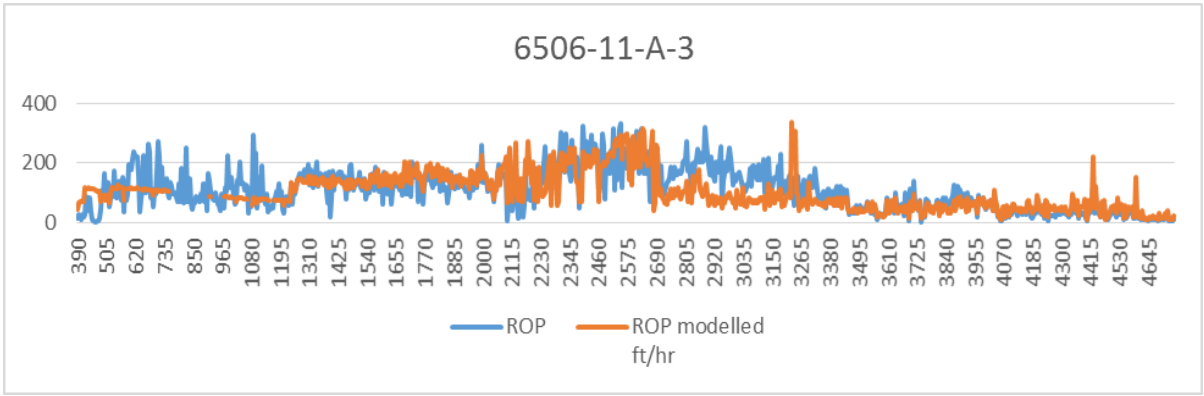

Figure 93: Least square with Bourgoyne & Young's model in well 6506/11-A-3

Shown here are the plotted results of ROP predicted by coefficients applied from close-by wells. The Ormen Lange wells are first presented. Well 6305/7-D-1 plots are shown in figures 94 and 95. Figure 94 has the predicted ROP by use of coefficients from well 6305/7-D-2. In figure 95, the ROP is modelled by coefficients from well 6305/7-D-3. Both predicted plots have fairly low deviation from the actual ROP. Coefficients from well 6305/7-D-3 appear more correlating.

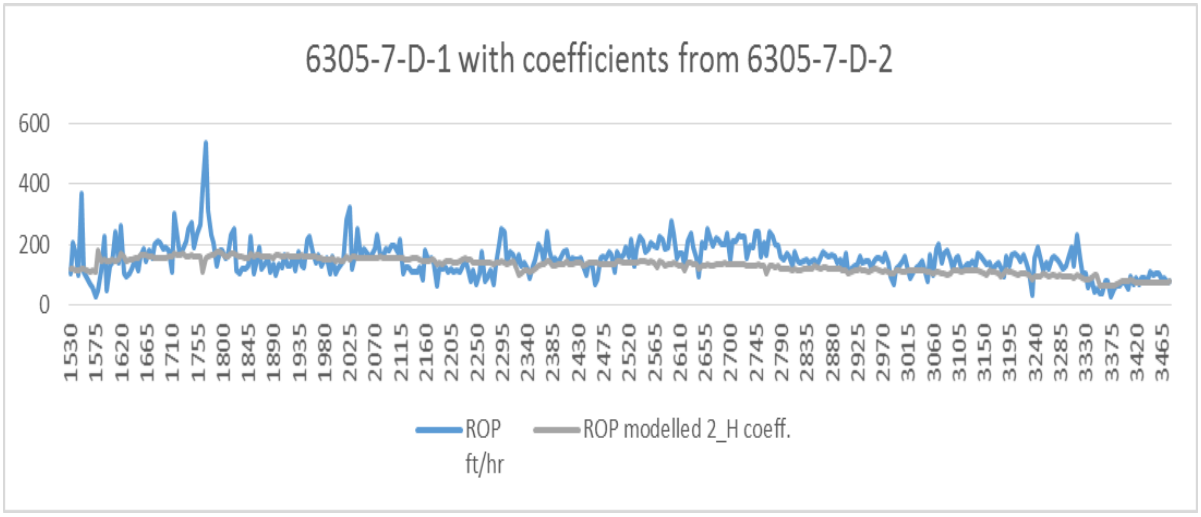

Figure 94: Least square with Bourgoyne & Young's model - 6305/7-D-1 with coefficients from 6305/7-D-2

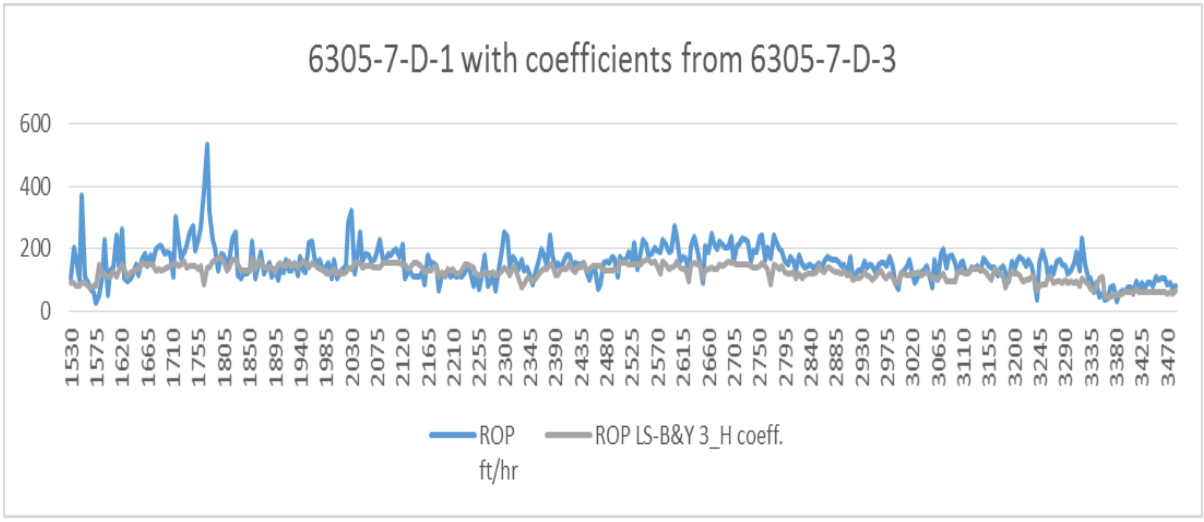

Figure 95: Least square with Bourgoyne & Young's model - 6305/7-D-1 with coefficients from 6305/7-D-3

Well 6305/7-D-2 with coefficients applied from neighboring wells are presented in figures 96 and 97. Figure 96 shows the plot of ROP predicted by well 6305/7-D-1 coefficients. The ROP modelled by well 6305/7-D-3 coefficients is displayed in figure 97. Both plots seem to correlate very well, though the one based on coefficients from well 6305/7-D-1 displays more deviation.

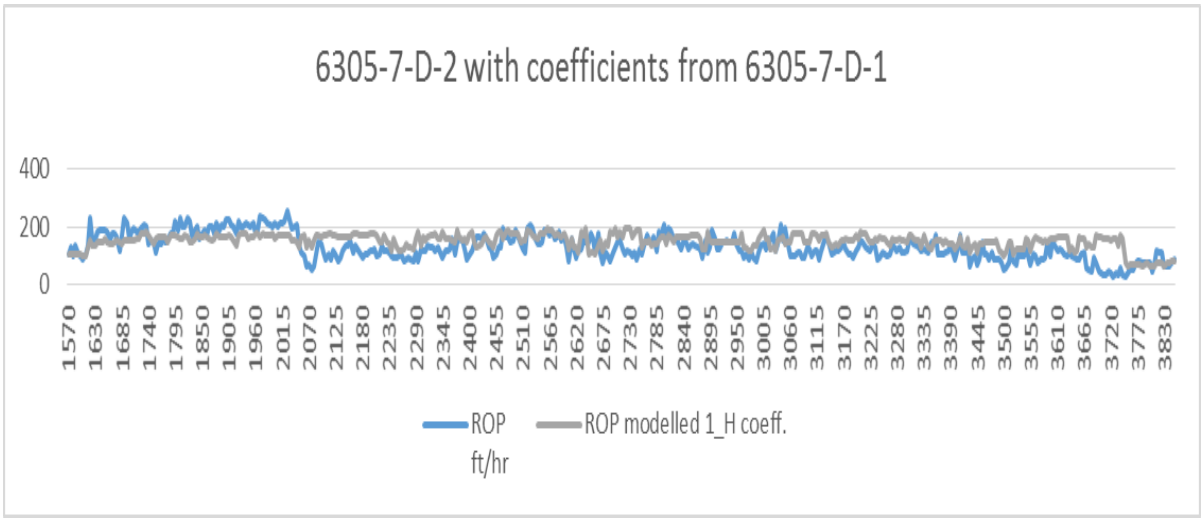

Figure 96: Least square with Bourgoyne & Young's model - 6305/7-D-2 with coefficients from 6305/7-D-1

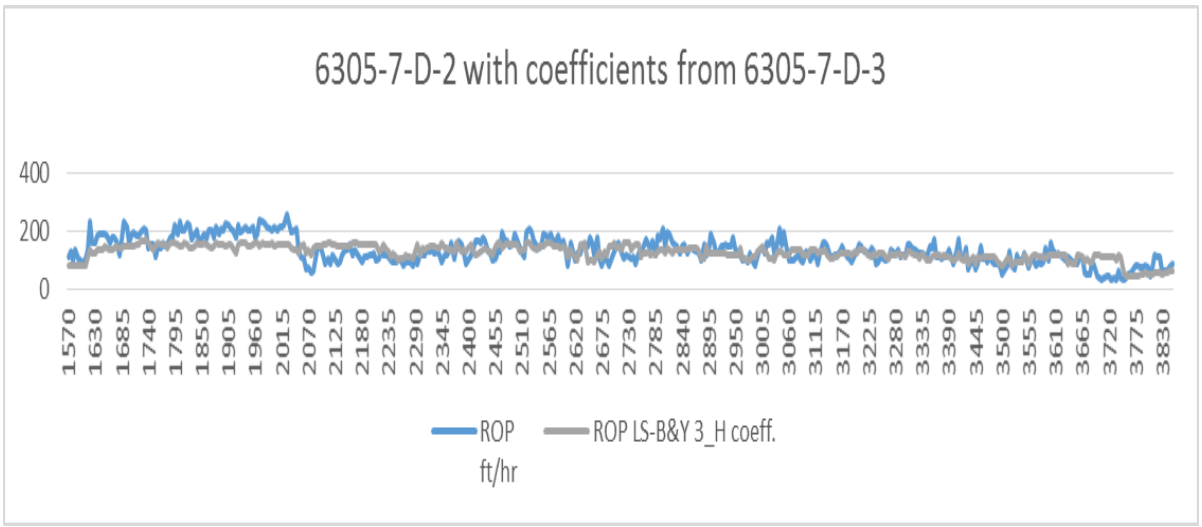

Figure 97: Least square with Bourgoyne & Young's model - 6305/7-D-2 with coefficients from 6305/7-D-3

Figures 98 and 99 presents well 6305/7-D-3 with coefficients applied from neighboring wells. Coefficients from well 6305/7-D-1 are used to model ROP in figure 98. In figure 99, ROP is modelled with coefficients from well 6305/7-D-2. These results are, as with the previous method, the weakest. However, there seems to be slight improvements with this method. Especially the coefficients from well 6305/7-D-1 are correlating far better.

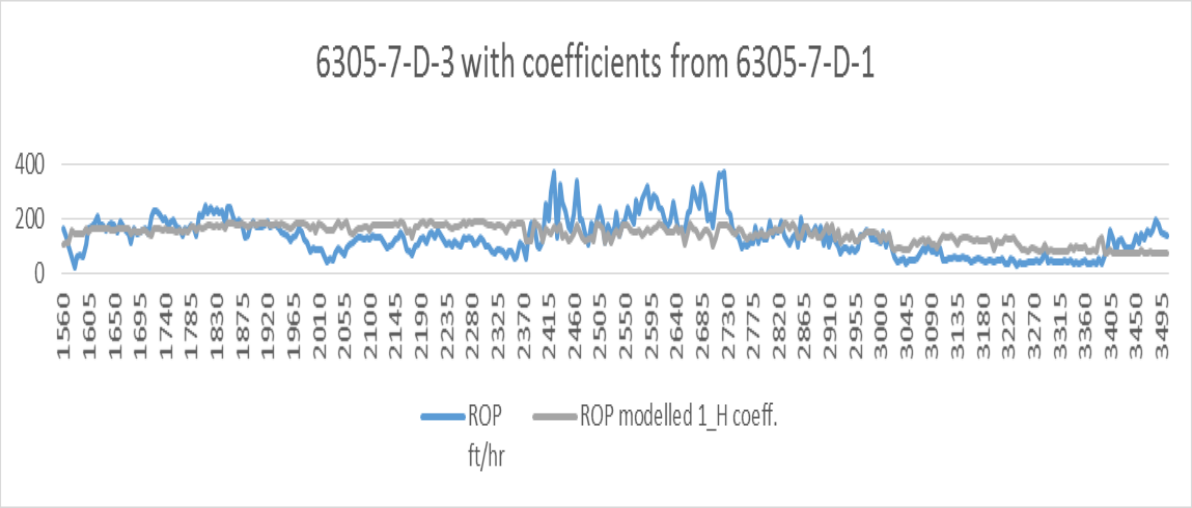

Figure 98: Least square with Bourgoyne & Young's model - 6305/7-D-3 with coefficients from 6305/7-D-1

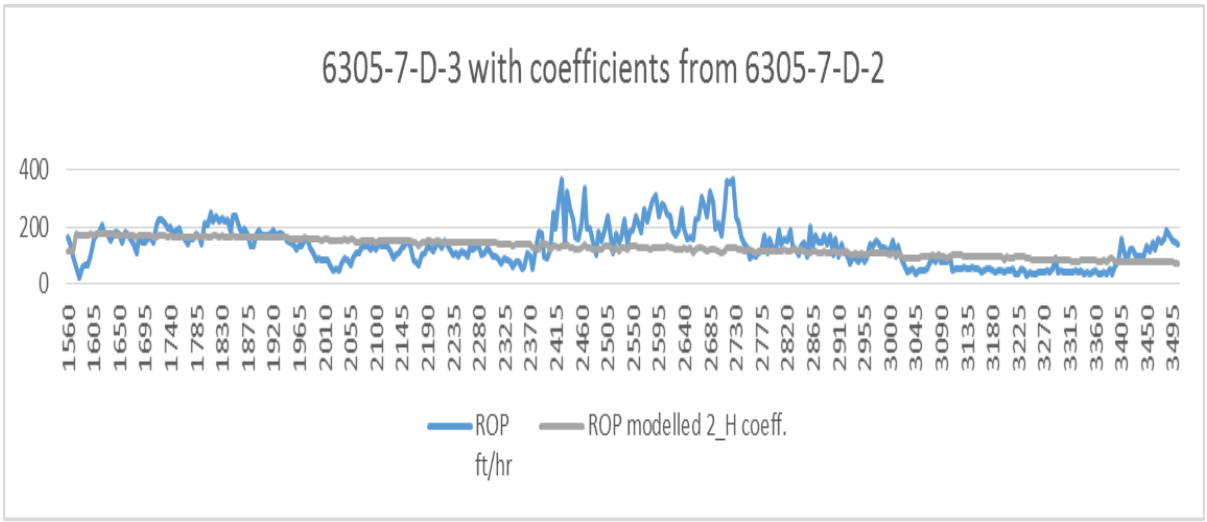

Figure 99: Least square with Bourgoyne & Young's model - 6305/7-D-3 with coefficients from 6305/7-D-2

The following figures are plots from the Morvin field wells. ROP plots of well 6506/11-A-1 with neighboring coefficients applied are displayed in figures 100 and 101. Figure 100 plots ROP modelled by well 6506/11-A-2 coefficients. In figure 101 the ROP is modelled by well 6506/11-A-3 coefficients. Although well 6506/11-A-2 coefficients give less deviation in the middle, well 6506/11-A-3 coefficients correlate far better towards the end of the plot.

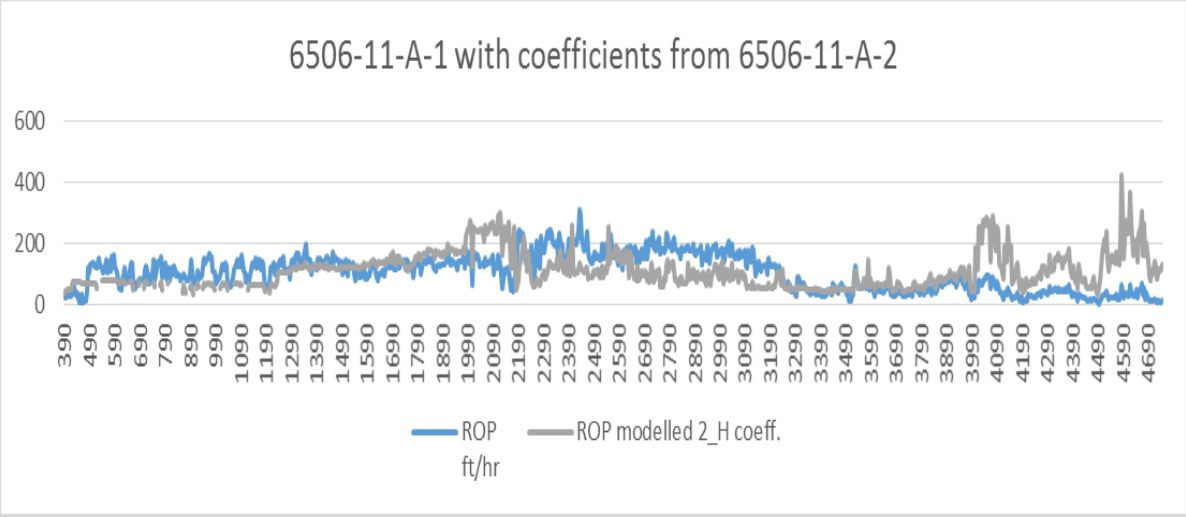

Figure 100: Least square with Bourgoyne & Young's model - 6506/11-A-1 with coefficients from 6506/11-A-2

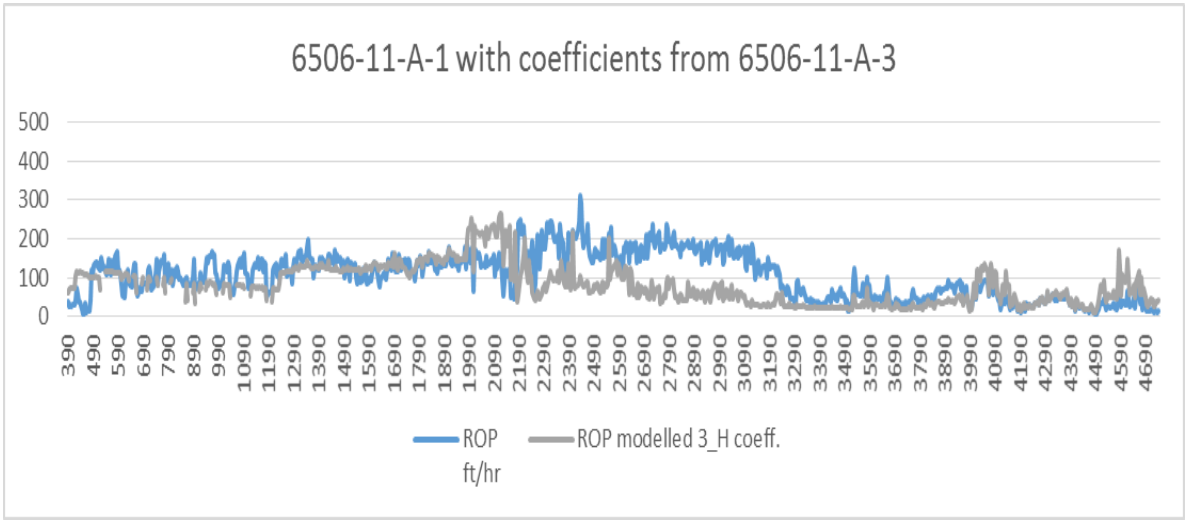

Figure 101: Least square with Bourgoyne & Young's model - 6506/11-A-1 with coefficients from 6506/11-A-3

Well 6506/11-A-2 with coefficients applied from neighboring wells is presented in figures 102 and 103. Figure 102 show the plot of ROP predicted by well 6506/11-A-1 coefficients. Plot of ROP predicted by well 6506/11-A-3 coefficients is displayed in figure 103. Both predicted plots seem to decline throughout to match the beginning and end of the actual plot. The Well 6506/11-A-3 coefficients plot additionally manages to correlate partly during the middle elevated actual ROP values. This plot correlates well before the elevated part of the actual ROP.

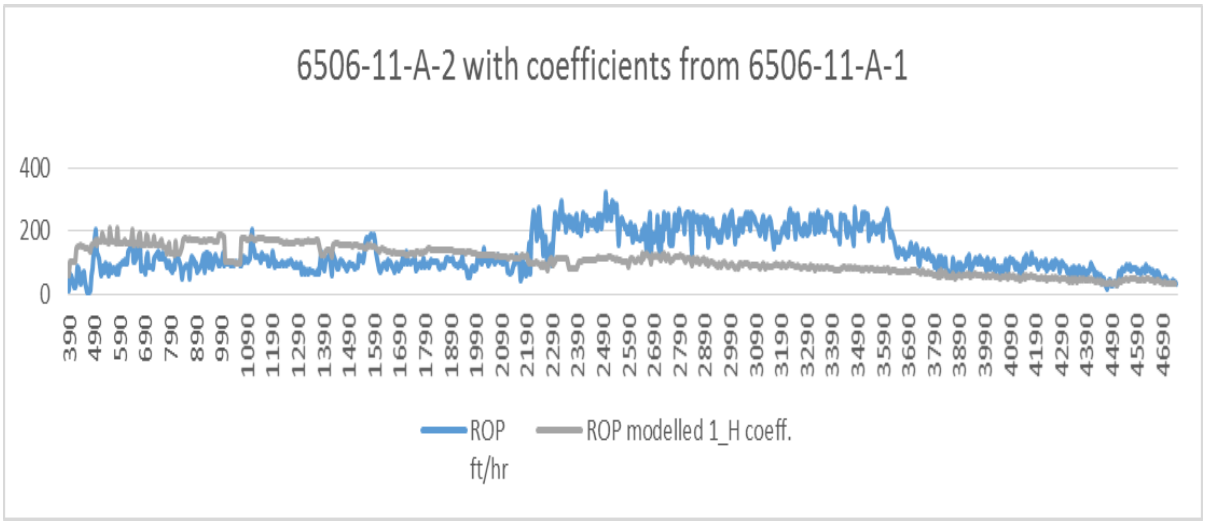

Figure 102: Least square with Bourgoyne & Young's model - 6506/11-A-2 with coefficients from 6506/11-A-1

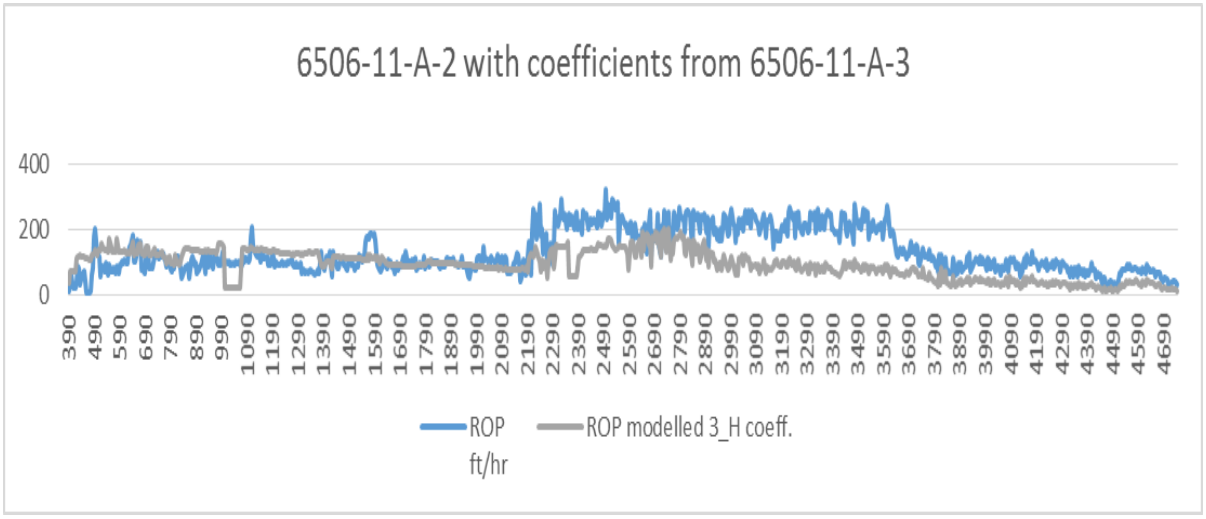

Figure 103: Least square with Bourgoyne & Young's model - 6506/11-A-2 with coefficients from 6506/11-A-3

To complete the testing results of the least square technique with Bourgoyne & Young's model in this thesis are the 6506/11-A-3 plots of modelled ROP from coefficients of close-by wells. Figure 104 shows the ROP predicted from well 6506/11-A-1 coefficients. Well 6506/11-A-2 coefficients displayed in figure 105. The two sets of coefficients applied in well 6506/11-A-3 seem to produce vastly different results. Neither of the results are bad, but the coefficients from well 6506/11-A-2 appear more accurate.

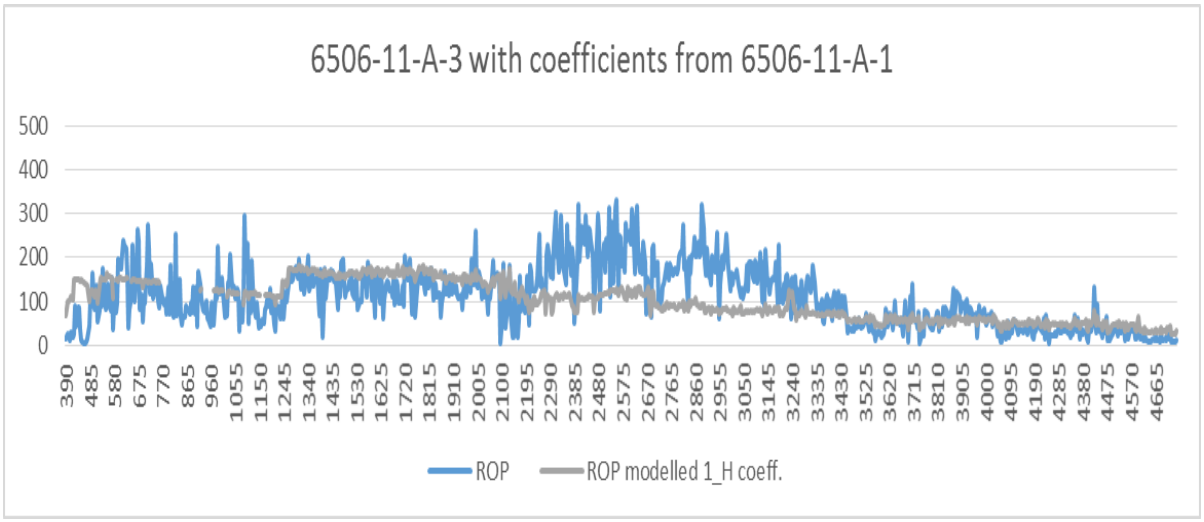

Figure 104: Least square with Bourgoyne & Young's model - 6506/11-A-3 with coefficients from 6506/11-A-1

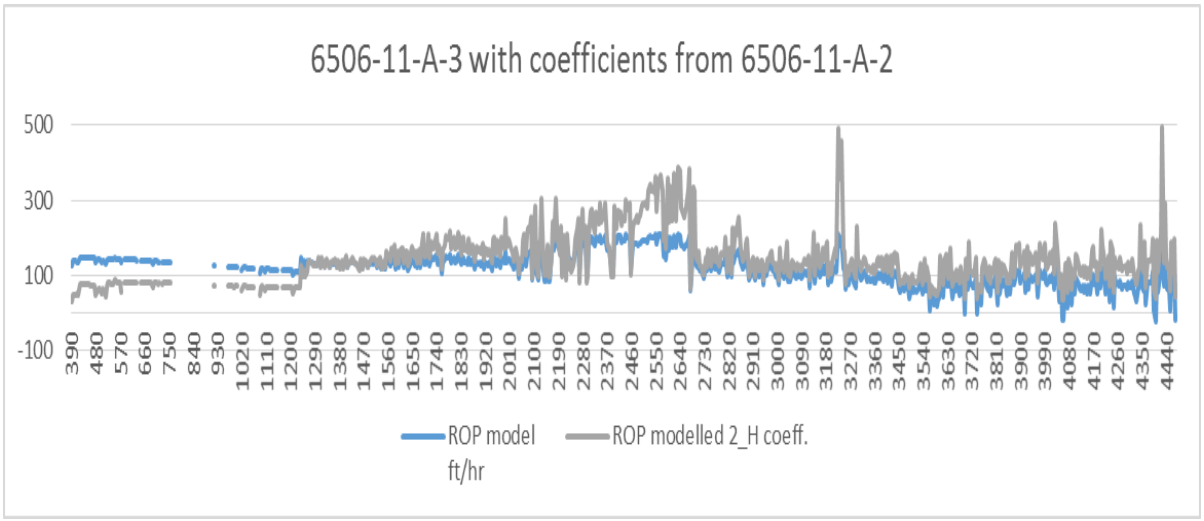

Figure 105: Least square with Bourgoyne & Young's model - 6506/11-A-3 with coefficients from 6506/11-A-2

5.5 D-Exponent

The results from using the D-Exponent method are available in this section. Results from using the D-Exponent method between wells 6305/7-D-1 and 6305/7-D-2 are presented in figures 106 to 108. In figure 106 the D-Exponents from the wells are compared. The plots are similar but several deviations occur. Results produced by the D-Exponent method in these wells are partly adequate. The deviations in figures 107 and 108 appear correlative to the deviations between the D-Exponents in figure 106. There is a clear difference of the magnitude between these deviations. These observations are also detected for all other wells.

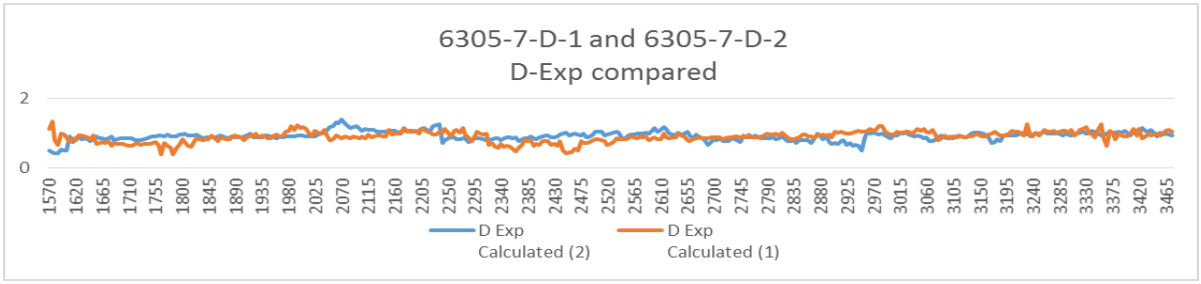

Figure 106: 6305/7-D-1 and 6305/7-D-2 d-exponents compared

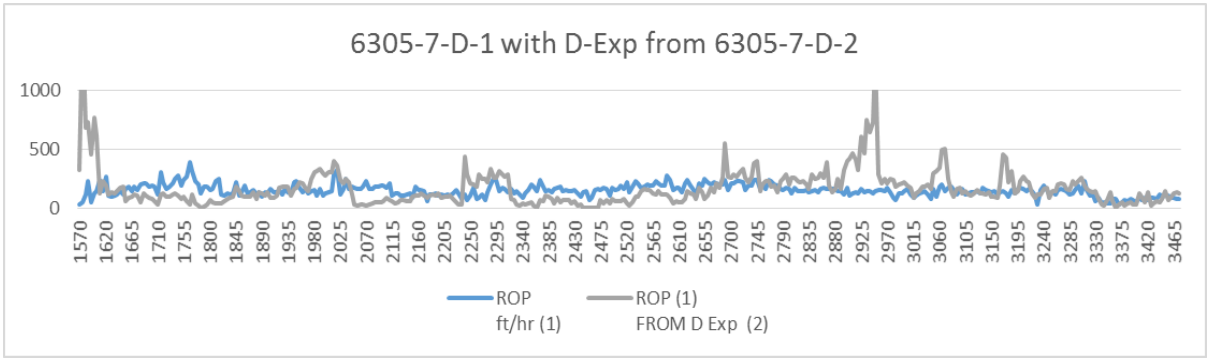

Figure 107: 6305/7-D-1 with d-exponent from 6305/7-D-2

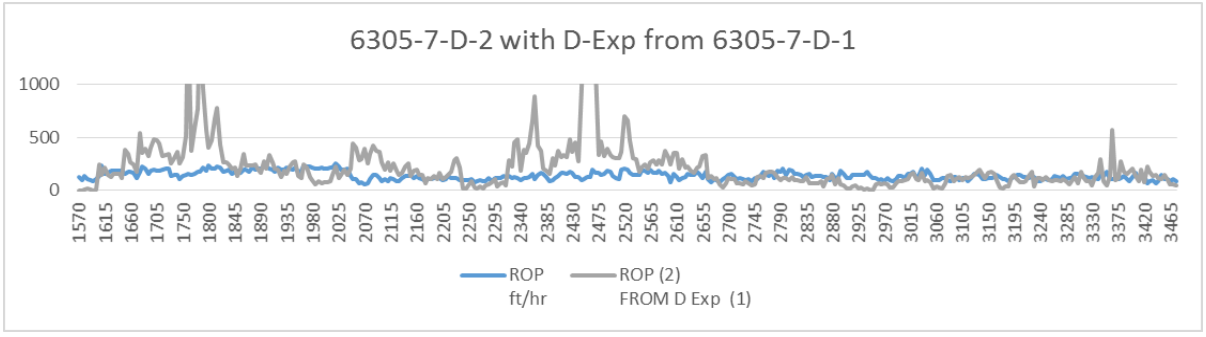

Figure 108: 6305/7-D-2 with d-exponent from 6305/7-D-1

Results from using the D-Exponent method between wells 6305/7-D-1 and 6305/7-D-3 are presented in figures 109 to 11. The compared D-Exponents correlate over large parts of the plot in figure 109.

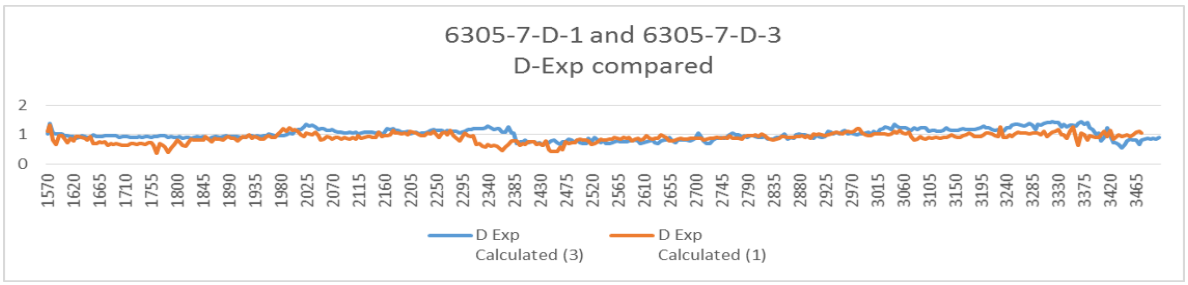

Figure 109: 6305/7-D-1 and 6305/7-D-3 d-exponents compared

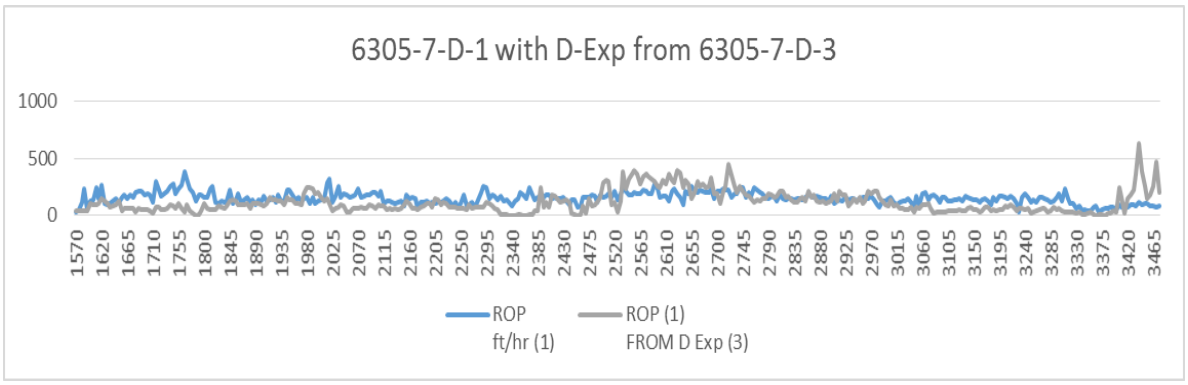

Figure 110: 6305/7-D-1 with d-exponent from 6305/7-D-3

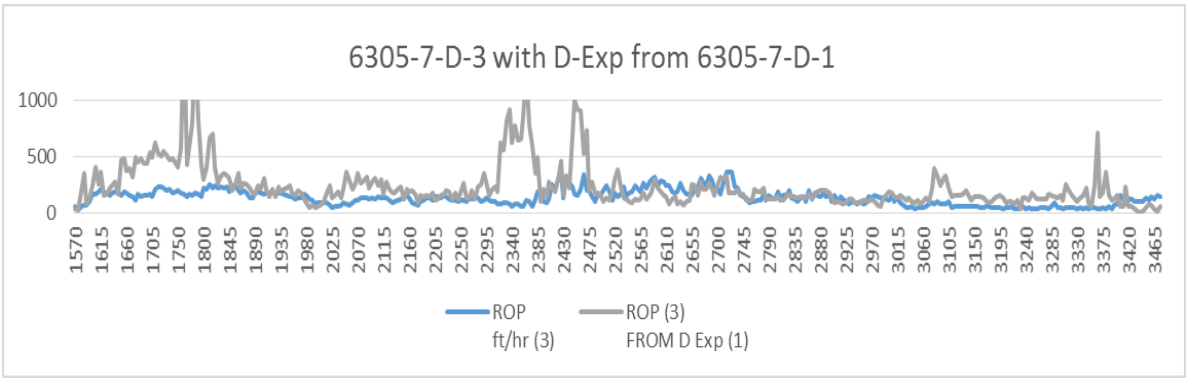

Figure 111: 6305/7-D-3 with d-exponent from 6305/7-D-1

Results from using the D-Exponent method between wells 6305/7-D-2 and 6305/7-D-3 are presented in figures 112 to 114. When compared the D-Exponent plots appear very close, but only partly completely correlate in figure 112.

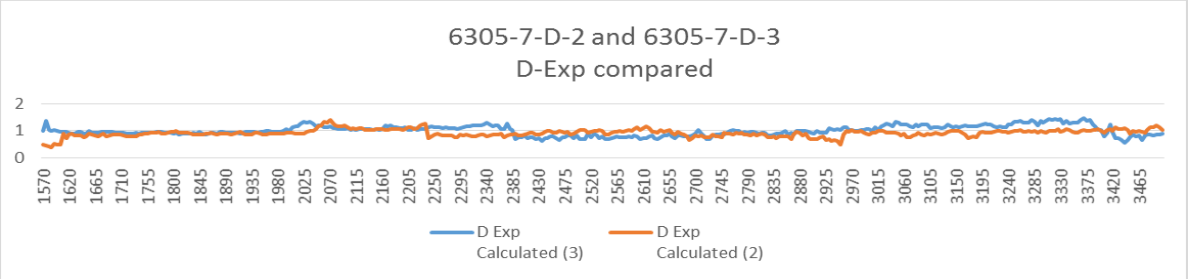

Figure 112: 6305/7-D-2 and 6305/7-D-3 d-exponents compared

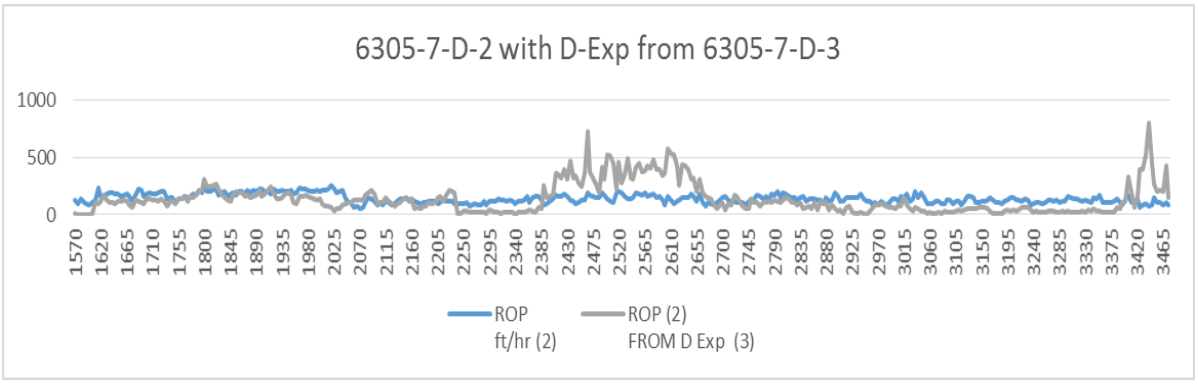

Figure 113: 6305/7-D-2 with d-exponent from 6305/7-D-3

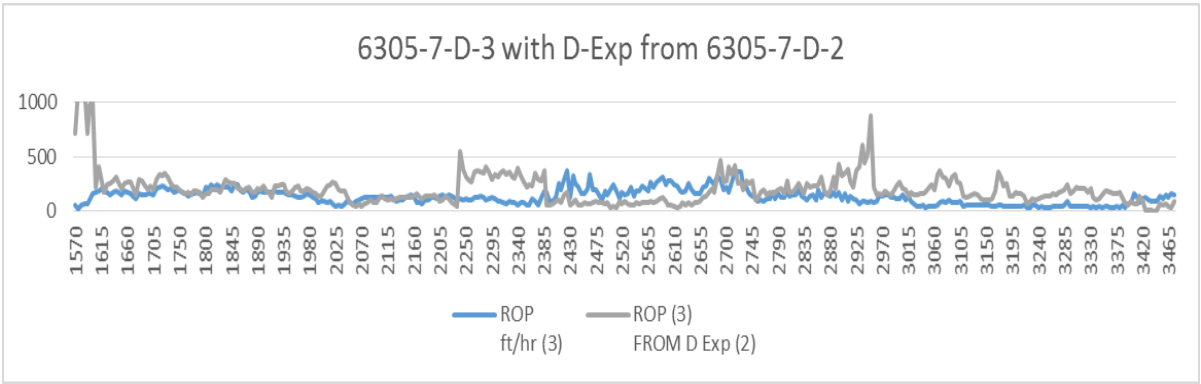

Figure 114: 6305/7-D-3 with d-exponent from 6305/7-D-2

Results from using the D-Exponent method between wells 6506/11-A-1 and 6506/11-A-2 are presented in figures 115 to 117. The D-Exponents compared show close similarity, though deviation seems to slowly increase with increasing depth.

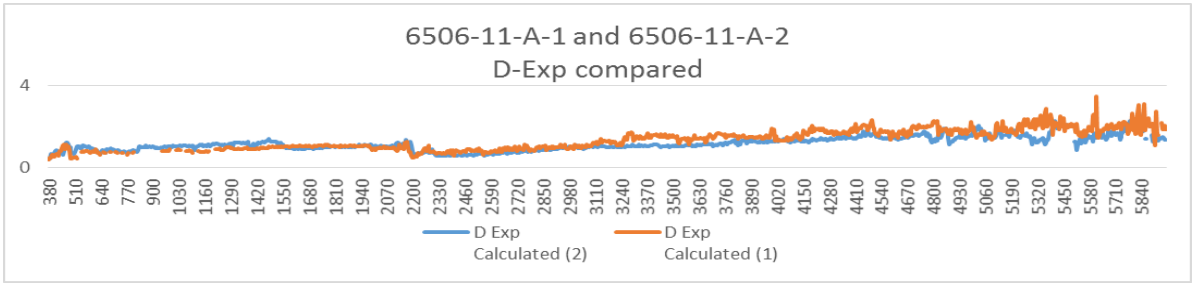

Figure 115: 6506/11-A-1 and 6506/11-A-2 d-exponents compared

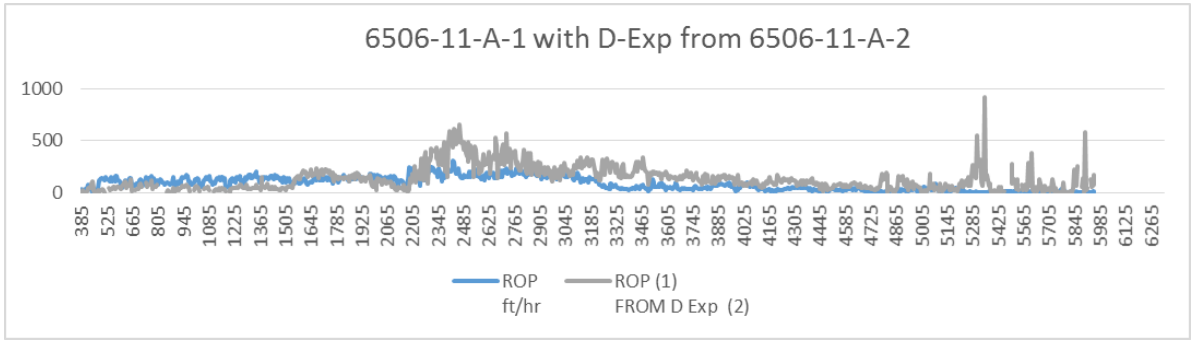

Figure 116: 6506/11-A-1 with d-exponent from 6506/11-A-2

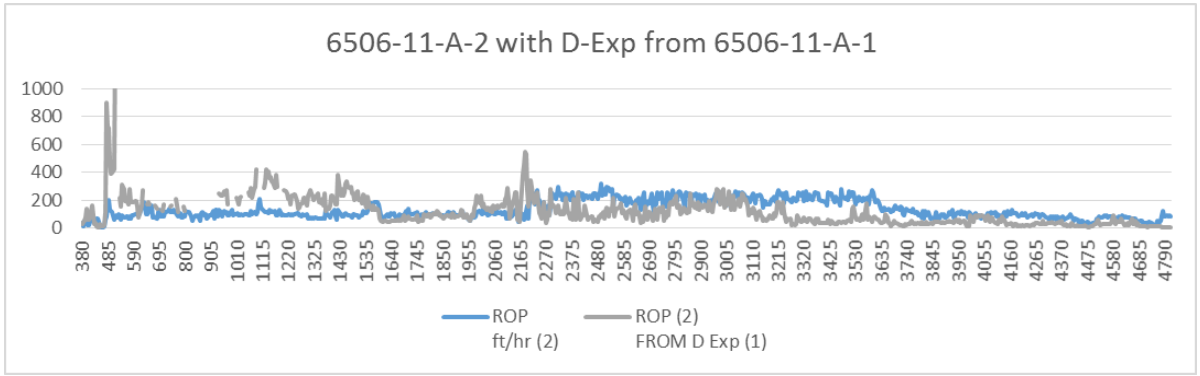

Figure 117: 6506/11-A-2 with d-exponent from 6506/11-A-1

Results from using the D-Exponent method between wells 6506/11-A-1 and 6506/11-A-3 are presented in figures 118 to 120. The D-Exponents compared are quite similar, and only a few visible deviations occur. Although there seems to be minimal deviation between the D-Exponents, there is a massive deviation of the predicted ROP in figure 119.

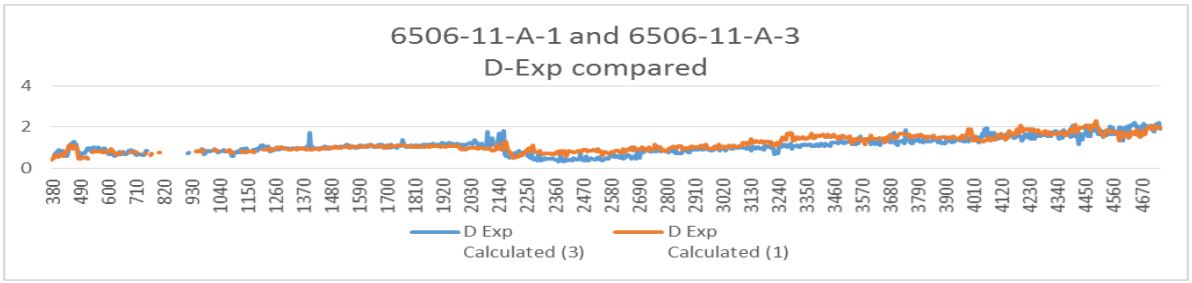

Figure 118: 6506/11-A-1 and 6506/11-A-3 d-exponents compared

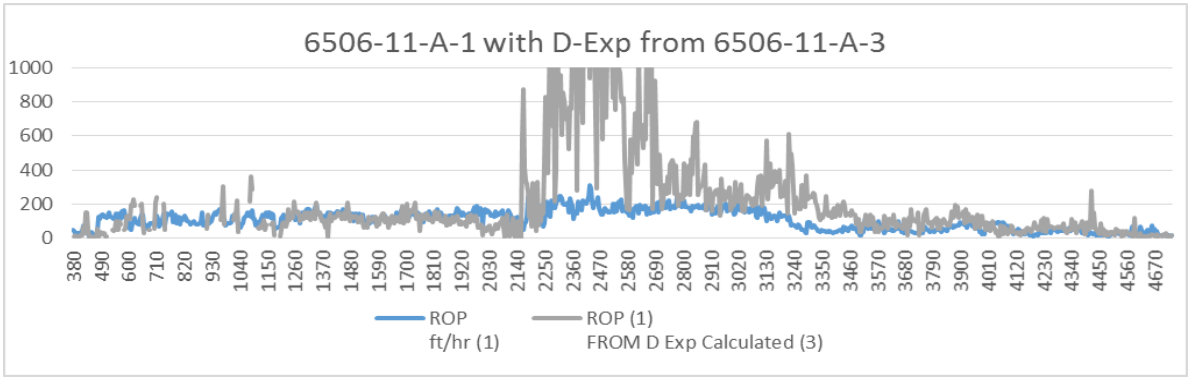

Figure 119: 6506/11-A-1 with d-exponent from 6506/11-A-3

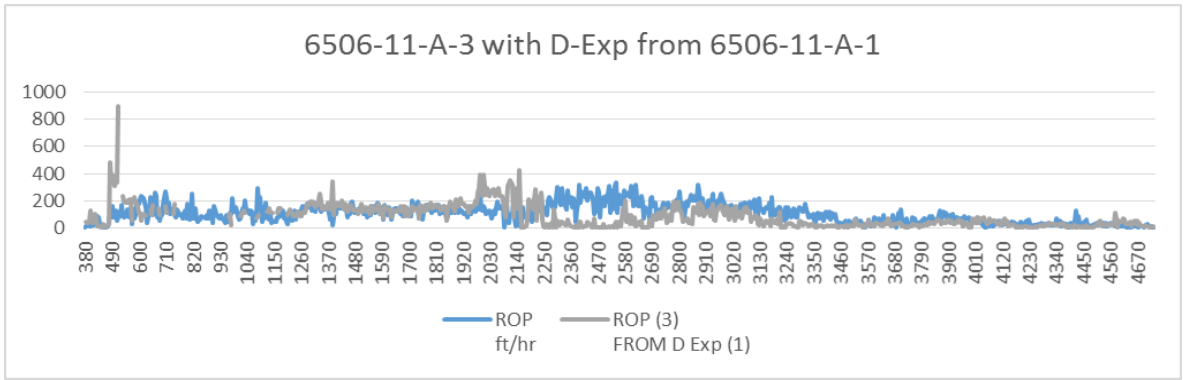

Figure 120: 6506/11-A-3 with d-exponent from 6506/11-A-1

Results from using the D-Exponent method between wells 6506-11-A-2 and 6506-11-A-3 are presented in figures 121 to 123. Again, the compared D-Exponents shows very little visible deviation. Also well 6506-11-A-2 has a high elevation of predicted ROP from the D-Exponents from well 6506-11-A-3. These elevations appear to be in the same location as in figure 119. The predicted ROP plot in figure 123 seems to be impressively correlating with the actual ROP.

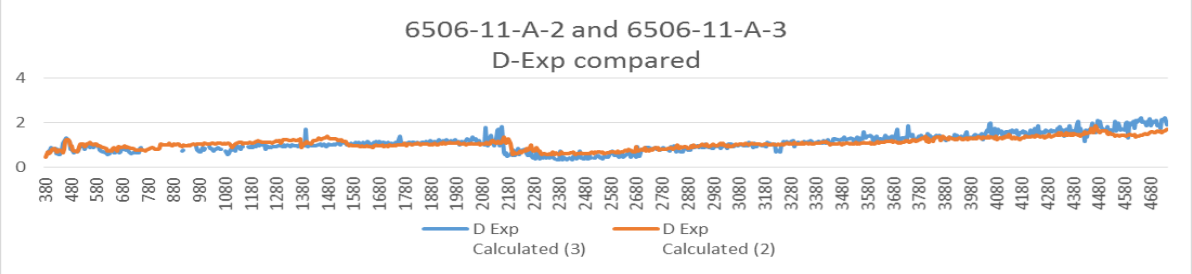

Figure 121: 6506/11-A-2 and 6506/11-A-3 d-exponents compared

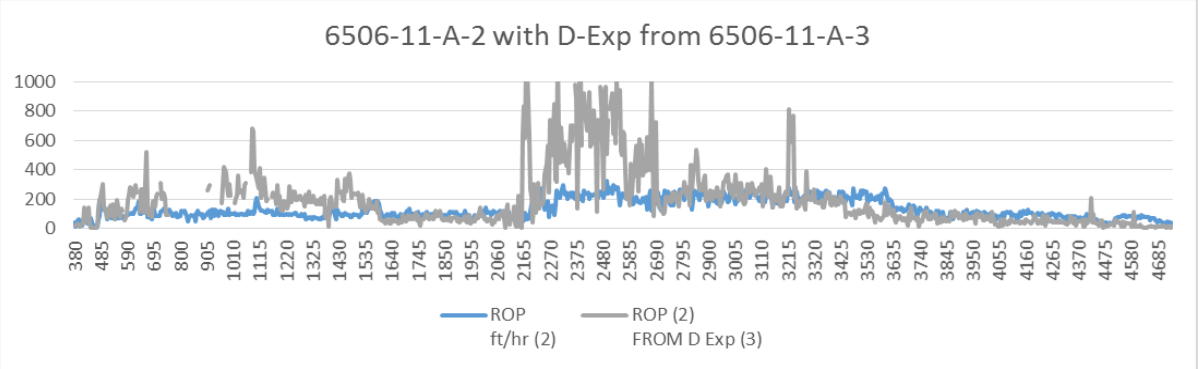

Figure 122: 6506/11-A-2 with d-exponent from 6506/11-A-3

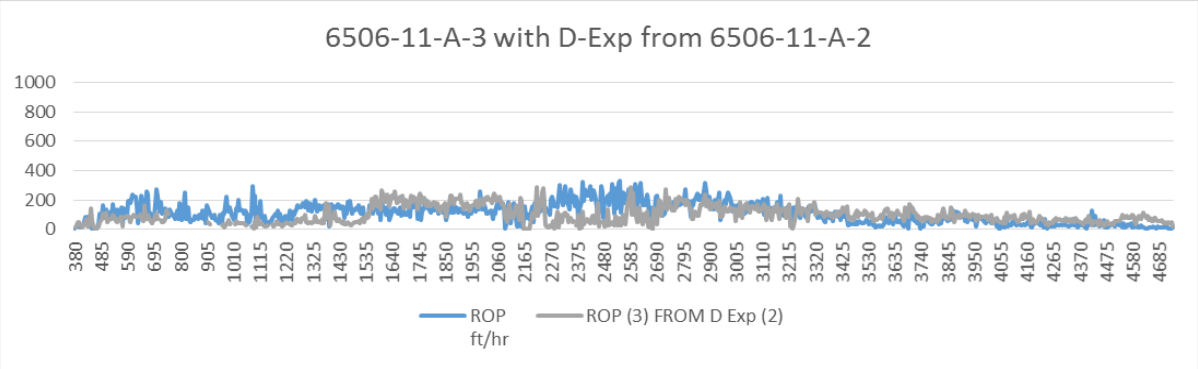

Figure 123: 6506/11-A-3 with d-exponent from 6506/11-A-2

5.6 MSE

The results from using the MSE method are available in this section. Comparing MSE is challenging, as the values may vary from one to over one thousand. This result in plots lacking the detail needed to see the correlation between the lower MSE values. The pattern is that the MSE compared values appear close for the lower depth lower MSE values, and then tend to deviate more with depth.

Results from using the MSE method between wells 6305/7-D-1 and 6305/7-D-2 are presented in figures 124 to 126. In figure 124 the MSE from the wells are compared. Results here correlate well with the actual ROP, with some clear deviations.

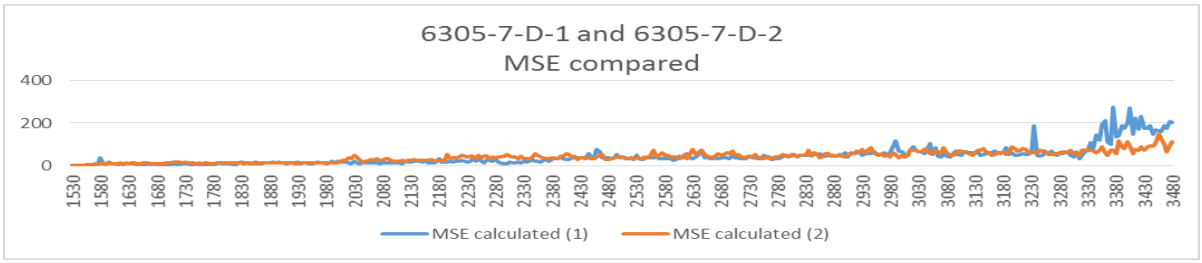

Figure 124: 6305/7-D-1 and 6305/7-D-2 MSE compared

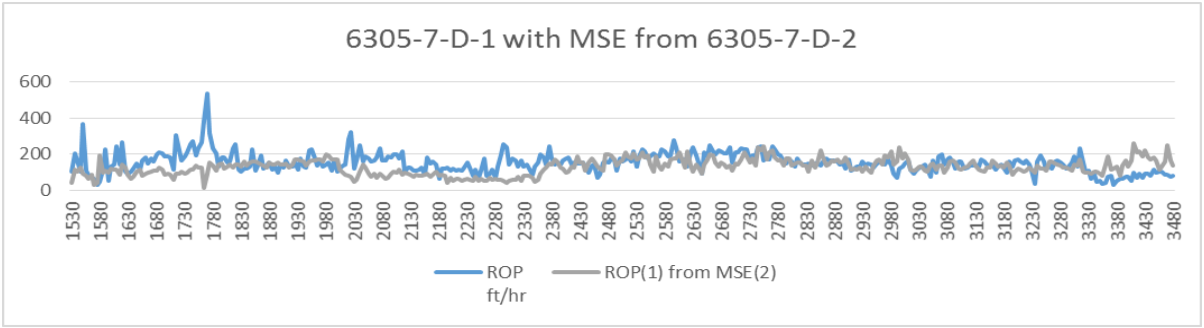

Figure 125: 6305/7-D-1 with MSE from 6305/7-D-2

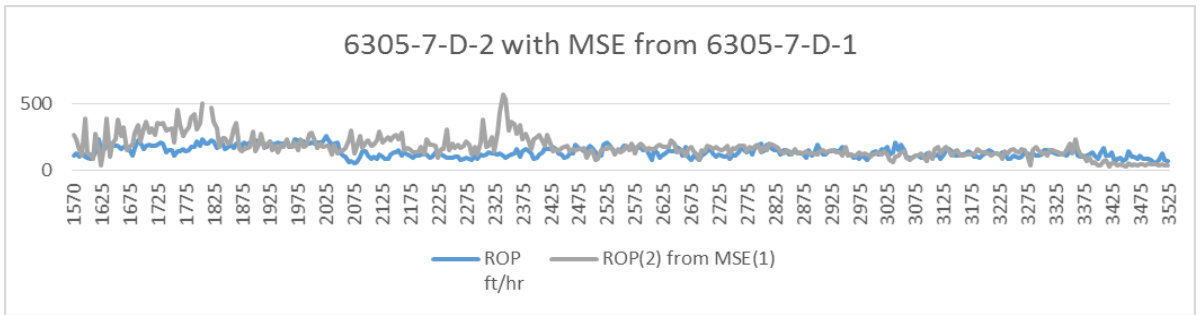

Figure 126: 6305/7-D-2 with MSE from 6305/7-D-1

Results from using the MSE method between wells 6305/7-D-1 and 6305/7-D-3 are presented in figures 127 to 129. The largest deviation between the MSE compared appear to be around the deeper depths of the plot. However, the largest deviations of the modelled ROP plots from these MSE values seem to be in the middle or beginning of the plots. This appears to be the case for the other wells as well. If anything, the modelled ROP seems to correlate well with the actual ROP in the deepest depths for the wells. Results for wells 6305/7-D-1 and 6305/7-D-3 are not terrible, but do have a lot of clear deviation from the actual ROP.

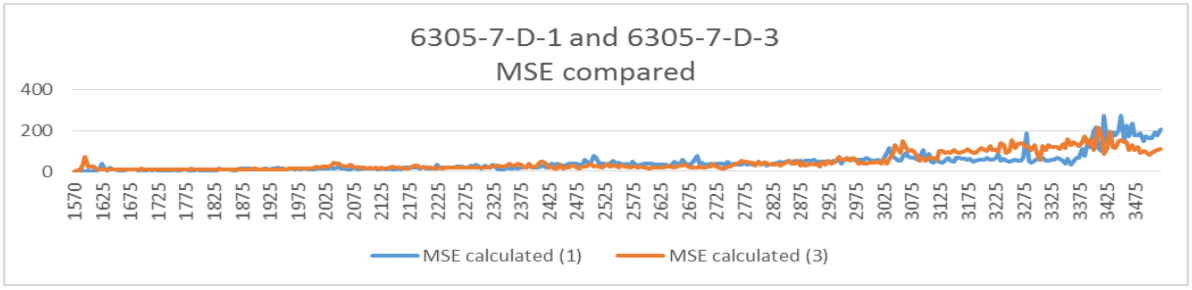

Figure 127: 6305/7-D-1 and 6305/7-D-3 MSE compared

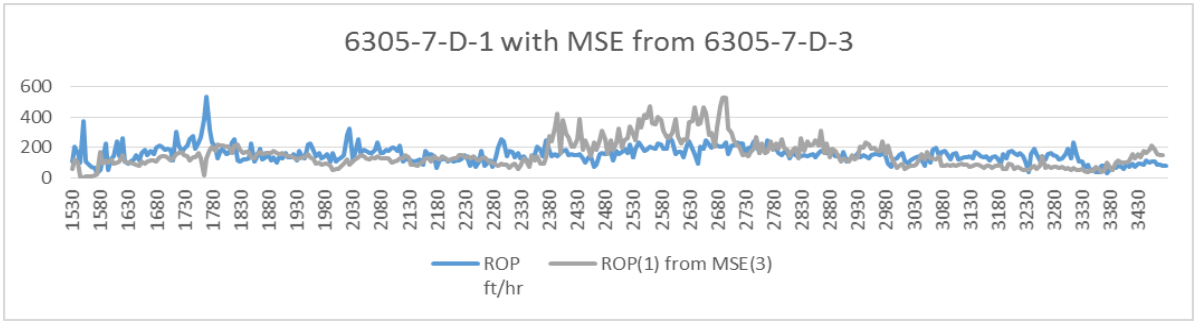

Figure 128: 6305/7-D-1 with MSE from 6305/7-D-3

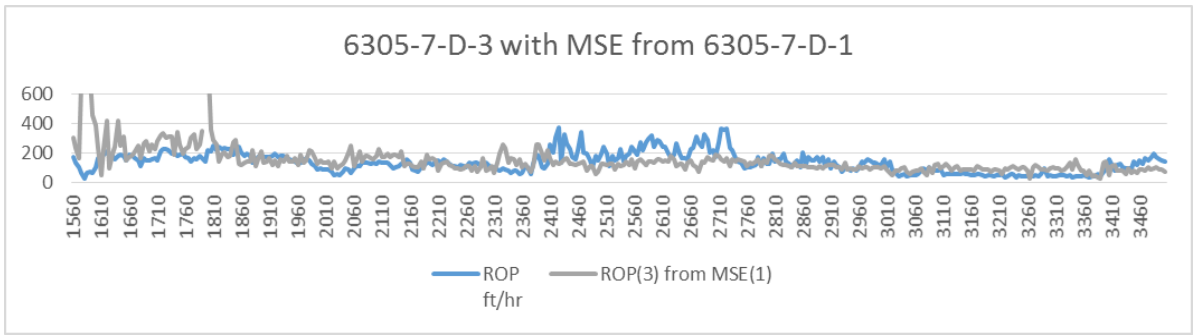

Figure 129: 6305/7-D-3 with MSE from 6305/7-D-1

Results from using the MSE method between wells 6305/7-D-2 and 6305/7-D-3 are presented in figures 130 to 132. Results here appear similar to the ones for wells 6305/7-D-1 and 6305/7-D-3.

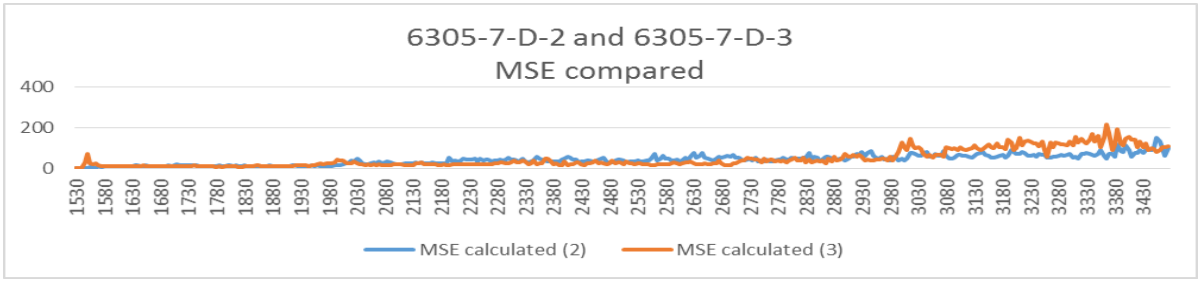

Figure 130: 6305/7-D-2 and 6305/7-D-3 MSE compared

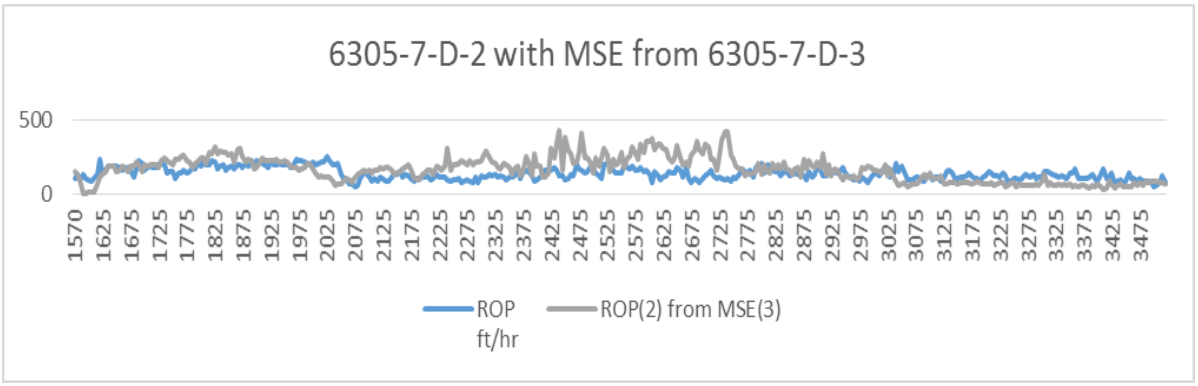

Figure 131: 6305/7-D-2 with MSE from 6305/7-D-3

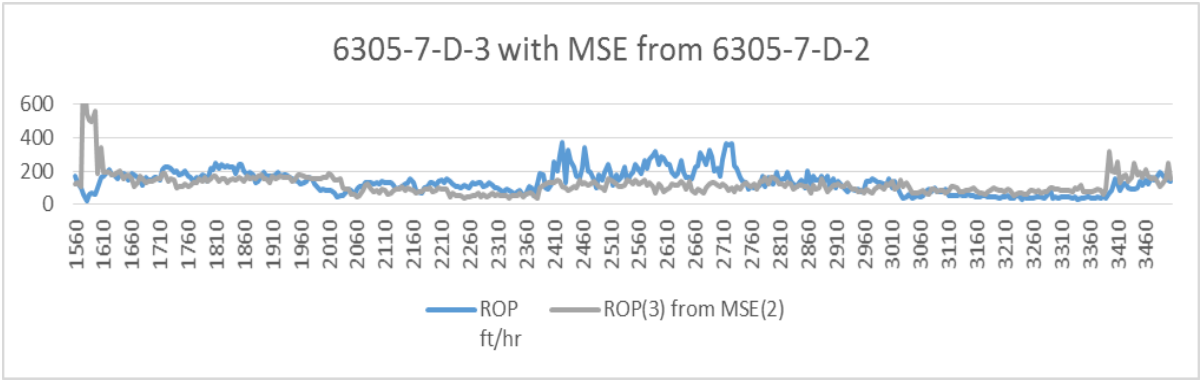

Figure 132: 6305/7-D-3 with MSE from 6305/7-D-2

Results from using the MSE method between wells 6506/11-A-1 and 6506/11-A-2 are presented in figures 133 to 135. In these wells the modelled ROP correlates better in the middle section of the plot than for previous wells. The lower depths however show significant deviation.

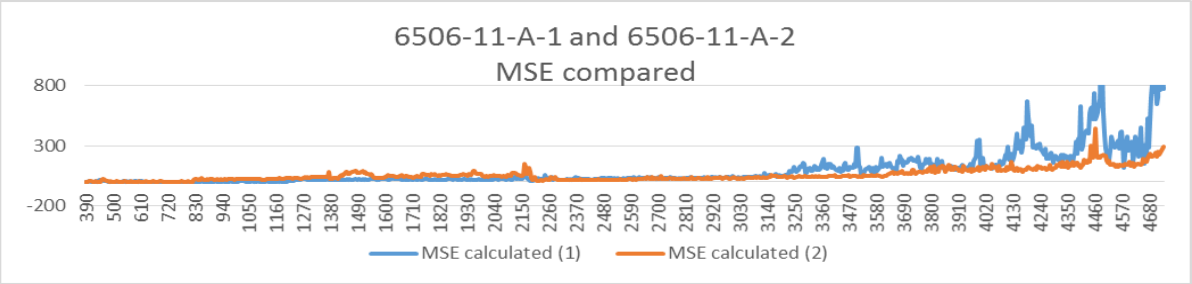

Figure 133: 6506/11-A-1 and 6506/11-A-2 MSE compared

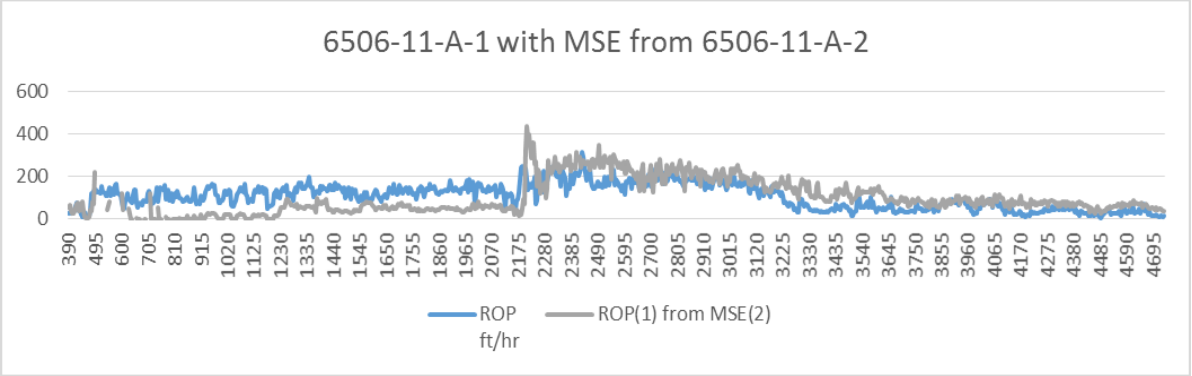

Figure 134: 6506/11-A-1 with MSE from 6506/11-A-2

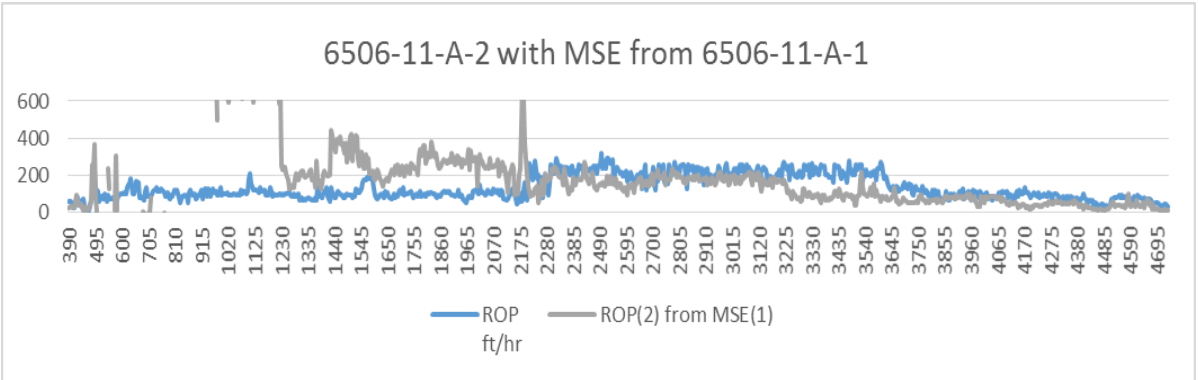

Figure 135: 6506/11-A-2 with MSE from 6506/11-A-1

Results from using the MSE method between wells 6506/11-A-1 and 6506/11-A-3 are presented in figures 136 to 138. The results for these wells appear very promising. The plots seem to correlate well, with only a few exceptions.

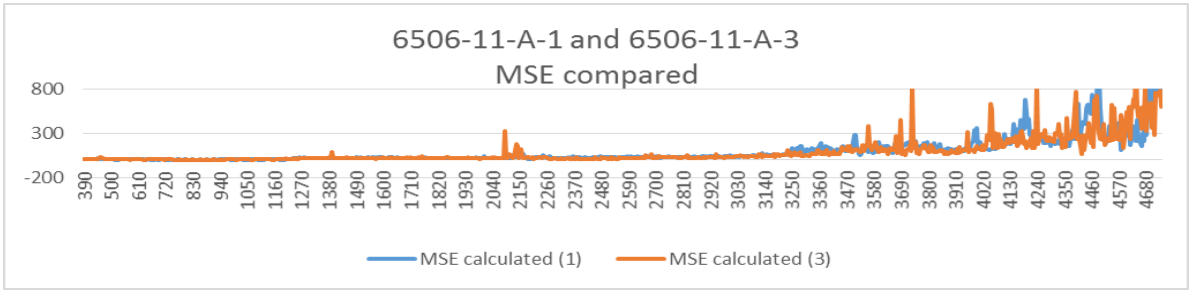

Figure 136: 6506/11-A-1 and 6506/11-A-3 MSE compared

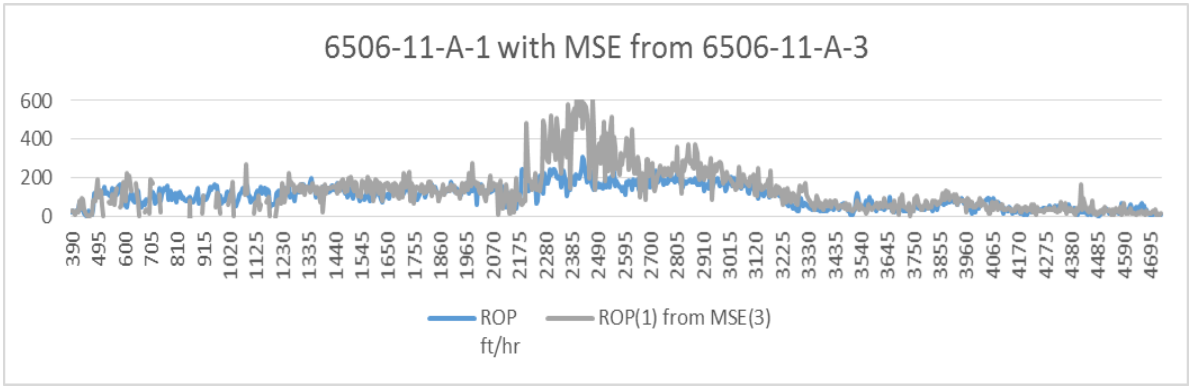

Figure 137: 6506/11-A-1 with MSE from 6506/11-A-3

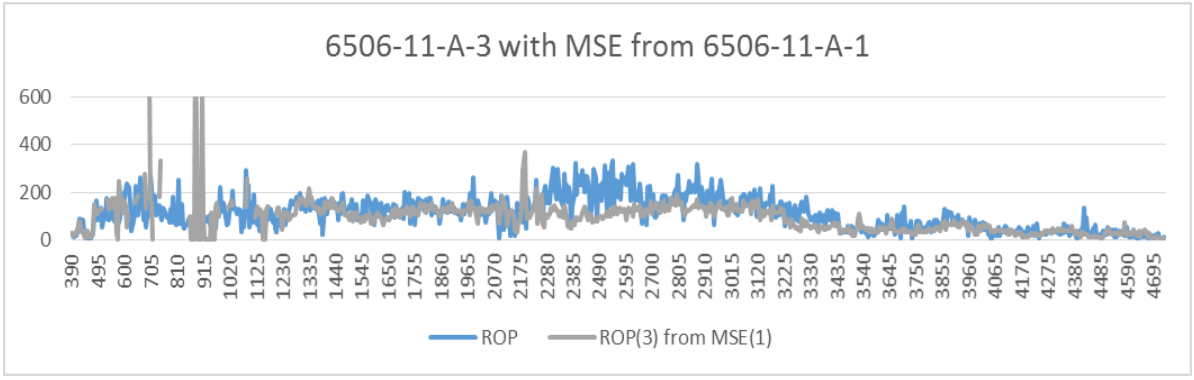

Figure 138: 6506/11-A-3 with MSE from 6506/11-A-1

Results from using the MSE method between wells 6506/11-A-2 and 6506/11-A-3 are presented in figures 139 to 141. Here the results look similar to the ones from 6506/11-A-1 and 6506/11-A-2. The modelled ROP correlates quite well from the middle of the plots, but is poor at the beginning of the plot.

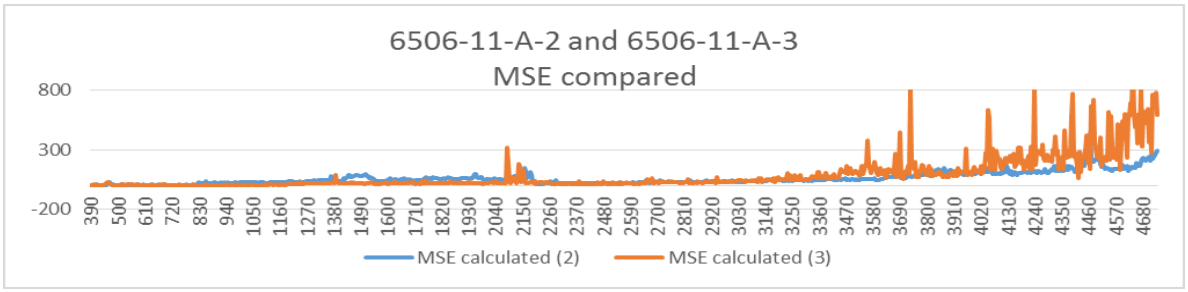

Figure 139: 6506/11-A-2 and 6506/11-A-3 MSE compared

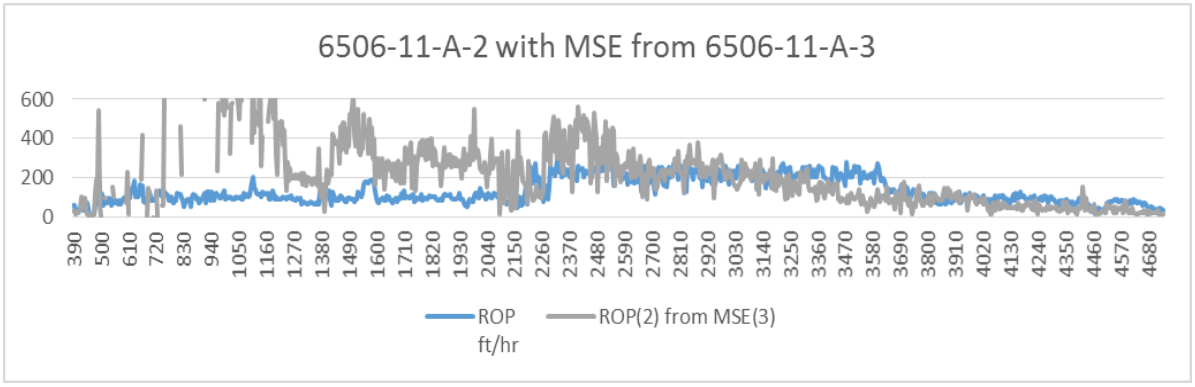

Figure 140: 6506/11-A-2 with MSE from 6506/11-A-3

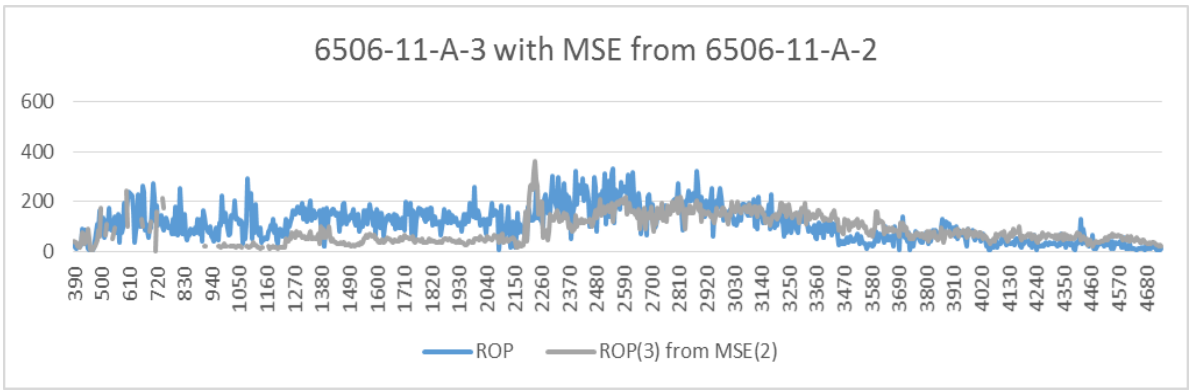

Figure 141: 6506/11-A-3 with MSE from 6506/11-A-2

5.7 Analysis: Plot comparison

The results from the analysis by plot comparison is available in this section. These results are presented by how much of the modelled ROP plot is within five or ten percent of the actual ROP, for each field location. Results of plot percentage within five percent from the Ormen Lange field wells is displayed in table 25. Percentage within ten percent of the actual ROP is available in table 26 for the same field. Table 27 presents plot percentage within five percent for the Morvin field wells. In table 28 the percentage of plot within ten percent is shown for the Morvin field.

The methods' results by use of coefficients in their originating well generally compares better to the actual ROP, as is expected. However, coefficients applied from the neighboring wells have occasionally produced results close to and even better than the original coefficients. The results from each method differ vastly depending on the well the coefficients or values are originated from, and the well they are implemented in. By organizing the results as in tables 25 to 28, it is possible to detect abnormalities. Abnormalities here may be that one of the several results from each method, deviates significantly from the others of same method. An abnormality found in table 25 is in the result of multiple regression with Bourgoyne & Young's model ("B&Y Mult. Regr") coefficients. Here the results vary from 5.50 % to 11.26 %, with one exception. For well -1 (6305/7-D-1) coefficients applied in well 6305/7-D-2, the result is a mere 0.52 %. This result lowers the average result of that method drastically, and may need to be investigated further. The same abnormality is visible in figure 143 where the result has only increased to 1.05 %, compared to the other results that are from 9.95 % to 21.99 % within 10 % of the actual ROP. In tables 27 and 28, there are no clear abnormalities. However, results within the methods frequently vary vastly. The best result of coefficients or values implemented in neighboring wells is 26.96 % of the plot within 10 % of the actual ROP. The prediction is computed by least square with Bourgoyne & Young's model ("B&Y Least Square") coefficients from well 6305/7-D-3 in well 6305/7-D-2.

Within 5%	Well		
Method	6305-7-D-1	6305-7-D-2	6305-7-D-3
Multiple Regression	13,35 %	13,09 %	11,78 %
Mult. Regression well-1 coefficients		8,90 %	6,81 %
Mult. Regression well-2 coefficients	7,07 %		6,28 %
Mult. Regression well-3 coefficients	2,09 %	2,88 %	
Least Square	16,49 %	13,61 %	7,85 %
Least Square well-1 coefficients		11,52 %	7,85 %
Least Square well-2 coefficients	10,21 %		5,76 %
Least Square well-3 coefficients	12,57 %	11,78 %	
B&Y Multiple Regression	17,28 %	11,26 %	16,49 %
B&Y Mult. Regr. well-1 coefficients		0,52 %	6,02 %
B&Y Mult. Regr. well-2 coefficients	7,33 %		11,26 %
B&Y Mult. Regr. well-3 coefficients	5,50 %	8,64 %	
B&Y Least Square	16,49 %	13,87 %	8,12 %
B&Y Least Square well-1 coefficients		12,30 %	11,52 %
B&Y Least Square well-2 coefficients	10,21 %		10,21 %
B&Y Least Square well-3 coefficients	10,21 %	12,83 %	
D Exp well-1 D-Exp		5,76 %	5,76 %
D Exp well-2 D-Exp	5,24 %		5,24 %
D Exp well-3 D-Exp	3,14 %	3,40 %	
MSE well-1 MSE		10,73 %	6,28 %
MSE well-2 MSE	10,47 %		7,07 %
MSE well-3 MSE	6,28 %	7,07 %	

Within 10%	Well		
Method	6305-7-D-1	6305-7-D-2	6305-7-D-3
Multiple Regression	30,89 %	27,75 %	20,94 %
Mult. Regression well-1 coefficients		17,54 %	13,61 %
Mult. Regression well-2 coefficients	14,92 %		12,30 %
Mult. Regression well-3 coefficients	4,19 %	6,02 %	
Least Square	31,94 %	25,92 %	14,40 %
Least Square well-1 coefficients		21,47 %	16,49 %
Least Square well-2 coefficients	18,06 %		14,66 %
Least Square well-3 coefficients	25,65 %	20,68 %	
B&Y Multiple Regression	33,51 %	27,49 %	30,89 %
B&Y Mult. Regr. well-1 coefficients		1,05 %	10,73 %
B&Y Mult. Regr. well-2 coefficients	15,97 %		21,99 %
B&Y Mult. Regr. well-3 coefficients	9,95 %	15,18 %	
B&Y Least Square	32,46 %	25,39 %	14,92 %
B&Y Least Square well-1 coefficients		20,42 %	18,59 %
B&Y Least Square well-2 coefficients	18,32 %		16,75 %
B&Y Least Square well-3 coefficients	19,37 %	26,96 %	
D Exp well-1 D-Exp		8,38 %	12,57 %
D Exp well-2 D-Exp	10,21 %		9,69 %
D Exp well-3 D-Exp	6,81 %	6,81 %	
MSE well-1 MSE		19,63 %	11,78 %
MSE well-2 MSE	21,47 %		14,14 %
MSE well-3 MSE	12,04 %	14,40 %	

Within 5%	Well		
Method	6506-11-A-1	6506-11-A-2	6506-11-A-3
Multiple Regression	9,31 %	8,39 %	8,74 %
Mult. Regression well-1 coefficients		4,25 %	6,09 %
Mult. Regression well-2 coefficients	4,94 %		6,55 %
Mult. Regression well-3 coefficients	6,90 %	7,01 %	
Least Square	7,47 %	6,78 %	5,40 %
Least Square well-1 coefficients		8,62 %	5,98 %
Least Square well-2 coefficients	10,23 %		7,93 %
Least Square well-3 coefficients	5,86 %	8,62 %	
B&Y Multiple Regression	11,03 %	12,53 %	12,30 %
B&Y Mult. Regr. well-1 coefficients		2,76 %	9,77 %
B&Y Mult. Regr. well-2 coefficients	6,67 %		6,32 %
B&Y Mult. Regr. well-3 coefficients	9,89 %	4,02 %	
B&Y Least Square	7,01 %	13,33 %	10,19 %
B&Y Least Square well-1 coefficients		2,53 %	7,15 %
B&Y Least Square well-2 coefficients	4,25 %		5,94 %
B&Y Least Square well-3 coefficients	7,01 %	5,29 %	
D Exp well-1 D-Exp		0,94 %	9,19 %
D Exp well-2 D-Exp	2,87 %		4,18 %
D Exp well-3 D-Exp	4,56 %	3,64 %	
MSE well-1 MSE		4,49 %	8,41 %
MSE well-2 MSE	3,63 %		5,94 %
MSE well-3 MSE	8,52 %	4,65 %	

Within 10%	Well		
Method	6506-11-A-1	6506-11-A-2	6506-11-A-3
Multiple Regression	16,78 %	15,63 %	19,20 %
Mult. Regression well-1 coefficients		9,89 %	12,18 %
Mult. Regression well-2 coefficients	9,77 %		14,02 %
Mult. Regression well-3 coefficients	14,02 %	14,02 %	
Least Square	12,99 %	12,37 %	12,41 %
Least Square well-1 coefficients		17,82 %	11,49 %
Least Square well-2 coefficients	19,20 %		15,06 %
Least Square well-3 coefficients	11,95 %	17,47 %	
B&Y Multiple Regression	21,38 %	24,71 %	24,71 %
B&Y Mult. Regr. well-1 coefficients		5,63 %	19,66 %
B&Y Mult. Regr. well-2 coefficients	15,17 %		13,91 %
B&Y Mult. Regr. well-3 coefficients	19,20 %	7,82 %	
B&Y Least Square	16,73 %	28,16 %	19,66 %
B&Y Least Square well-1 coefficients		4,94 %	14,20 %
B&Y Least Square well-2 coefficients	8,30 %		12,86 %
B&Y Least Square well-3 coefficients	14,41 %	9,77 %	
D Exp well-1 D-Exp		1,29 %	21,80 %
D Exp well-2 D-Exp	7,13 %		9,78 %
D Exp well-3 D-Exp	9,39 %	7,29 %	
MSE well-1 MSE		8,92 %	16,41 %
MSE well-2 MSE	7,44 %		9,73 %
MSE well-3 MSE	16,04 %	10,18 %	

5.8 Analysis: Time comparison

The results obtained from the analysis by time comparison is available in this section. These results are presented by percent of estimated time deviating from the actual drilling time, for each field location. The results of time comparison from the Ormen Lange field wells is displayed in table 29. Table 30 presents the time comparison for the Morvin field wells.

The methods' result by use of coefficients in their originating well is generally significantly closer to the actual drilling time, compared to applying them in neighboring wells. Still, there are results of coefficients or values applied in neighboring wells only deviating a few percent. The variations of results within methods are very significant. In table 29 for multiple regression ("Mult. Regression") coefficients, the results vary from 8.47 % to 209.74 % predicted time deviation. In table 30 for MSE values, results estimate times from 0.97 % to 33.30 % below actual drilling time. It is visible in table 30 that the multiple regression method applied in well 6506/11-A-3 has managed to estimate a time prediction with a 0.00 % deviation. Closer inspection reveals that the time estimate is off by 13 seconds for a 128.64-hour drilling operation. The best resulting prediction of coefficients or values implemented in neighboring wells is only 0.48 % below. This prediction is computed by multiple regression with Bourgoyne & Young's model ("B&Y Mult. Regr") coefficients from well 6506/11-A-3 in well 6506/11-A-2. Only 30.9 minutes below the correct 107.14-hour drilling operation.

	Well		
Method	6305-7-D-1	6305-7-D-2	6305-7-D-3
Multiple Regression	-0,38 %	0,65 %	-0,66 %
Mult. Regression well-1 coefficients		-13,32 %	-21,31 %
Mult. Regression well-2 coefficients	8,47 %		-23,14 %
Mult. Regression well-3 coefficients	209,74 %	176,50 %	
Least Square	-0,44 %	4,42 %	-1,32 %
Least Square well-1 coefficients		-10,61 %	-14,81 %
Least Square well-2 coefficients	16,10 %		-4,28 %
Least Square well-3 coefficients	14,21 %	2,55 %	
B&Y Multiple Regression	3,92 %	4,22 %	4,14 %
B&Y Mult. Regr. well-1 coefficients		-40,50 %	-32,28 %
B&Y Mult. Regr. well-2 coefficients	20,16 %		7,92 %
B&Y Mult. Regr. well-3 coefficients	9,08 %	9,56 %	
B&Y Least Square	4,19 %	4,78 %	9,36 %
B&Y Least Square well-1 coefficients		-9,36 %	-8,52 %
B&Y Least Square well-2 coefficients	17,28 %		3,23 %
B&Y Least Square well-3 coefficients	23,27 %	7,05 %	
D Exp well-1 D-Exp		-18,87 %	-29,86 %
D Exp well-2 D-Exp	8,70 %		-21,73 %
D Exp well-3 D-Exp	70,76 %	31,93 %	
MSE well-1 MSE		-21,43 %	-7,58 %
MSE well-2 MSE	20,59 %		12,37 %
MSE well-3 MSE	0,64 %	-16,90 %	

	Well		
Method	6506-11-A-1	6506-11-A-2	6506-11-A-3
Multiple Regression	0,40 %	6,73 %	0,00 %
Mult. Regression well-1 coefficients		32,01 %	9,56 %
Mult. Regression well-2 coefficients	14,07 %		-3,00 %
Mult. Regression well-3 coefficients	24,25 %	27,01 %	
Least Square	-0,01 %	-1,50 %	-2,13 %
Least Square well-1 coefficients		27,46 %	6,15 %
Least Square well-2 coefficients	-21,38 %		-23,16 %
Least Square well-3 coefficients	-2,78 %	20,70 %	
B&Y Multiple Regression	2,23 %	5,37 %	4,57 %
B&Y Mult. Regr. well-1 coefficients		-10,42 %	-11,27 %
B&Y Mult. Regr. well-2 coefficients	-5,34 %		-15,24 %
B&Y Mult. Regr. well-3 coefficients	6,44 %	-0,48 %	
B&Y Least Square	10,48 %	6,48 %	6,80 %
B&Y Least Square well-1 coefficients		24,67 %	10,40 %
B&Y Least Square well-2 coefficients	-6,35 %		-21,28 %
B&Y Least Square well-3 coefficients	30,73 %	44,29 %	
D Exp well-1 D-Exp		-52,21 %	-6,40 %
D Exp well-2 D-Exp	-8,37 %		-17,57 %
D Exp well-3 D-Exp	57,74 %	61,68 %	
MSE well-1 MSE		-22,76 %	21,89 %
MSE well-2 MSE	-0,97 %		26,35 %
MSE well-3 MSE	-21,32 %	-33,30 %	

6 CONCLUSION

Similar lithology and conditions make it possible to correlate with respect to computing the ROP with close-by wells. As formation properties has a major impact on drillability, MSE and drilling variables effects, it also affects the ROP. The use of coefficients and values from close-by wells with the techniques introduced in this thesis to give a predicted ROP has produced promising results. Most of the modelled ROP plots appear to correlate close to the actual ROP. That said these are still modelled predictions and in some cases deviate significantly from the actual data.

Well 6305/7-D-3 results appear to have most frequently produced poor results. This is also apparent in figure 146 showing the overall time deviation for the predicted ROP. Well 6305/7-D-3 results have the three clearly most deviating results. For multiple regression, the time deviation is no less than 209.74 % and 176.50 % when applying the neighboring well coefficients. Additionally for the d-exponent method, the deviation is 70.76 % from one of the close-by well coefficients. One possible reason for this has been remarked in the final well report, from where the data for the tests were retrieved, where it states “To maintain template orientation and level restrictions all 30” conductors and 20” surface casings on 3 wells were installed. The wells were drilled in batch mode. The 3 wells where 20” surface casing were installed include: 6305/7-D-3 H, 6305/7-D-6 H, 6305/7-D-7 H pilot hole and 6305/7-D-7 AH.” This suggests that well 6305/7-D-3 drilling may have been conducted differently, providing discrepancy in the data when they later returned to re-enter and complete the well. Another reason may be that the actual ROP varies more than for other wells.

The other results that may be regarded as failing to predict ROP, due to significant deviation is well 6506/11-A-2 with neighboring coefficients. For the Morvin field wells, wells 6506/11-A-1 and 6506/11-A-3 seem to correspond the best. Also for these wells, a possible answer is in the final well report. While both 6506/11-A-1 and 6506/11-A-3 wells were drilled with 36”, 26”, 17 ½” and 12 ¼” sections, the 6506/11-A-2 well was drilled with 36”, 26”, 17 ½”x20”, 12 ¼”x17 ½” and 12 ¼” sections. Therefore, also here it seems the differences may be a result of conducting the drilling process differently.

A conclusion over the validity and performance of the techniques may be derived from the overall results displayed in tables 31 and 32. Within 5 % deviation of the actual ROP, the least square technique with and without the Bourgoyne & Young's model clearly performs the best. The outcome is similar for within 10 % deviation of the actual ROP. Here the least square method is noticeably the strongest performer. The least square technique has good results for time deviation results, only the technique of multiple regression with Bourgoyne & Young's model has better results here.

6305/7-D wells	MULT.REG	MULTIPLE REGRESSION COEFF.	LEAST SQ	LEAST SQUARE COEFF.	LEAST SQR B&Y	LEAST SQR B&Y COEFF.	D-EXP	MSE	MULT.REG B&Y COEFF.	MULT. REG. B&Y
6305/7 average within 5%:	0,1274	0,056719023	0,12653	0,0994764	0,12827	0,1121291	0,0475567	0,079843	0,065445	0,15009
6506/11-A wells										
6506/11 average within 5%:	0,08812	0,059578544	0,06552	0,0787356	0,1018	0,0536189	0,0422993	0,0594	0,0657088	0,11954
TOTAL WELLS AVERAGE WITHIN 5%:	**10,78 %**	**5,81 %**	**9,60 %**	**8,91 %**	**11,50 %**	**8,29 %**	**4,49 %**	**6,96 %**	**6,56 %**	**13,48 %**
6305/7-D wells	MULT.REG	MULTIPLE REGRESSION COEFF.	LEAST SQ	LEAST SQUARE COEFF.	LEAST SQR B&Y	LEAST SQR B&Y COEFF.	D-EXP	MSE	MULT.REG B&Y COEFF.	MULT. REG. B&Y
6305/7 average within 10%:	0,26527	0,114310646	0,24084	0,1950262	0,24258	0,2006981	0,0907504	0,155759	0,1247818	0,30628
6506/11-A wells										
6506/11 average within 10%:	0,17203	0,123180077	0,1259	0,1549808	0,21516	0,1074773	0,0944594	0,114537	0,1356322	0,23602
TOTAL WELLS AVERAGE WITHIN 10%:	**21,87 %**	**11,87 %**	**18,34 %**	**17,50 %**	**22,89 %**	**15,41 %**	**9,26 %**	**13,51 %**	**13,02 %**	**27,11 %**

31

6305		Multiple Regression	Multiple Regression Coefficients	Least Square	Least Square Coefficients	Least Square B&Y	Least Square B&Y Coefficients	D-EXP	MSE	Multiple Regression B&Y Coefficients	Multiple Regression B&Y
	6305 average deviation:	0,24965864	32,0351397	0,9116	4,49119828	2,7225	4,8450791	13,0865	4,60699	8,76445803	1,7891056
	% deviation:	0,00571511	0,73333823	0,0209	0,10281108	0,0623	0,11091201	0,29957	0,10546	0,20063318	0,0409556
6506											
	6506 average deviation:	2,58155442	21,8574419	1,4546	20,325637	9,9485	27,4529755	40,3584	25,3668	10,2813329	4,8817354
	% deviation:	0,0208834	0,17681508	0,0118	0,1644236	0,0805	0,22207997	0,32648	0,2052	0,08317052	0,0394906
ALL	Total average deviation	1,41560653	26,9462908	1,1831	12,4084176	**6,3355**	16,1490273	26,7224	14,9869	**9,52289546**	3,3354205
	% deviation:	**1,69 %**	**32,21 %**	**1,41 %**	**14,83 %**	**7,57 %**	**19,31 %**	**31,95 %**	**17,92 %**	**11,38 %**	**3,99 %**

32

The final conclusion is that the results in general appear to correlate closely with the actual ROP, and many techniques show promise. The least square technique may be considered the overall best technique to predict the ROP from the data sets used in this thesis. With more available data and development of the techniques, it is believed that the results may improve and become more accurate. The techniques may then possibly be used to optimize planning for operations and expenses. From the experience in this thesis, it is recommended that the techniques be implemented for wells that are to be drilled with a similar procedure as the reference well, as this has been shown to be a possible cause of deviation.

REFERENCES

[1] Teale, R., “The Concept of Specific Energy in Rock Drilling”,(1965), Int. J. Rock Mechanic Mining Science

[2] Macini, P., SPE, “Bit Performance Evaluation Revisited by Means of Bit Index and Formation Drillability Catalogue”, SPE/IADC 107536, (2007)

[3] Dr. Kök M. V., “Drilling optimization”, Middle East Technical University, Dept. of Petroleum & Natural Gas Engineering, retrieved from https://www.metu.edu.tr/~kok/pete424/PETE424_CHAPTER2.pdf, 24.02.2015

[4] Borgouyne & Young, 1974 // A multiple regression approach to optimal drilling and abnormal pressure detection // SPE J. 14 (4): 371-384

[5] Morton, E.K. and Clements, W.R., “The Role of Bit Type and Drilling Fluid Type in Drilling Performance”, SPE 14073, (1986)

[6] Bourgoyne A.T. Jr., Millheim K.K., Chenevert M.E., and Young F.S., "*Applied Drilling Engineering*", Society of Petroleum Engineers Text Book Series, Vol.1, Richardson, TX, 1986)

[7] Warren, T.M., and Armagost, W.K., SPE, Amoco Production Co., “Laboratory Drilling Performance of PDC Bits”, SPE 15617, (June 1988)

[8] T.M. Warren, SPE, Amoco Production Co. (1987), Penetration-Rate Performance of Roller-Cone Bits

[9] Hareland, G. and Rampersad, P.R., Drag - Bit Model Including Wear; paper SPE 26957 presented at the SPE Latin America/ Caribbean Petroleum Engineering Conference, Buenos Aires, Argentina, 27-29 April 1994.

[10] Singh et al., “Cutting Structure for Roller Cone Bits”, United States Patent, United States Patent and Trademark Office, Patent #: US006374930, Sheet 2 of 8, http://www.uspto.gov/, (23. April, 2002)

[11] WISE J.L., GROSSMAN, J.W., WRIGHT, E.K., GRONEWALD, P.J., BERTAGNOLLI, K. and COOLEY, C.H., Latest Results of Parameter Studies on PDC Drag Cutters for Hard Rock Drilling; GRC Transactions, Vol. 29, 2005.

[12] Swenson , D.V., Wesenberg , D.L. and Jones , A.K., Analytical and Experimental Investigations of Rock Cutting Using Polycrystalline Diamond Compact Drag Cutters; paper

SPE 10150 presented at the SPE Annual Technical Conference and Exhibition, San Antonio, TX, 4-7 October 1981.

[13] Warren , T.M. and Armagost , W.K., Laboratory Drilling Performance of PDC Bits; SPE Drilling Engineering, Vol. 3, No. 2, pp. 125-135, June 1988.

[14] Zeuch , D.H. and Finger , J.T., Rock Breakage Mechanisms with a PDC Cutter; paper SPE 14219 presented at the SPE Annual Technical Conference and Exhibition, Las Vegas, NV, 22-26 September 1985.

[15] Brett , J.F., Warren , T.M. and Behr , S.M., Bit Whirl: A New Theory of PDC Bit Failure; paper SPE 19571 presented at the SPE Annual Technical Conference and Exhibition, San Antonio, TX, 8-11 October 1989.

[16] Hareland, G, et.al, "Cutting Efficiency of a Single PDC Cutter on Hard Rock" (2007)

[17] Warren, T.M and Sinor, A., Amoco Production Co.,.: "Drag Bit Performance Modeling", (October 1986), SPE 15618

[18] "PDC bit profile", PetroWiki by SPE International, http://petrowiki.org/, Created Aug 29, 2012, Retrieved April 3, 2015, from PetroWiki by SPE International, http://petrowiki.org/, Copyrights by Smith Bits, http://petrowiki.org/File%3ADevol2_1102final_Page_247_Image_0001.png

[19] B. Rashidi, G. Hareland, R. Nygaard, 'Real-Time Drill Bit Wear Prediction by Combining Rock Energy and Drilling Strength Concepts', paper for presentation at the Abu Dhabi International Petroleum Conference and Exhibition, Abu Dhabi, UAE [3rd – 6th November 2008]

[20] D.S.I.R. Crushing and Grinding; a Bibliography. H.M.S.O., London (1958)

[21] WALKER D. R. and SHAW M.C. Mining Engng 6, 313-20 0954

[22] SPE/IADC 92194, Dupriest, F.E., "Maximizing Drill Rates with Real-Time Surveillance of Mechanical Specific Energy", 2005

[23] Pessier, R.C and Fear, M.J., "Quantifying Common Drilling Problems with Mechanical Specific Energy and Bit-Specific Coefficient of Sliding Friction", IADC/SPE 24584, (1992)

[24] Eren, T., "Real-Time-Optimization of Drilling Parameters During Drilling Operations", (2010)

[25] Maurer, W. C.: “The ‘Perfect Cleaning’ Theory of Rotary Drilling”, J. Pet. Tech. (Nov. 1962) 1270-1274; Trans., AIME, Vol. 225.

[26] Murray A. S., and Cunningham, R. A.: “The Effect of Mud Column Pressure on Drilling Rates”, Trans., AIME (1955) Vol. 204, 196-204.

[27] Combs, G. D.: “Prediction of Pore Pressure From Penetration Rate”, Proc., Second Symposium on Abnormal Subsurface Pore Pressure, Baton Rouge, La. (Jan. 1970)

[28] Vidrine, D. J., and Denit, E. J.: "Field Verification of the Effect of Differential Pressure on Drilling Rate,"]. Pet. Tech. (July 1968) 676-682.

[29] Cunningham, A. J., and Eenink, J. G.: "Laboratory Study of Effect of Overburden, Formation and Mud Column Pressure on Drilling Rate of Permeable Formations," Trans., AIME (1959) Vol. 216, 9-17.

[30] Garnier, A. J., and van Lingen, N. H.: "Phenomena Affecting Drilling Rates at Depth," Trans., AIME (1959) Vol. 216, 232-239.

[31] Edwards, J. H.: “Engineering Design of Drilling Operations”, Drill. and Prod. Prac. API (1964) 39.

[32] Galle, E. M., and Woods, A. B.: “Best Constant Weight and Rotary Speed for Rotary Rock Bits”, Drill. and Prod. Prac. API (1963) 48.

[33] Graham, J. W., and Muench, N. L.: “Analytical Determination of Optimum Bit Weight and Rotary Speed Combinations”, paper SPE 1349-G presented at SPE-AIME 34th Annual Fall Meeting, Dallas, Oct. 4-7, 1959.

[34] Jorden, J. R., and Shirley, O. J.: “Application of Drilling Performance Data to Overpressure Detection”, J. Pet. Tech. (Nov. 1966) 1387-1394.

[35] Maratier, J.: “Optimum Rotary Speed and Bit Weight for Rotary Drilling”, MS thesis, Louisiana State U., Baton Rouge (June 1971).

[36] Eckel, J. J.: “Microbit Studies of the Effect of Fluid Properties and Hydraulics on Drilling Rate”, J. Pet. Tech. (April 1967) 541-546; Trans. AIME, Vol. 240.

[37] Galle, E. M. and Woods, H.B.: "Variable Weight and Rotary Speed for Lowest Drilling Cost," paper presented at the AAODC Annual Meeting, New Orleans, Sept. 27, 1960

[38] Estes, Jack C. and Randall, B.V.: "Practical Application of Optimized Drilling Operations," paper presented at the IADC Drilling Technology Conf., New Orleans, March 16-18, 1977

[39] Warren, T.M.: "Drilling Model for Soft-Formation Bits," JPT, (June 1981) 963-70.

[40] (Wardlaw, H.W.R.: "Optimization of Rotary Drilling Parameters," PhD dissertation, U. of Texas, Austin (Aug. 1971))

[41] Hareland, G., and Hoberock, L.L.: "Use of Drilling Parameters to Predict In-Situ Stress Bounds," SPE paper 25727, presented at the 1993 SPE/ IADC Drilling Conference, Amsterdam, The Netherlands, February 23-25, 1993

[42] Darley, H. C., "Designing Fast Drilling Fluids", Journal of Petroleum Technology, April, 1965, 465-470

[43] Cheatham, J. B., "Tooth Penetration Into Dry Rock at Confming Pressures of 0 to 5000 psi", Texas Conference on Drilling and Rock Mechanics, Austin Texas, Jan. 20-21,1965

[44] Hunt, E., Hoberock, L. L., and Hareland, G., "Investigation of an In-Situ Stress Profile Model Using Drilling Parameters", Topical Report, Sept., 1992, Contract 5091-221-2229, Gas Research Institute, 8600 West Bryn Mawr, Chicago, IL, 60631

[45] P. R. Rampersad, G. Hareland, P. Boonyapaluk, "Drilling Optimization Using Drilling Data and Available Technology", SPE paper 27034, presented at the 3rd Latin American/Caribbean Petroleum Engineering Conference held in Buenos Aires, Argentina, April 27-29, 1994

[46] Appl, F. C. and Rowley, D. S.: "Analysis of the cutting Action of a Single Diamond" Soc. of Pet Eng. J. (Sept 1968), 269-280

[47] Peterson, J. L.: "Diamond Drilling Model Verified in Field and Laboratory Tests" Journal of Petr Tech. (Feb. 1976), 213-223

[48] Warren, T. M. and Sinor, L. A.: "Drag Bit Wear Model" SPE Paper No. 16699, Presented at the 62nd SPE Annual Technical Conference and Exhibition, Dallas, TX (Sept. 1987)

[49] Millheim, K. K and Higgins, R. L.: "The Engineering Simulator for Drilling (Part 2) paper SPE 12075 presented at the 1983 SPE Annual Technical Conference and Exhibition, San Francisco, Oct. 5-8

[50] “New Approach in Real-Time Bit Wear Prediction” Behrad Rashidi (University of Calgary) | Geir Hareland (U. of Calgary) | Andrew Wu (University of Calgary), SPE-136008-MS, (2010)

[51] Fasheloum, M.: ”INVESTIGATION OF DRILLING PARAMETERS INDICATORS”, (April 1997), The University of Nottingham, department of mineral resources engineering

[52] Ozbayoglu M.E., Miska S.Z., Reed T., and Takach N., “Analysis of the Effects of Major Drilling Parameters on Cuttings Transport Efficiency for High-Angle Wells in Coiled Tubing Drilling Operations,” SPE 89334, SPE/IcoTA CT Conf. and Exhb., Houston, TX, March 2004

[53] Montgomery D.C., and Runger G.C., “Applied Statistics and Probability for Engineers” Third Edition, John Wiley & Sons, Inc, USA, 2003, pp 482)

[54] Davis J.C., “Statistics and Data Analysis in Geology” Third Edition, John

Wiley & Sons, USA, Inc, 2002, pp 461)

[55] Explorable.com (Jun 18, 2009). Multiple Regression Analysis. Retrieved Feb 20, 2015 from Explorable.com: https://explorable.com/multiple-regression-analysis

[56] Dale E. Berger “Introduction to Multiple Regression”, (2003), Claremont Graduate University

[57] Engineering Statistics Handbook, 4.4.3.1 Least Squares. Retrieved April 12, 2015 from http://www.itl.nist.gov, http://www.itl.nist.gov/div898/handbook/pmd/section4/pmd431.htm

[58] Rabia H., Entrac Consulting, “Well Engineering & Construction”, p. 26-29, (2002), ISBN: 0954108701. Retrieved April 12, 2015 from http://faculty.ksu.edu.sa, http://faculty.ksu.edu.sa/shokir/PGE472/Textbook%20and%20References/RABIA%20-%20WELL%20ENGINEERING%20%20CONSTRUCTION.pdf

[59] Ablard P., et al., “The Expanding Role of Mud Logging”, Oilfield Review Spring 2012: 24, no. 1., p. 31-32, (2012), Copyright Schlumberger

[60] Jordan J.R and Shirley O.J (1966)"Application of drilling performance data to overpressure detection" JPT

[61] Rehm B and McClendon R (1971) "Measurement of formation pressures from drilling data" SPE 3601, AIME Annual Fall Meeting, New Orleans.

[62] Rider M. and Kennedy M., “The Geological Interpretation of Well Logs”, 3rd edition, p. 401, (2011)

[63] Bjørlykke K., «Sedimentologi og petroleumsgeologi», p. 177, (2001)

[64] Bjørlykke K., «Sedimentologi og petroleumsgeologi», p. 40 (2001)

[65] Aadnøy, B. S., “Mordern Well Design”, 2nd edition, (2010)

[66] Schlumberger Oilfield Glossary, “wildcat”. Retrieved April 16, 2015, from http://www.glossary.oilfield.slb.com, http://www.glossary.oilfield.slb.com/en/Terms.aspx?LookIn=term%20name&filter=wildcat

[67] SUBSEAIQ, “Ormen Lange”. Retrieved May 5, 2015, from http://www.subseaiq.com/, http://www.subseaiq.com/data/PrintProject.aspx?project_id=222&AspxAutoDetectCookieSupport=1

[68] SUBSEAIQ, “Morvin”. Retrieved May 5, 2015, from http://www.subseaiq.com/ http://subseaiq.com/data/Project.aspx?project_id=360&AspxAutoDetectCookieSupport=1